5 CPT

NASA CR-151918

FEASIBILITY STUDY OF MODERN AIRSHIPS

Phase II

VOLUME I - HEAVY LIFT AIRSHIP VEHICLE

BOOK II - APPENDICES TO BOOK I

(NASA-CR-151918) FEASIBILITY STUDY OF MODERN AIRSHIPS, PHASE 2. VOLUME 1: HEAVY LIFT AIRSHIP VEHICLE. BOOK 2: APPENDICES TO BOOK 1 (Goodyear Aerospace Corp.) 142 p HC A07/MF A01 [illegible] N77-[illegible] Unclas [illegible]

GOODYEAR AEROSPACE CORPORATION
AKRON, OHIO

SEPTEMBER 1976

CONTRACT NAS2-8643

PREPARED FOR AMES RESEARCH CENTER
MOFFETT FIELD, CALIFORNIA

NASA CR-151918

FEASIBILITY STUDY OF MODERN AIRSHIPS (PHASE II)

Volume I - Heavy Lift Airship Vehicle

Book II - Appendices to Book I

Contract NAS2-8643
September 1976

Prepared for

Ames Research Center, Moffett Field, California

by

Goodyear Aerospace Corporation, Akron, Ohio

FOREWORD

Goodyear Aerospace Corporation (GAC) under a jointly sponsored NASA/Navy Contract (NAS2-8643) .as conducted a Phase II investigation into the feasibility of modern airships. The Ames Research Center and the Navy Air Development Center were the respective NASA/Navy sponsoring agencies. The Phase II investigation has involved further study of mission/vehicle combinations defined during the Phase I portion of the contract. NASA Contractor Report NASA CR-137692 summarizes the GAC Phase I investigation.

Volume I of the Phase II final report summarizes the work performed relative to a Heavy Lift Airship combining buoyant lift derived from a conventional helium filled airship hull with propulsive lift derived from conventional helicopter rotors. Contract funding for the effort reported in Volume I was $96,000.

Dr. Mark Ardema, the NASA Project Monitor, provided valuable technical guidance and direction to the entire study effort. Mr. Ralph Huston was the GAC Program Manager. Gerald Faurote was the Project Engineer for the Heavy Lift Airship investigation. Other principal personnel included:

Senior Technical Analyst	W. N. Brewer
Engineering Design	N. D. Brown
Control Systems Analyst	D. W. Lichty
Computer Analyst	N. P. Tomlinson

Subcontractors supporting the GAC study team included:

Aerodynamics/Stability & Control
Nielsen Engineering & Research

Institutional/Operational Constraints
Battelle Columbus Laboratories

Helicopter Performance/Operational Data
Piasecki Aircraft Corporation

Other contributors were:

CH-54 Weight, Cost, Performance, and Aerodynamic Characteristics; CH-54B Modification Guidance
Sikorsky Aircraft

Heavy-Lift-Helicopter Fly-By-Wire Technology
General Electric Corporation

Heavy-Lift Helicopter Precision Hover System Technology
Radio Corporation of America

The contractor wishes to acknowledge that NASA Ames Research Center (ARC) provided the use of the ARC 7 x 10-foot Wind Tunnel Facility for the purpose of an exploratory evaluation of the Phase II Heavy Lift Airship.

OVERALL TABLE OF CONTENTS

TABLE OF CONTENTS

REFERENCES

1. Minimum Weight Analysis of Compression Structures; George Gerard; New York University Press 1956

2. Durand, W. F.; Aerodynamic Theory; January 1934

3. Model Specification for U. S. Army CH-54B Helicopter - SER-64279 Rev. 8 dated 26 February 1971

APPENDIX A

OPTIMUM DESIGN OF COMPRESSION STRUTS AND BOX TRUSSES

CONVERSION FACTOR FOR APPENDIX A

t_K	=	$(5/9)(t_F + 459.67)$
1.0 ft	=	3.048×10^{-1} m
1.0 in	=	2.54×10^{-1} m
1.0 sq in	=	6.45×10^{-2} m
1.0 in lb	=	1.152×10^{-1} m kg
1.0 Ksi	=	$6.89 \times 10^{+6}$ N/m^2
1.0 lb	=	4.536×10^{-1} m/s
1.0 lb/sq in	=	$6.89 \times 10^{+3}$ N/m^2
1.0 lb/cu in	=	$2.77 \times 10^{+4}$ kg/cu m

A.1 GENERAL

This Appendix reports details of the in-cial parametric studies of the interconnecting structure. The results of the work reported in this Appendix led to the interconnecting structure finally selected (see Section 5.4 of Book I of this volume of the report).

A.2 OPTIMUM DESIGN OF COMPRESSION STRUTS

As shown by George Girard (Reference 1) and others the optimum stress for a compression strut of uniform, stable, cross section is expressed by:

$$\sigma_0 = \left(\frac{\pi^2 C \rho^2}{A}\right)^{1/2} E_t^{1/2} \left(\frac{P}{L^2}\right)^{1/2}$$

where:

σ_0 is the optimum stress

C is the end fixity coefficient

ρ is the radius of gyration of the cross section

A is the area of the cross section

E_t is the tangent modulus of the material at the stress σ_0

P is the strut load

L is the unsupported length

It will be shown in the following derivations that in general the optimum stress is expressed by:

$$\sigma_0 = K\left(\frac{P}{L^2}\right)^n \qquad \text{(See Figure A.1)}$$

for failure in the elastic range where K is related to the material properties and the strut design, (P/L^2) is the "structural index" and n depends on the strut design and failure mode characteristics.

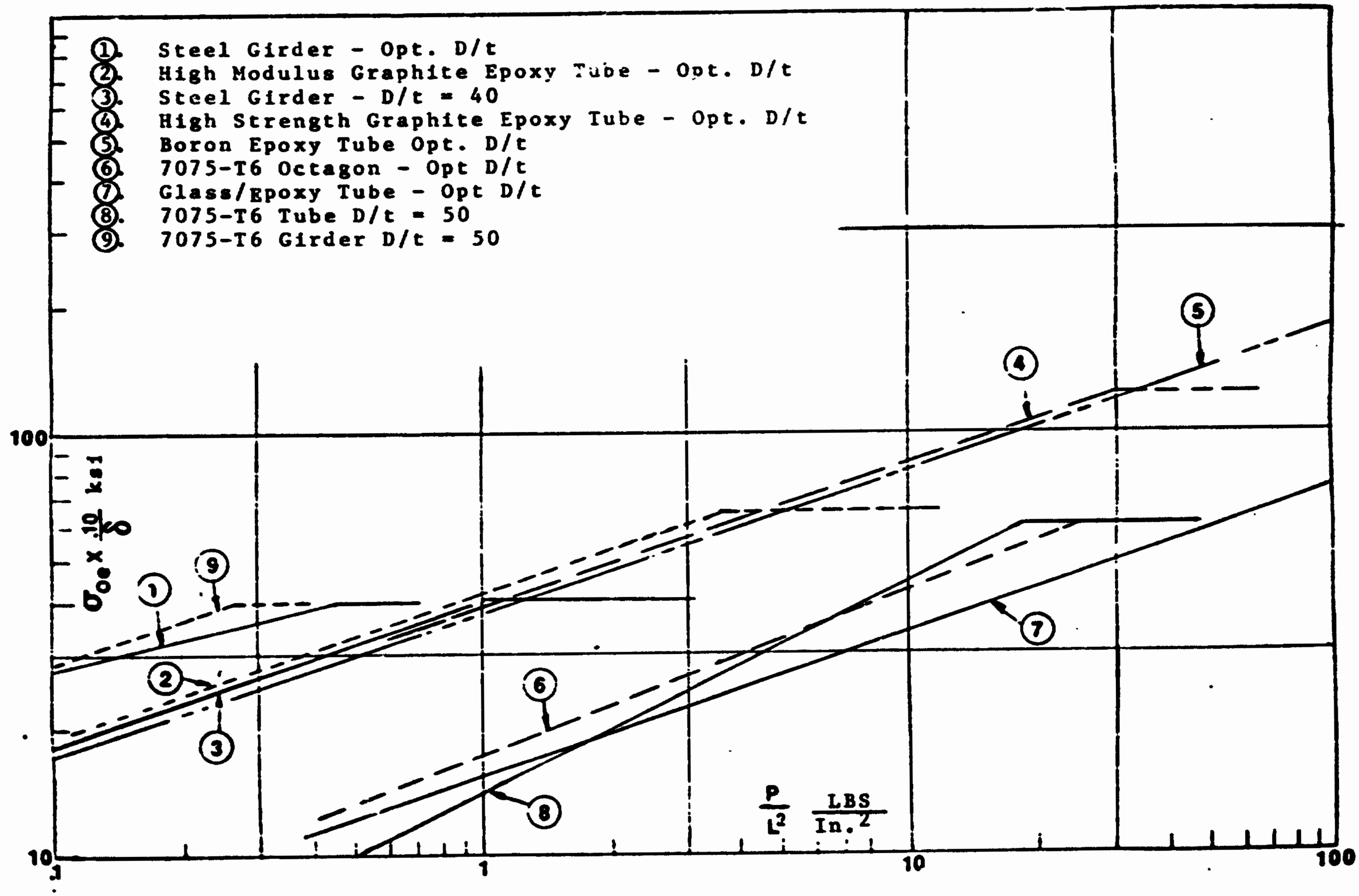

FIGURE A.1 - OPTIMUM DESIGN STRESS - COMPRESSION STRUTS

High values of the structural index produce values of σ_0 [from the above equation] which are greater than the proportional limits of the material. In this case the K value is not a constant but varies with the tangent modulus of the material to some power which also depends on the strut characteristics. The tangent modulus must correspond to the stress σ_0 and the equation for σ_0 is evaluated by choosing values of σ_0, computing K from the tangent modulus at σ_0, solve for P/L^2. This data is then plotted as σ_0 vs P/L^2 from which curve the σ_0 can be read directly for any value of P/L^2. A simple approximation for this behavior can be made by using the elastic characteristics with a cutoff at the yield stress of the material. In all of the following derivations when E appears, it should be interpreted to mean tangent modulus.

A.2.1 Struts with Stable Cross Sections

This class of strut is subject to a single failure mode; long column buckling. Thin tubular struts are typical of this class and exhibit the following characteristics:

$$A = \frac{\pi D^2}{D/t}, \quad I = \frac{\pi D^4}{8D/t}, \quad \frac{\rho^2}{A} = \frac{D/t}{8\pi},$$

$$\sigma_0 = \left(\frac{\pi}{8}\frac{D}{t}\right)^{1/2} E_t^{\,1/2}\left(\frac{P}{L^2}\right)^{1/2}$$

$$A = \frac{P}{\sigma_0} = \frac{LP^{1/2}}{\left[\left(\frac{\pi E}{8}\right)\left(\frac{D}{t}\right)\right]^{1/2}}$$

$$\text{Strut Wt.} = \frac{L \quad P^{1/2}}{(\pi/8\ D/t)^{1/2}} \quad \left(\frac{\delta}{E^{1/2}}\right)$$

For aluminum tubes with $D/t = 50$, $E = 10^7$

$$\sigma_0 = 14{,}000\left(\frac{P}{L^2}\right)^{1/2}$$

Note that the weight is a strong function of the length, a weak function of the load P. Note also that the material factor is $\delta/E^{1/2}$ where δ is the material density.

A.2.2 Thin Walled Tubes Subject to Local Buckling

The local buckling stress for a thin walled circular tube can be taken as:

$$\sigma_{cr} = .25E\,\frac{t}{R} = \frac{.50E}{D/t}$$

The long column buckling characteristic is:

$$\sigma_{col} = \frac{\pi^2 E}{8\,(L/D)^2}$$

The applied stress is

$$\sigma = \frac{P}{\pi D t}$$

Gerard [Reference 1] argues that the optimum design occurs when:

$$\sigma = \sigma_{cr} = \sigma_{col}$$

From which:

$$\sigma_0 = \left(\frac{\pi}{16}\right)^{1/3} E^{2/3} \left(\frac{P}{L^2}\right)^{1/3}$$

with L/D and D/t set at the optimum ratios of:

$$(L/D)_{opt} = \left(\frac{\pi^2 E}{8\sigma_0}\right)^{1/2}$$

$$(D/t)_{opt} = \frac{1}{2}\ \frac{E}{\sigma_0}$$

For $E = 10^7 \quad \sigma_0 = 27{,}000\left(\frac{P}{L^2}\right)^{1/3}$

Note that K has changed from 14,000 for the stable cross section to 27,000 for D/t set high enough to produce simultaneous local and long column buckling. Note also that $n = \frac{1}{3}$ instead of $\frac{1}{2}$ for the stable cross section case.

A.2.3 Three Boom Girders Constructed from Thin Walled Tubes

The girder is envisioned to be similar to the classic rigid airship design with the three booms placed at the corners of an equilateral triangle. The lattice tubes are arranged in a warren truss pattern forming equilateral triangles in the three side planes.

Three modes of failure are possible: local buckling of boom tubes, short column buckling of boom tubes, and long column buckling of the girder.

Let b = girder cross section dimension from center to center of booms

L = girder unsupported length

D = boom tube diameter

t = boom tube thickness

For convenience the lattice tubes are assumed to be of one-half the diameter of the boom tubes and the same D/t. This produces a "Ginger Bread Factor" of 1.50. This means that the weight of the complete girder is 1.5 times the weight of the booms, alternately the "effective" optimum stress σ_{0e} is $\frac{2}{3}$ the actual working stress in the booms.

Setting the L/b and D/t ratios to produce simultaneous buckling in the three modes yields:

$$\sigma_{0e} = \frac{1}{9} \left(\frac{3\pi E}{2} \right)^{3/4} \left(\frac{P}{L^2} \right)^{1/4}$$

where L/b and D/t are optimum at

$$(L/b)_{opt} = \frac{\pi}{3} \left(\frac{E}{\sigma_{0e}} \right)^{1/2}$$

$$(D/t)_{opt} = \frac{1}{3} \frac{E}{\sigma_{0e}}$$

For $E = 10^7 \quad \sigma_{0e} = 63{,}300 \left(\frac{P}{L^2} \right)^{1/4}$

$E = 3 \times 10^7 \quad \sigma_{0e} = 144{,}000 \left(\frac{P}{L^2} \right)^{1/4}$

A.2.4 <u>Three Boom Girders - Stable Cross Section Tubes</u>

If the D/t of the tubes is arbitrarily assigned a value less than that required to prevent local buckling the character of the optimum design becomes:

$$\sigma_{0e} = \frac{\pi}{18} (9E^2)^{1/3} \left(\frac{D}{t}\right)^{1/3} \left(\frac{P}{L^2}\right)^{1/3}$$

where the cross sectional dimensions are optimum at:

$$b_{opt} = \frac{L}{\frac{\pi}{3}\left(\frac{E}{\sigma_{0e}}\right)^{1/2}}$$

$$D_{opt} = \frac{L}{\frac{\pi^2}{12}\left(\frac{E}{\sigma_{0e}}\right)}$$

$$t_{opt} = \frac{D_{opt}}{D/t}$$

In the above, D/t is arbitrary but not more than:

$$(D/t)_{max} = \frac{1}{3} \frac{E}{\sigma_{0e}}$$

This configuration is of particular interest using HP9420 steel tubes which are assembled by welding with a yield stress of 180,000 psi after welding with no subsequent heat treatment.

$$D/t = 40 \quad \sigma_{0e} = 120{,}000\left(\frac{P}{L^2}\right)^{1/3}$$

$$D/t = 50 \quad \sigma_{0e} = 129{,}000\left(\frac{P}{L^2}\right)^{1/3}$$

A.2.5 Fiber Reinforced Epoxy Tubes

Several combinations are considered. In every case the tubes are proportioned such that local buckling and long column buckling occur simultaneously. Multiple layers are assumed in an isotrophic pattern so that homogeneous properties are appropriate. The local buckling failure is taken conservatively at:

$$\sigma_{cr} = .2E\frac{t}{R}$$

$$\sigma_0 = \left(\frac{.2\pi}{4}\right)^{1/3} E^{2/3}\left(\frac{P}{L^2}\right)^{1/3},$$

$$K = .53956\ E^{2/3}$$

$$V_F = \text{Fiber Volumeric Fraction}$$

Properties of candidate composite materials are given in Table A.1.

Table A.1 - Composite Properties

Composite	Boron Epoxy	GRAPHITE/EPOXY High Strength	GRAPHITE/EPOXY High Modulus	Glass Epoxy
V_F	.50	.60	.60	.60
F_{CU} (KSI)	135	69	38	60
E ($X10^{-6}$)	11.44	8.09	9.42	3.0
K (KSI)	27.394	21.744	24.066	11.223
Density, δ, #/In^3	.0725	.056	.058	.072
K/δ [Inches]	377,848	388,286	414,931	155,875
F_{cu}/δ [Inches]	1,862,000	1,232,000	655,000	833,000

A.2.6 Fabricated Octagon

Design studies on the H frame using extruded aluminum alloy tubes of circular or octagon cross section revealed a fabrication problem. Optimum design proportions indicated D/t values of 60 or more are necessary to achieve minimum weight. The loads involved in the heavy lifter H frame require sections of 10 inches or more in diameter. The largest extrusion presses available are not capable of extruding these large sections in high strength alloys with the high D/t ratios required.

The octagon section [Figure A.2] fabricated from sheet [plate] stock of high strength alloys was investigated as an alternate approach which permits control over the D/t ratio to create the desired value. In this design the optimum stress is

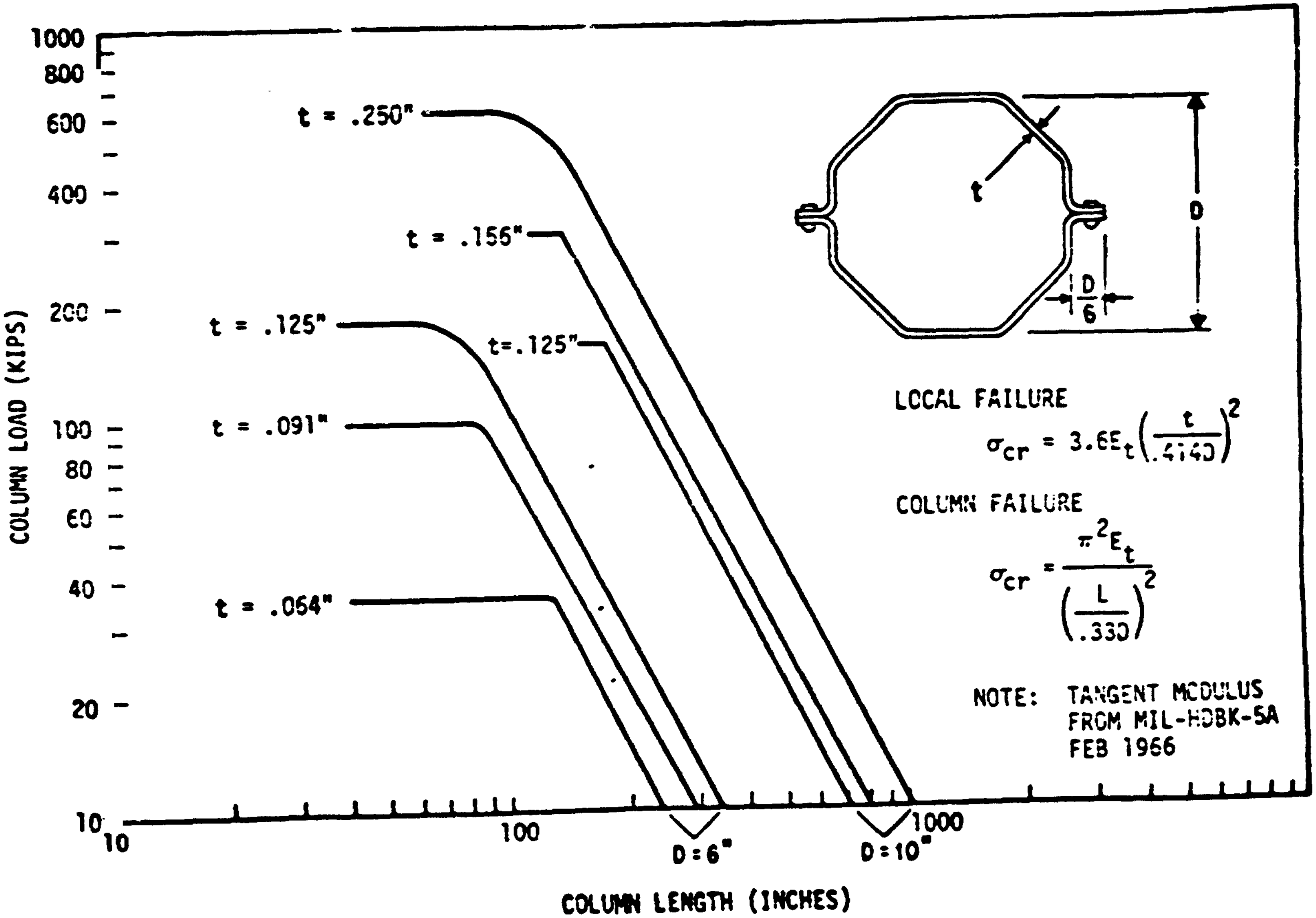

FIGURE A.2 - COLUMN STRENGTH - OCTAGONS, 7075-T6 ALCLAD again derived by establishing proportions which result in simultaneous buckling locally and as a long column.

$$A = 3.98\ Dt, \quad \rho = .33D$$

$$\sigma_{cr} = 3.6E\left(\frac{t}{.414D}\right)^2$$

$$\sigma_{col} = \frac{\pi^2 E}{\left(\frac{L}{.33D}\right)^2}$$

$$\sigma = \frac{P}{3.98Dt}$$

with P, L and E given, and $\sigma = \sigma_{cr} = \sigma_{col}$

$$\sigma_0 = 1.089E^{.6}\left(\frac{P}{L^2}\right)^{.4}$$

$$(L/D)_{opt} = .33\pi\left(\frac{E}{\sigma_0}\right)^{1/2}$$

$$(D/t)_{opt} = 4.583\left(\frac{E}{\sigma_0}\right)^{1/2}$$

Taking $E = 10^7$, $\sigma_0 = 17{,}250\left(\frac{P}{L^2}\right)^{.4}$

The above deviation for the fabricated octagon presumes that the column curve for sections of this type can be represented by a tangent modulus long column curve with a cutoff at the local buckling stress. In order to verify this presumption a series of test specimens was fabricated from bare 7075T6 material and tested. This data and analysis is presented in Section A.4 of this Appendix.

A.3 BOX TRUSSES IN BENDING AND TORSION

The initial estimate of the strength requirements for the keel of the H Frame, see Figure A.3, was based on a maximum limit rotor thrust equal to 3 g's based on the normal gross weight of a CH54B helicopter. It was further assumed that two diagonally opposite helicopters would tug against a payload with the other two helicopters dead. This assumed condition [later found to be much too conservative] creates a torsional strength requirement of the keel on the order of 150×10^6 inch pounds combined with a less demanding bending moment and direct shear.

Numerous design approaches for the keel beam were evaluated including typical airplane fuselage construction, rectangular and circular sandwich shells, and box trusses with rigid bracing as well as cable [or wire] braced box beams. As a result of these studies the box truss was judged to be the most suitable construction for the keel member for minimum weight, simplicity of construction and relative ease of adaptability toward providing strong points for attachment of payload slings, suspension cables, tie down cables, etc. In general, the rigidly braced [X pattern] box beams with secondary bracing to the compression booms provided the least weight design with optimum depths on the order of 16' → 25' depending on the specific configuration.

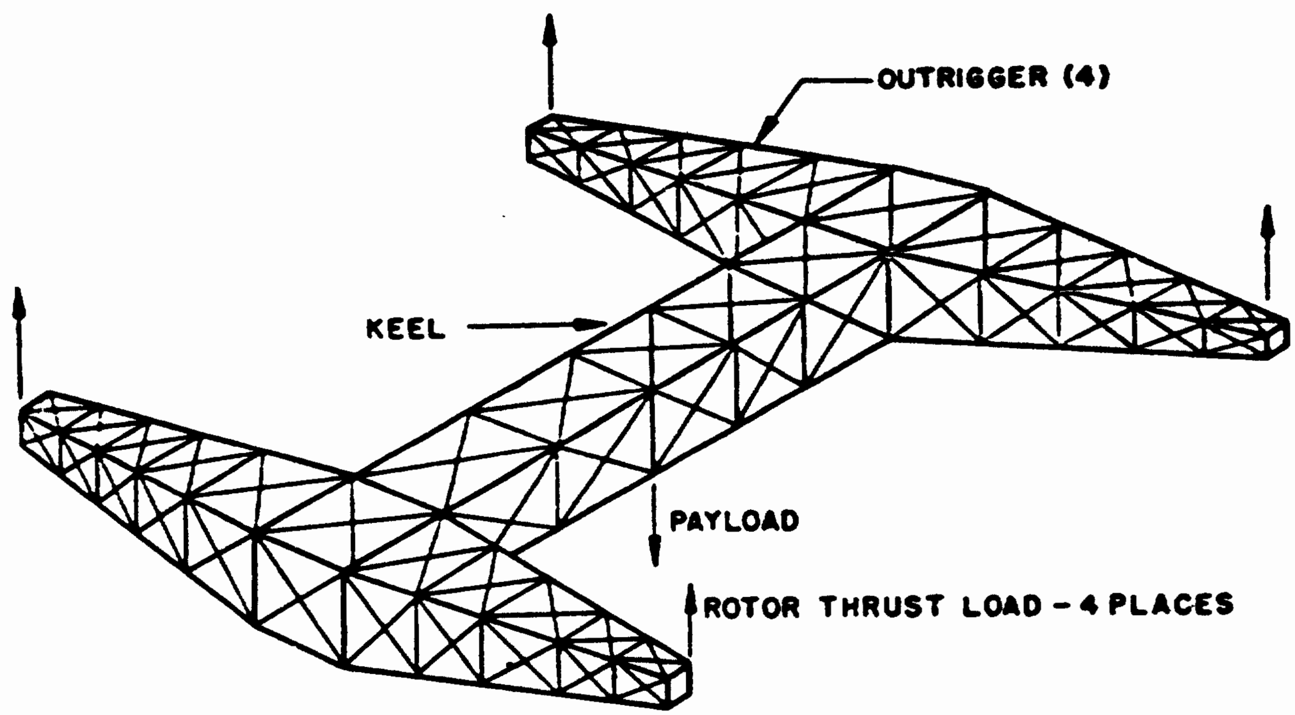

- HELICOPTER LOADS (ONE ENGINE OUT) DICTATE OVERALL STRUCTURAL REQUIREMENTS
- MATERIAL: 7050 T76 ALUMINUM ALLOY

FIGURE A.5 - H-FRAME - KEEL/OUTRIGGER INTERCONNECTING STRUCTURE

Several interesting results were developed during these design studies. The most interesting results are most easily illustrated by the optimum design characteristics of the cable braced box beam.

The type of construction being considered and the principle results are illustrated in Figure A.4 .

Observe that the "doodle box" beam is defined to present square surface panels with 45° bracing so that longitudinal and transverse struts are of equal lengths. In the pure torsion condition all cables [one set] are equally loaded and all struts are equally loaded.

b	=	diameter of inscribed circle
N	=	number of sides
T	=	Torsional moment inch lbs
P	=	strut compression - lbs
L	=	strut length - inches
n & K		are from the optimum stress eq. $\sigma_0 = K\,(P/L^2)^n$ of Section A.2.
$(\sigma/\delta)_c$		is the strength weight ratio of the cables
W_s		is the weight of the struts per inch of beam length
W_c		is the weight of the cables per inch of beam length

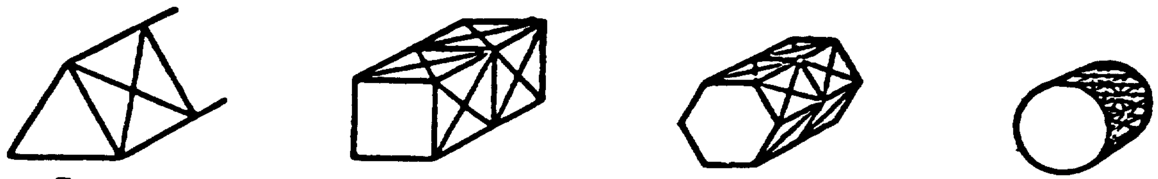

N 3 4 6 ∞

b IS DIA OF INSCRIBED CIRCLE

$$P/L^2 = \frac{2T}{b^3\ N\tan^2\left(\frac{\pi}{N}\right)}$$

$$W_s = \frac{(2)^{2-n}\ N^n\ T^{1-n}\ b^{3n-1}\left(\tan\frac{\pi}{N}\right)^{2n}}{(K/\delta)_s}, \qquad W_c = \frac{8T}{b(\sigma/\delta)_c}$$

$$b_{opt} = \left(\frac{(2)^{n+1}R}{3n-1}\right)^{1/3n} \cdot \left(\frac{T}{N\tan^2\left(\frac{\pi}{N}\right)}\right)^{1/3}, \qquad R = \frac{(K/\delta)_s}{(\sigma/\delta)_c}$$

$$W_B = \left(\frac{(2)^{\frac{8n-1}{3n}} \times 3n}{(3n-1)^{\frac{3n-1}{3n}}}\right)\left(\frac{\left(N\tan^2\left(\frac{\pi}{N}\right)\right)^{1/3} T^{2/3}}{\left(\frac{\sigma}{\delta}\right)_c^{\frac{3n-1}{3n}} \left(\frac{K}{\delta}\right)_s^{1/3n}}\right)$$

FIGURE A.4 - N-SIDED DOODLE BOX TRUSS - PURE TORSION

In Figure A.4, note that the weight of the struts [W_s] can increase with "b", decrease as "b" increases or remain constant as "b" changes depending on the value of "n". The cable weight is inversely proportional to "b".

The W_s expression is based on elastic action of the struts and is subject to two limitations:

1) σ_0 must not exceed the yield cutoff stress σ^* on the one extreme and

2) Minimum gage limitations must not be exceeded.

When $n > \frac{1}{3}$ an optimum diameter "b" can be calculated from the equation and may or may not fall within the elastic range on the struts. Within these limitations, the optimum weight equation applies for cases where $n > \frac{1}{3}$.

An interesting case is $n = \frac{1}{3}$. The strut weight is independent of the choice of "b" subject to the elastic limitations which requires that b be greater than the minimum shown.

As b increases such that b becomes much larger than the minimum, the optimum strut stress decreases and the overall weight goes down due to decreasing cable weight. This characteristic drives the diameter into the very large range area and will eventually face minimum gage limitations. Note that the strut weight is independent of the strength/weight ratio of the strut material and the trend for minimum weight is toward low stresses in the struts.

The ratio [K/δ] is the parameter of significance. Further exploration in the area is illustrated in Figure A.5 where the number of sides N is introduced as a open parameter along with "b".

This procedure results in a minimum weight curve:

$$W_b = \frac{T}{b}\left\{4\,\frac{\delta_s}{\sigma^*} + 8\,\frac{\delta_c}{\sigma_c}\right\}$$

in which case N is chosen to create a yield limited condition $\sigma_0 = \sigma^*$

$$N \tan^2\left(\frac{\pi}{N}\right) = \left(\frac{K}{b\sigma^*}\right)^3 \quad (2T)$$

The significance of this result lies in the fact that the minimum weight structure is now clearly a direct reflection of the strength/weight ratio of the materials independent of Youngs modulus except for the appropriate value of N to use. It is precisely the strength/weight ratio of the materials which have been greatly improved with the development of new exotic materials. This result therefore suggests that great improvements in structural efficiency can be realized by the proper application of new materials.

Extension of this analysis to the case of shear and bending provides a similar result:

$$W_B = \frac{2M}{D_0}\left[4\left(\frac{\delta}{\sigma^*}\right)_s + 8\left(\frac{\delta}{\sigma}\right)_c\right]$$

where:

$$D_0 = \frac{2M}{V} \quad \text{and} \quad N = \left(\frac{\sigma^*}{K}\right)^{1/n}\left(\frac{2\pi^2 M^2}{V^3}\right)$$

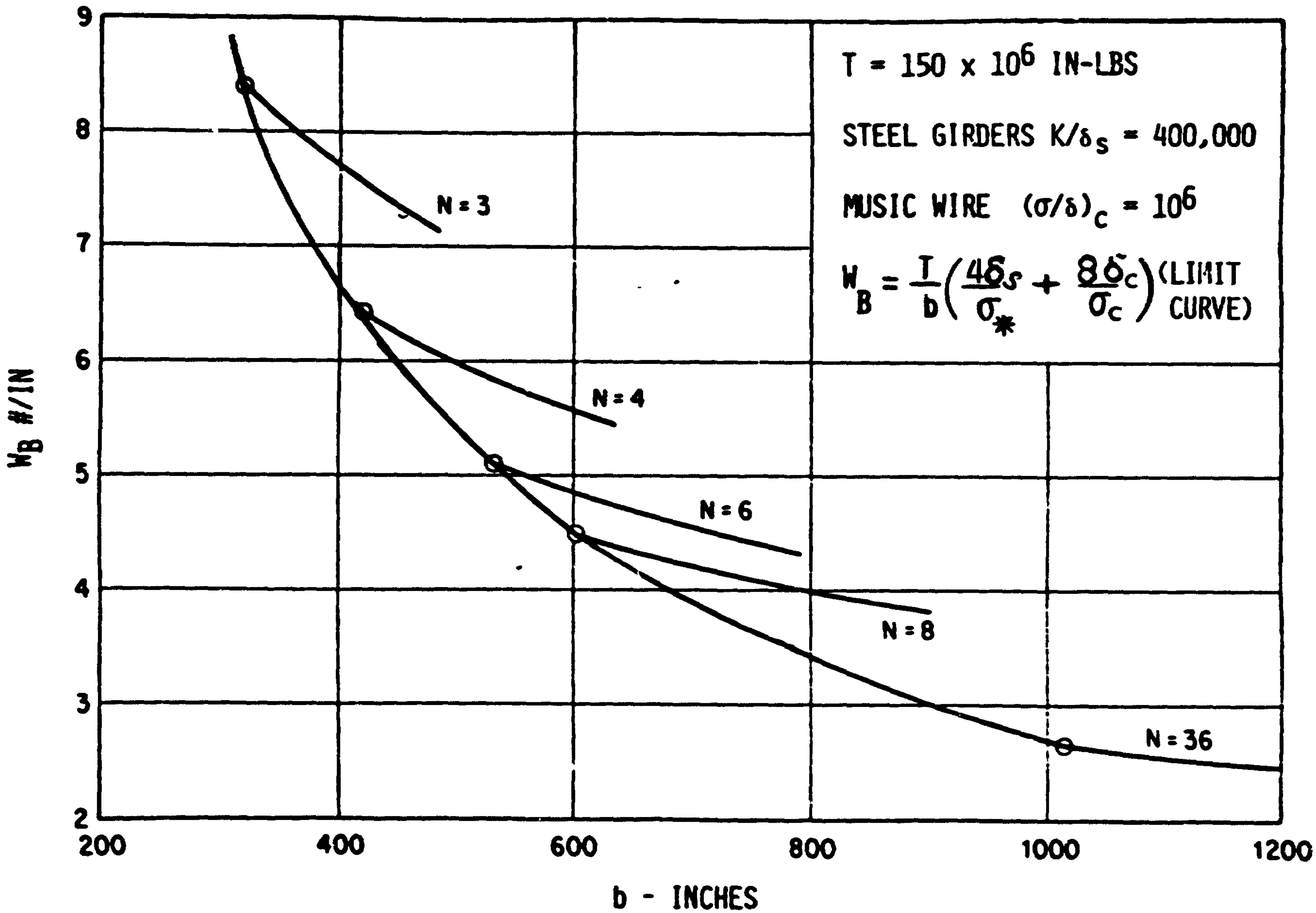

FIGURE A.5 MINIMUM WEIGHT - DOODLEBOX TRUSS - PURE TORSION

D_0 is the optimum diameter, M the design bending moment and V the design shear force. Bending and shear may be applied in any direction to the cross section.

A.4 EVALUATION OF OCTAGONAL COLUMNS

A.4.1 Introduction

Structural members having an octagonal cross-section are being considered for the HLA. The strength of these members has been computed on the assumption that local and general instability depend upon the tangent modulus of the material and that there is no interaction between the two modes of failure. Tests of octagonal sections were made and the results compared to the predicted values.

A.4.1 Theory

A.4.2.1 Section Properties

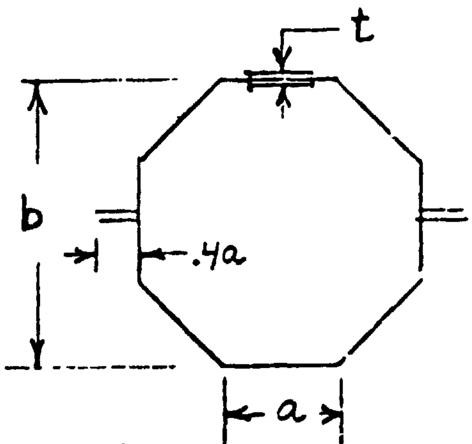

$$a = b \tan\frac{\pi}{8} = 0.4142\ b \qquad \text{Eq. 1}$$

$$A = 9.6\ a\ t \quad \text{in.}^2 \qquad \text{Eq. 2}$$

$$= 3.976\ bt$$

$$I = a^3 t \left[\frac{1}{3} + \frac{1}{\tan^2 \pi/8}\right] = 6.1618\ a^3 t \qquad \text{Eq. 3}$$

$$= 0.4379\ b^3 t$$

$$\rho = 0.3319\ b \qquad \text{Eq. 4}$$

A.4.2.2 Tangent Modulus E_t

The tangent modulus in terms of the Ramburg-Osgood parameters is given by

$$E_t = \frac{E}{1 + \frac{3}{7} n \left(\frac{\sigma}{F_{0.7}}\right)^{n-1}} \qquad \text{Eq. 5}$$

A.4.2.3 General Instability σ_{col}

$$\sigma_{col} = \frac{\pi^2 E_t \rho^2}{L^2} \qquad \text{Eq. 6}$$

$$\sigma_{col} \left[1 + \frac{3}{7} n \quad \frac{\sigma_{col}}{F_{0.7}}^{n-1}\right] = \frac{\pi E \rho^2}{L^2}$$

A.4.2.4 Local Instability

$$\sigma_{LOC} = 3.6 E_t \left(\frac{t}{a}\right)^2 \qquad \text{Eq. 7}$$

$$\sigma_{LOC} \left[1 + \frac{3}{7} n \quad \frac{\sigma_{LOC}}{F_{0.7}}^{n-1}\right] = 3.6 E \left(\frac{t}{a}\right)^2$$

A.4.2.5 Section Crippling σ_{cc}

If the section consisted of 8 identical sides, which could be the case with an extrusion, then the local instability stress is also the section crippling stress.

If the elements of the section are not the same then it is assumed that each section will carry a load consistent with its local instability and the section crippling stress is a weighted average.

$$\sigma_{cc} = \frac{\Sigma_{i=1} A_N \, \sigma_{LOC_N}}{\Sigma_1^N \, A_N} \qquad \text{Eq. 8}$$

For the test specimen it is assumed the six plain sides buckle at a stress σ_{LOC_1} based on t/a. For the other two sides plus the flanges the buckling stress σ_{LOC_2} is based upon 2t/a. The section crippling stress is then given by

$$\sigma_{cc} = \frac{3.6 \, \sigma_{LOC_2} + 6 \, \sigma_{LOC_1}}{9.6} \qquad \text{Eq. 9}$$

A.4.2.6 Initial Eccentricity

If a column has an initial eccentricity, y_o, at no load, the deflection will increase to y_T when an axial load is applied. A good approximation for the deflection is given by

$$y_T = \frac{y_o}{1 - P/P_{col}} \qquad \text{Eq. 10}$$

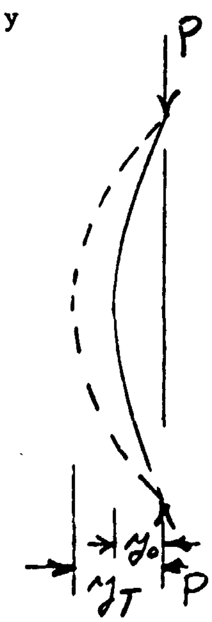

The maximum compression stress in the section is given by

$$f = \frac{P}{A} + \frac{P y_T \; c}{I}$$

$$= \frac{P}{A} \left(1 + \frac{y_T b}{2\rho^2}\right)$$

$$= \frac{P}{A} \left[1 + \frac{y_o \; b}{2 \; \rho^2 \; (1 - P/P_{col}}\right]$$

$$f = \sigma \; \left[1 + \frac{y_o b}{2\rho^2 \; \left(1 - \frac{\sigma}{\sigma_{COL}}\right)}\right. \qquad \text{Eq. 11}$$

The failing stress is the local instability of flat element as given by Equation 7. Letting σ_F denote the failing P/A stress then

$$\sigma_F \; \left[1 + \frac{y_o b}{2\rho^2 \; (1 - \sigma_F/\sigma_{COL})}\right] = \sigma_{LOC} \qquad \text{Eq. 12}$$

A.4.2.7 Transverse Test Displacement

Let y_o be the initial displacement as before. If an axial load is applied the measured transverse deflection is y and the total deflection y_T. Equation 10 again applies except now we separate y_T into two parts, thus

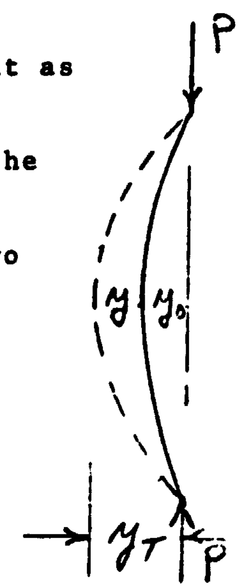

$$y + y_o = \frac{y_o}{1 - P/P_{cr}}$$

This equation can be manipulated to the following form

$$P = P_{cr} - y_o \frac{P}{y} \qquad \text{Eq. 13}$$

which is a straight line when P is plotted versus P/y. The intercept at the ordinate is P_{cr} and the slope of the curve is the initial displacement.

A.4.3 Test Program

A.4.3.1 Specimen

The specimens were fabricated from 7075-T6 bare sheet. They were formed in two halves and riveted together along the flange. The ends were machined square and parallel.

A.4.3.2 Test Setup and Procedure

The tests were run in the Baldwin Universal test machine. The specimen was loaded through a hemisphere of hardened steel at each end. Centering stops were attached to the flat side of the hemisphere to ensure that the specimen centroid coincided with the centers of the hemispheres. A level was used to check that the specimen was vertical.

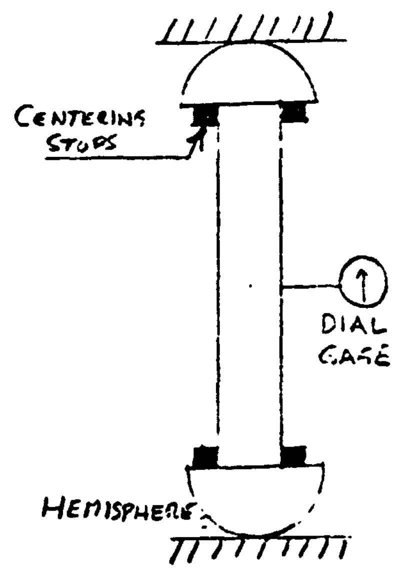

For the long specimen a dial gage was mounted at the midpoint of the specimen to measure the transverse deflection. For the shorter specimen only the head travel or axial deflection was measured. In either case the machine operator would call out at predetermined load increments and another operator would record the deflection.

Dimensions of each specimen and their weight were also recorded. Table A.2 contains the dimensions, weight, and maximum compression load for each specimen. Table A.3 shows the load-vertical deflection data for the short specimen. Table A.4 shows the load-transverse deflection data for the long specimen.

The maximum stress for each specimen was determined as follows. The length and weight of the specimen was used to calculate the cross-sectional area assuming a material density of 0.101 pci. The maximum load was then divided by the area to obtain the maximum stress. These data are shown in Table A.5.

Table A.5 Compression Test Results

Spec. No.	t IN.	L IN.	W	A $IN.^2$	P_{MAX} LBS	σ_{MAX} PSI
1	0.052	15	414.8 gr	0.6036	39,400	65,274
2	0.052	15	415.6	0.6048	39,200	64,818
3	0.034	15.125	261.8	0.3778	16,300	43,143
4	0.0335	15.125	259.8	0.3749	15,850	42,275
5	0.034	15.125	261.2	0.3769	16,350	43,374
6	0.052	25	690.4	0.6028	38,300	63,538
7	0.052	25	693.7	0.6057	38,600	63,731
8	0.052	35	969.0	0.6043	37,600	62,220
9	0.052	34	943.9	0.6060	35,700	58,913
10	0.051/0.052	40	1105.7	0.6034	33,600	55,687
11	0.052	40	1104.5	0.6027	31,000	51,434
12	0.052/0.051	45	1237.3 gr	0.6002	29,150	48,567
13	0.0515/ 0.052	45	2.76 lb	0.6073	29,700	48,908
14	0.051/ 0.0515	75	4.52	0.5967	10,200	17,094
15	0.052	75	4.55 lb	0.6007	10,500	17,481

$\gamma = 0.101$ PCI $\qquad A = \dfrac{W}{L\gamma}$ or $\dfrac{W}{453.6\ \gamma\ L}$

Table A.2 Octagon Dimensions, Weight, and Maximum Compression Load Data

GOODYEAR AEROSPACE
CORPORATION

DEPARTMENT 450
PHYSICAL TEST LABORATORY

TYPE OF TESTS COMPRESSION R&D 988118 FOR G. FAUROTE

MAT'L & TYPE OF SPECIMENS RIVETED ALUM. TUBES DATE REC'D 12-4-75

SPECIMEN NO	DIMENSION	AREA	YIELD LOAD	ULTIMATE LOAD	YIELD PSI	ULTIMATE PSI	ELONGATION PER CENT	OTHER		
		AVG.	ULT.	WIDTH		DIMEN		SIONS-AVG.		
	LENGTH IN.	THK.	LOAD	A		B		C	D	WEIGHT
1	15.0	.052	39,400	2.996		2.977		3.027	3.039	414.8 gr.
2	15.0	.052	39,200	3.003		3.034		3.009	3.004	415.6 gr.
3	15.1	.034	16,300	3.085		3.059		2.962	2.932	261.8 gr.
4	15.1	.0335	15,350	3.071		2.979		2.963	3.011	259.8 gr.
5	15.1	.034	16,350	3.004		3.025		3.027	3.009	261.2 gr.
6	25	.052	39,300	2.979		3.006		3.020	3.027	690.4 gr.
7	25	.052	39,600	2.968		2.979		3.037	3.039	693.7 gr.
8	35	.052	37,600	2.970		3.014		3.033	3.003	969.0 gr.
9	~~35~~ 34	.052	35,700	2.972		2.996		3.001	2.996	943.9 gr.
10	40	.0515	33,600	2.988		3.022		3.042	3.023	1105.7 gr.
11	40	.052	31,000	2.975		3.005		3.062	3.060	1104.5 gr.
12	45	.0515	29,150	2.988		2.970		3.023	3.033	1237.3 gr. 2.74 LB.
13	45	.0515	29,700	2.997		3.021		3.034	3.049	2.76 LB.
14	75	.0515	10,200	2.944		3.012		3.084	3.052	4.52 LB.
15	75	.052	10,500	2.964		2.997		3.072	3.064	4.55 LB.

IDENTITY NO. POINTING DOWN

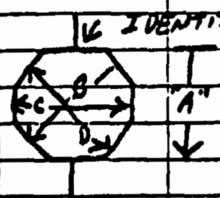

"A"

A, B, C & D ARE OUTSIDE DIMENSIONS.

THK. @ EACH END ON "C" DIRECTION.
LENGTH ON "C" DIRECTION SIDES.

REMARKS TEST @ ROOM TEMP. APPROX. 71°F.
LOAD RATE APPROX. 3 MINUTES TO FAILURE.

WITNESSES

TESTED BY J. Snider R. V. Dalwell DATE 12-5-75 TO 12-8-75

Table A.3 Load - Vertical Deflection Data

PHYSICAL TEST LAB
DEPARTMENT 486

TYPE OF TEST Compression w/Hemispheres. **DATE** 12-5-75 & 12-8-75

MATERIAL 7075-T6 Alum. **BY** J.B. R.

FOR G. Fairote

VERTICAL. DEFLECTION - INCHES

LOAD LBS.	34" L.			1000 lb. increments. (Specimen Number)			2000 lb. increments.			
	No. 9	7	6	5	4	3	2	1		
200	[illegible]	[illegible]	[illegible]	[illegible]	[illegible]	[illegible]	[illegible]	[illegible]		
2000	.017	.014	.0155	1 .0055	.006	.0065	.009	.011		
4	.033	.027	.0285	2 .012	.0125	.014	.0185	.020		
6	.048	.039	.040	3 .018	.019	.020	.027	.029		
8	.061	.050	.052	4 .0245	.025	.0265	.0345	.036		
10,000	.075	.061	.063	5 .0305	.031	.0325	.043	.0435		
12	.088	.072	.074	6 .036	.0365	.038	.0505	.0515		
14	.101	.0825	.085	7 .042	.042	.044	.058	.059		
16	.114	.093	.095	8 .047	.047	.0495	.0655	.0665		
18	.127	.103	.105	9 .053	.053	.055	.0725	.0735		
20,000	.140	.1135	.1155	10 .059	.0585	.061	.0795	.080		
22	.153	.124	.1255	11 .064	.064	.067	.087	.0875		
24	.166	.1345	.136	12 .070	.071	.0745	.094	.094		
26	.179	.145	.146	13 .0785	.079	.082	.101	.101		
28	.192	.156	.156	14 .087	.088	.0905	.1085	.1085		
30,000	.206	.167	.167	15 .0955	.0965	.099	.1155	.1155		
32	.219	.1785	.177	16 .106	.1055	.1085	.123	.1225		
34	.233	.191	.1875	.112 @	.116 @	.112 @	.130	.130		
36	.246 @	.203	.198	16,350 lb	15,850 lb	16,300 lb	.137	.137		
38	35,200 lb	.216	.210 @				.145	.144		
40,000		.220 @	38,300 lb				.150 @	.151 @		
		38,600					39,200 lb.	39,400 lb.		

ORIGINAL PAGE IS

Table A.4 Load - Transaverse Deflection Data

PHYSICAL TEST LAB
DEPARTMENT 486

TYPE OF TEST Compression w/Hemispheres DATE 12-5-75

MATERIAL 7075-T6 Alum. BY JS. RH

FOR G. Faurote

Sidewise. DEFLECTION - INCHES

LOAD LBS.	Specimen Number								
	No. 15	No. 14	Load	No. 13	No. 12	No. 11	No. 10	No. 8		
500	[illegible]	[illegible]	[illegible]	[illegible]	[illegible]	[illegible]	[illegible]	[illegible]		
1000	.5045	.501	2	.502	.504	.494	.5005	.503		
2000	.5125	.505	4	.5045	.509	.487	.501	.506		
3000	.521	.510	6	.507	.514	.480	.502	.5085		
4000	.5315	.5155	8	.509	.5195	.473	.502	.5115		
5000	.543	.523	10	.5115	.525	.466	.5025	.5145		
6000	.5565	.534	12	.5135	.531	.458	.503	.5175		
7000	.576	.551	14	.515	.537	.449	.5035	.5205		
8000	.605	.584	16	.516	.544	.440	.5035	.523		
9000	.661	.662	18	.5165	.552	.429	.503	.525		
10000	.845	1.120	20	.516	.562	.417	.5025	.5275		
11000	1.880		22	.513	.573	.402	.501	.5295		
12000			24	.506	.591	.384	.4985	.5315		
			26	.490	.619	.361	.4945	.533		
	ULT. 10,500	ULT. 10,300	28	.448	.682	.327	.488	.5345		
			30			.270	.476	.5355		
						.100 @	.449	.5355		
				ULT. 29,700	ULT. 29,150	31,000 LB.	.375 @	.534		
							33,600 LB.	.527		
								.500		
								37,600 LB.		

A.4.4 Predicted Values

A.4.4.1 Typical Sections

The dimensional data shown in Table A.2 was averaged to determine the typical cross section to be used in the calculations. The pertinent section properties are shown below in Table A.6.

Table A.6 Typical Section Properties

t	in.	0.052	0.034
b_{ave}	in.	2.957	2.991
A	in.^{2}	0.6113	0.4043
ρ		0.9893	0.9846
t/a		0.0425	0.0274

A typical stress-strain curve for 7075-T6 bare sheet is not available. In Bruhn's "Analysis and Design of Flight Vehicle Structures", the Romberg-Osgood parameters are given for many materials. The values of 7075-T6 bare sheet and extrusions are shown in Table A.7. The calculations were carried out using both sets of values so that the sensitivity of the predicted values to the shape of the stress-strain curve could be determined.

Table A.7 Romburg-Osgood Parameters

Item	Bare Sheet	Extrusion
E_c	10.5×10^6	10.5×10^6
$F_{0.7}$	70,000	72,000
n	9.42	16.6

A.4.4.2 General Instability

Equation 6 was used to calculate the stress, σ_{col}, for general instability. The section properties of Table A.6 for the sheet thickness of 0.052 were used along with the above Romburg-Osgood parameters. The results are shown in Table A.8. The column labeled R.S. is the value of the right side of Equation 6. The equation was solved by trial and error using the criteria that the absolute value of the difference between the left and right sides of Equation 6 be less than 10.

Table A.8 Calculated General Instability

Length In.	R.S.	σ_{COL} - PSI	
		Bare Sheet	Extrusion
100	10,143	10,140	10,143
80	15,848	15,845	15,848
75	18,032	18,030	18,031
60	28,175	28,120	28,175
50	40,572	39,330	40,536
40	63,393	50,455	55,846
35	82,800	54,772	59,734
30	112,700	58,719	62,591
25	162,288	62,665	65,138
15	450,800	72,287	70,717

A.4.4.3 Local Instability and Section Crippling

Equation 7 was used to calculate the stress σ_{LOC} for local instability. The section properties of Table A.6 and the material parameters of Table A.7 were used in the calculations. The values of σ_{LOC} were then used to compute the crippling stress, σ_{cc}, according to Equation 9. The results of these calculations are shown in Table A.9.

Table A.9 Calculated Local and Crippling Stresses

t	t/e	R.S.	Type Instability	Stress - PSI	
				Bare Sheet	Extrustion
0.052	0.0425 0.0850 x	68,276 273,104 x	Local Local Crippling	51,875 67,670 57,798	57,162 68,135 61,277
0.034	0.0274 0.0548 x	28,379 113,516 x	Local Local Crippling	28,330 58,803 39,767	28,375 62,648 41,227

A.4.4.4 Initial Eccentricity

The effect of initial eccentricity on the failing stress was determined for one case, the 0.052 thick section was an initial eccentricity of 0.1 inch. Equation 12 was used to determine the failing stress, σ_F. The values of b and ρ are from Table A.6, σ_{COL} from Table A.8 and σ_{LOC} from Table A.9. The results of these calculations are shown in Table A.10.

Table A.10 Calculated Failing Stress for Initial Eccentricity of 0.1

L	σ_{COL}	σ_{LOC}	σ_F
100	10,143	57,162	9,822
80	15,848		14,990
75	18,031		16,880
60	28,175		24,870
50	40,536	57,162	32,438

A.4.5 Discussion of Results

A.4.5.1 Stress-Strain Curves

The calculated stress-strain curves using the Romburg-Osgood parameters of Table A.7 are shown in Figure A.6. These will be useful if actual stress-strain curves for the material used to make the specimen are obtained.

It should be noted that the following discussions are made without benefit of actual material properties. It would be desirable to apply material correction to the test data.

A.4,5.2 General Instability

The calculated values of σ_{COL} from Table A.8 are plotted in Figure A.7 versus the column length. For column lengths greater than 60 inches there is virtually no difference between bare sheet and extrusion. The extrusion gives higher values than the bare sheet except for lengths less than 20 inches. The maximum difference bwtween the two curves is about 5,000 PSI at a length near 35 inches.

The test points for the 0.052 thick material are plotted as circles. For lengths greater than 25 inches the test points lie above the sheet curve except at a length of 75 inches. At 75 inches the test points are slightly below the curve. This is due to initial eccentricity of the specimen and will be discussed later in more detail. The test points are in better agreement with the extrusion curve than the bare sheet curve, however two points (at L = 34 and 40) are below the extrusicn curve.

A.4.5.3 Local Instability and Section Crippling

The various stresses of interest are shown in Table A.11. The local buckling and crippling stress are from Table A.9. For comparison the failing stress for the shortest length columns is also shown. The test values are from Table A.5 and are the average of two tests for the 0.052 members and three tests for the 0.034 members.

Figure A.6 CALCULATED STRESS-STRAIN FOR 7075-T6

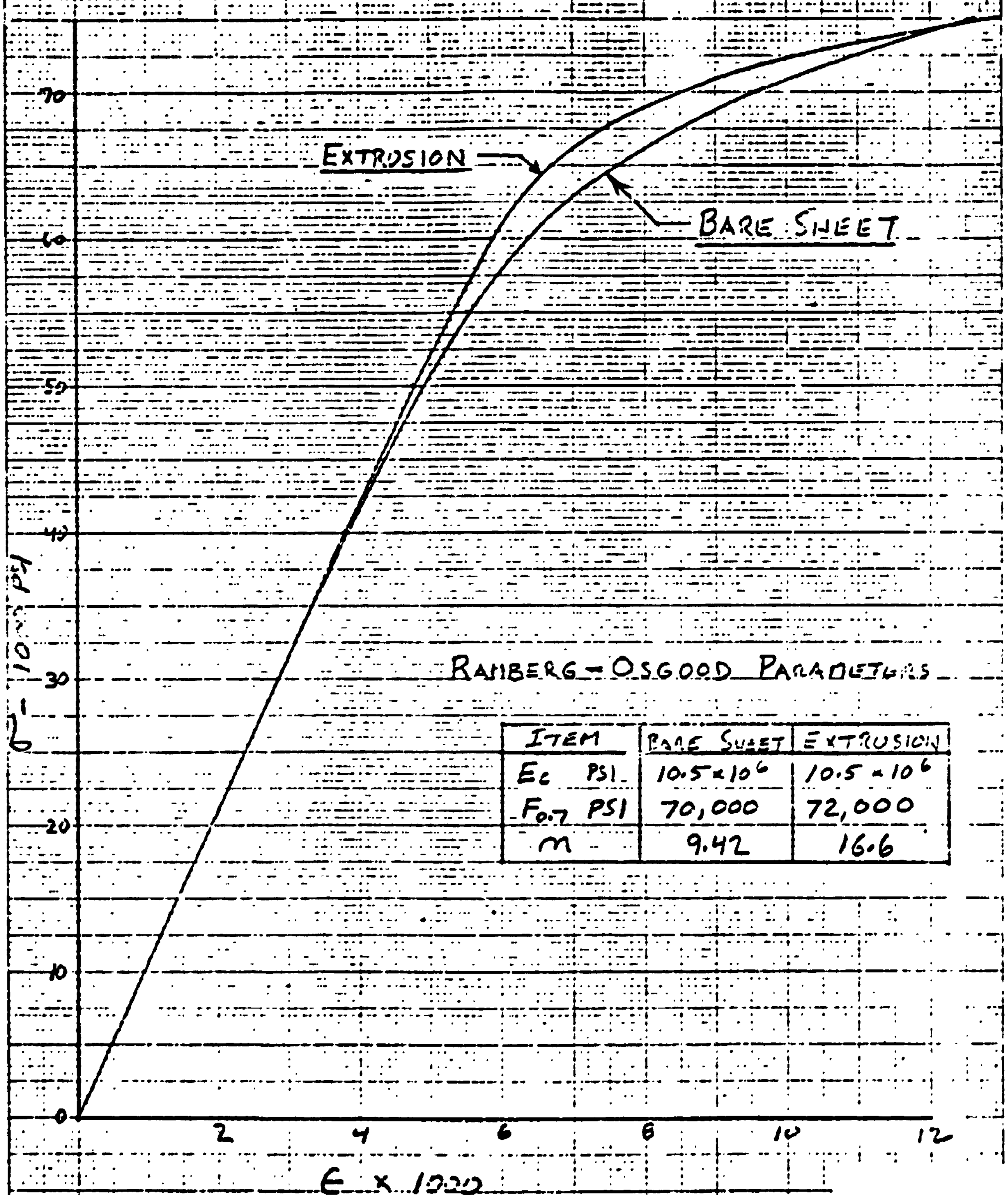

ITEM	BARE SHEET	EXTRUSION
E_c PSI	10.5×10^6	10.5×10^6
$F_{0.7}$ PSI	70,000	72,000
m	9.42	16.6

Figure A.7 COMPRESSION TEST DATA FOR 7075-T6

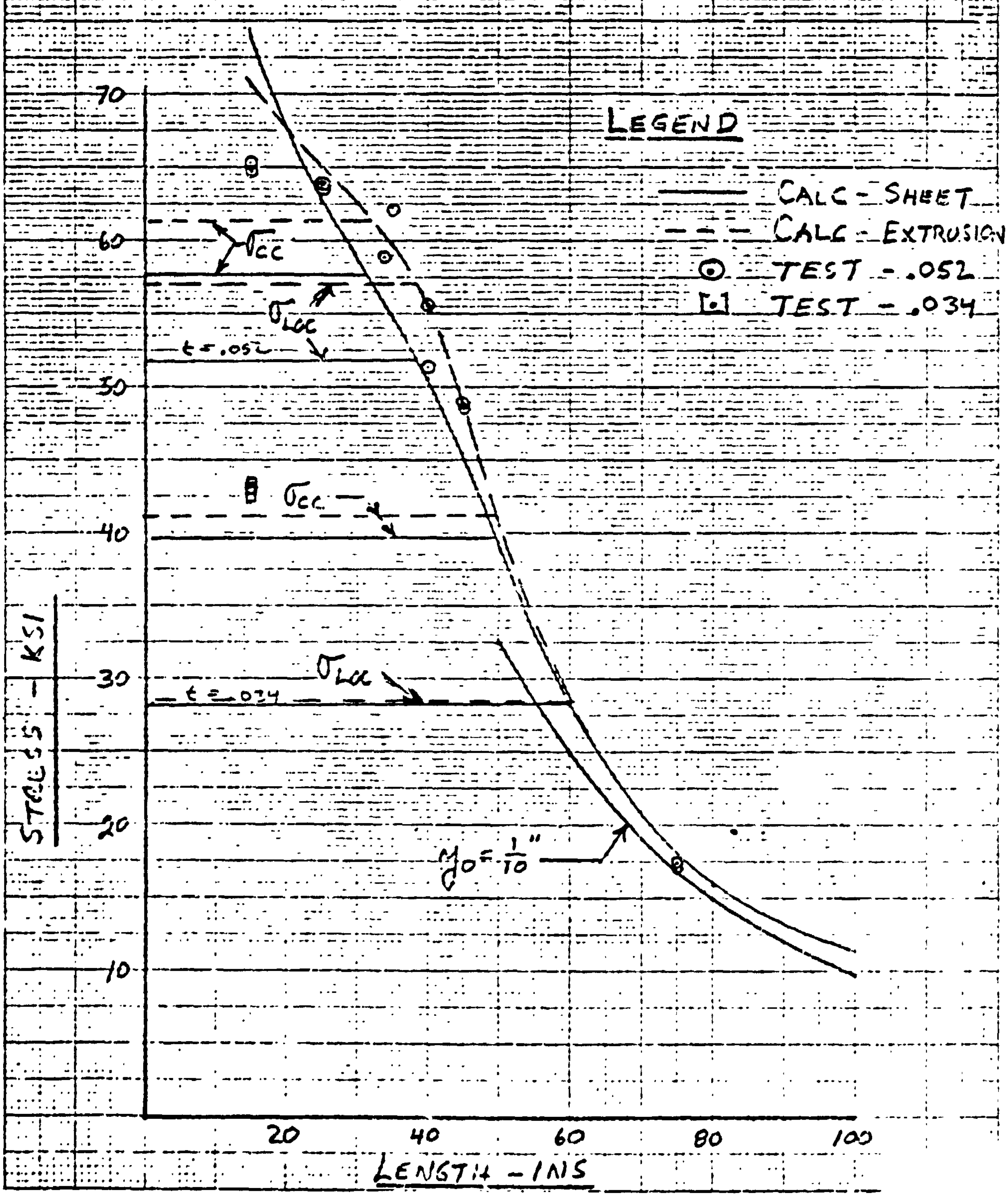

Table A.11 Cripping Stress Comparison

Source	t = 0.052		t = 0.034	
	Sheet	Extr.	Sheet	Extr.
CALC - LOCAL - σ_{LOC}	51,875	57,162	28,330	28,375
CALC - CRIPPLING σ_{CC}	57,798	61,277	39,757	41,227
TEST AV - 15" MEMBER	65,046		42,930	

It is evident from the above table that the use of σ_{LOC} to predict the failing stress for short columns is very conservative. It is the most conservative for the 0.034 member based on sheet properties. It is the least conservative for the 0.052 member based on extrusion properties. The minimum and maximum percent of the test values were 66 and 88 respectively.

The crippling stress is also conservative for predicting the failing stress of short columns, but far less conservative than the lo^al buckling. The best agreement is with 0.034 extrusion calculations where the predicted value is 96% of the test value. The poorest agreement is with 0.052 sheet calculations where the predicted value is 89% of the test value.

It is recommended that the crippling stress method be used to predict the failure of short columns for the type of construction tested.

A.4.5.4 Interaction

One concern in the prediction of the failing stress is that there may be a strong interaction between the crippling stresses and the column stress. Most of the specimen lengths of the 0.052 members were selected to be in the range where interaction was expected to occur, namely lengths between 25 and 45 inches. The test points and the predicted stresses are shown in Figure A.7 for comparison.

It is not evident from the plot that there is interaction between the crippling and column stress. If there is any interaction, its effect is not pronounced and is hidden in the scattered test points in this region. More test points would be required before a definite conclusion could be made.

Of greater practical interest is not whether there is interaction but whether the assumption that there is no interaction is a satisfactory basis for design. If the test points are compared to the predicted values based on bare sheet properties it is seen that the test points are in all cases higher than the predicted values. Therefore, based on this limited data it is concluded that the predicted values using bare sheet properties are conservative and can be used for design.

Compared to the extrusion curves it is seen that two of the test points lie within the predicted envelope. For this reason it must be concluded that the predicted values using the extrusion properties are non-conservative.

A.4.5.5 Initial Eccentricity

The predicted failing stress for a long column with an intiial eccentricity of 0.1 inch, note Table A.10, is also plotted in Figure A.7. The failing stress for the two long specimens (L = 75") lie between the column curves with zero eccentricity and the 0.1 inch eccentricity, indicating if the analysis is correct that there was some initial eccentricity and that this eccentricity was less than 0.1 inch.

The transverse deflection data (Table A.4) was taken with the objective of determining the initial eccentricity of the long columns. The discussion following Equation 13, explains how this is done. The data of Table A.4 was used to generate the test points in Figure A.8. In the Figure the Load, P, is plotted against the load, p, divided by the measured transverse deflection y. According to Equation 13 the test points should plot as a straight line. In the case of specimen 14 the test points do lie in a straight line and for specimen 15 they do not. The reason for this is thought to be as follows. The deflection y should be theoretically the deflection associated with general instability of the column. In these test specimens the thin flat element of the face where the measurements were taken showed some waviness which changed as the load was applied. The measured deflection therefore contained contributions from both local deflection as well as that due to general instability. Therefore it is assumed that if the data does not plot as a straight line then local deflections were present and the data can not be analyzed according to Equation 13.

The plot for specimen 14 is a straight line and can be considered valid. The intercept at the ordinate is 10,470 lbs and is the buckling load. This corresponds to a buckling stress of 17,546 psi which is in good agreement with the calculated value of 18,031, note Table A.8. The slope of the curve is 0.0252 inch, which is the initial deflection, y_o.

This initial deflection is consistent with the test points and the predicted failing stress with and without initial eccentricity. The method of analysis used to account for the initial eccentricity seems to yield reasonable values.

It is evident that the failing stress for this type of cross section is sensitive to initial eccentricity. This factor must be taken into account in design of structures using similar types of cross section.

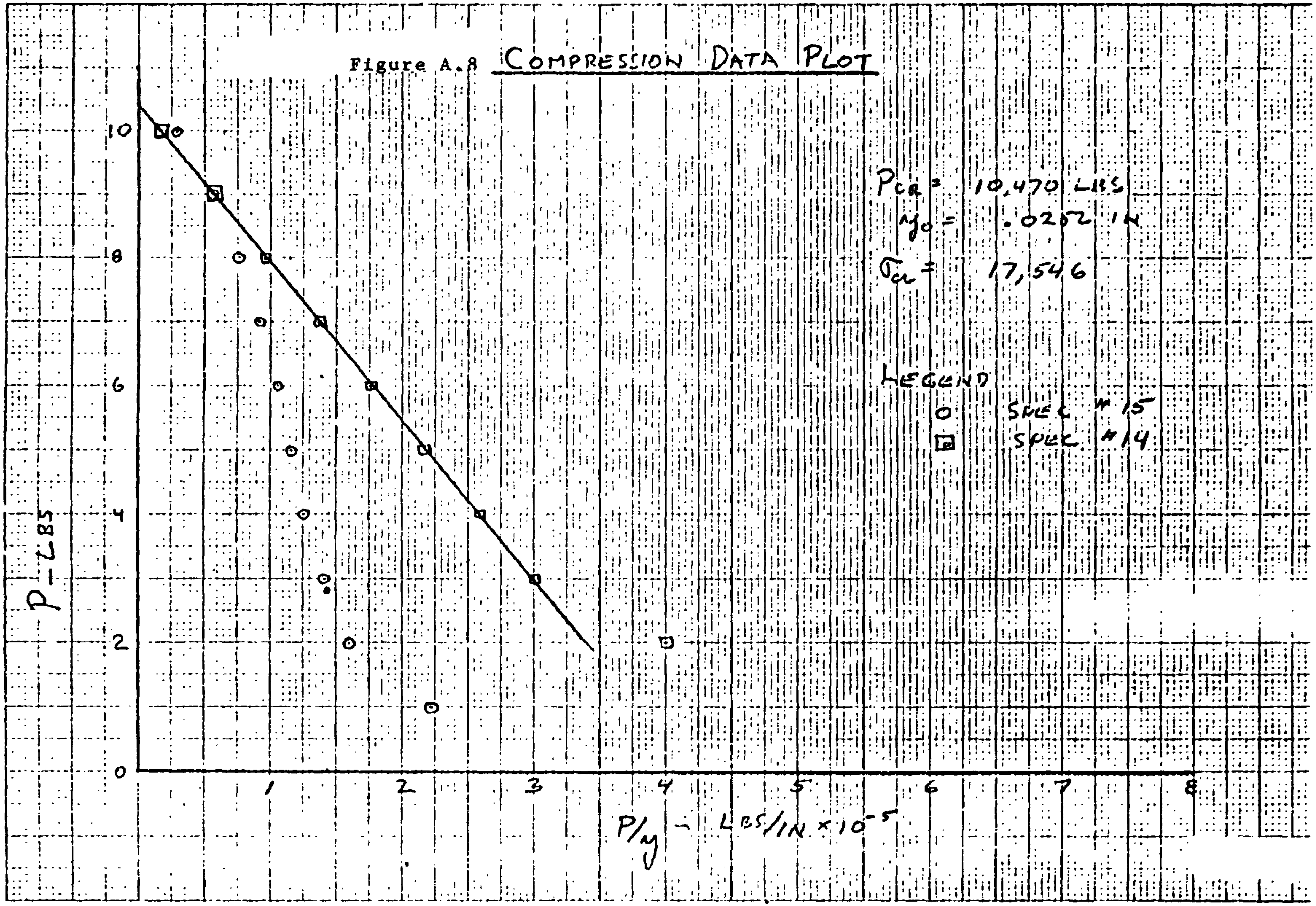

Figure A.8 COMPRESSION DATA PLOT

A.4.6 Conclusions

A.4.6.1 The tangent modulus can be used to predict both general and local instability.

A.4.6.2 The crippling stress should be used for the failing stress of short columns.

A.4.6.3 There appears to be little interaction between general and local instability.

A.4.6.4 The failing stress of long columns is sensitive to initial eccentricity.

A.4.6.5 Equation 12 can be used to predict the failing stress of long columns.

A.4.7 Recommendations

A.4.7.1 Stress-strain curves of the material from which the specimens were fabricated should be obtained in order to correct for material properties.

A.4.7.2 Additional specimens be tested to ensure with greater confidence that the above conclusions are correct.

APPENDIX B

DYNAMIC RESPONSE AND DESIGN LOADS

CONVERSION FACTORS FOR APPENDIX B

1.0 ft/sec	= 3.048×10^{-1} m/s
1.0 lb	= 4.536×10^{-1} kg
1.0 lb/ft	= 1.38×10^{-1} kg/m
1.0 lb/sq ft	= 4.788×10^{1} N/sq m
1.0 lb/sec	= 4.536×10^{-1} kg/s
1.0 mph	= 4.47×10^{-1} m/s
1.0 sq ft	= 9.29×10^{-2} sq m

B.1 DYNAMIC RESPONSE

Two of the flight conditions (1.1 and 2.1) and the two landing conditions have been analyzed as dynamic conditions in which the response of the structural system has been taken into account on a simplified basis (see Section 5.6 of Book I of this Volume of the report). The analysis has been made on the basis of a 3 mass, 2 spring system with no damping. "M_1" represents the mass of the helicopters including contents and a fraction of the outrigger weights. "M_2" represents the mass of the central portion of the frame work including payload if any. "M_3" represents the mass of the envelope group, ballonet air, helium and additional effective mass.

The springs in the system are S_{12} which works between M_1 and M_2 and represents the elastic deflection of the outriggers and supporting structure and S_{23} which works between M_2 and M_3 and represents the deflection of the envelope and suspension system. The spring constants have been estimated at K_{12} = 125,000 lbs per ft for (4) outriggers and K_{23} = 75,000 lbs per ft.

B.1.1 Dynamic Collective Pitch

The forcing function for the dynamic collective pitch condition was based on full collective pitch superimposed on the heavy hover condition. According to Sikorsky, the maximum rotor load that can be expected is 1.8 x 47,000 lbs = 84,600 lbs per rotor, and this peak can be expected approximately one second after the collective pitch application is started. These loads are to be superimposed on a static heavy hover condition with the steady state load on each rotor equal to 45,200 lbs. The dynamic load on four rotors therefore peaks at 4 (84,600 - 45,200) = 157,600 lbs. This loading was represented by

$$P = P_0 \left[1 - e^{-\left(\frac{t}{T_1}\right)}\right] e^{-\left(\frac{t}{T_2}\right)}$$

with P_0 = 630,400, T_1 = 2.32 and T_2 = 2.32

The peak load reaches 157,597 lbs @ t = 1.6 sec with an initial slope of:

$$\left(\frac{dP}{dT}\right)_0 = 272{,}000 \text{ lbs/sec}$$

Other constants used:

$$M_1 = 3068, \quad M_2 = 5652, \quad M_3 = 9000,$$

$$K_{12} = 125{,}000, \quad K_{23} = 75{,}000$$

Results are shown in Figure B.1.

B.1.2 Landing Conditions

In the four point landing condition the airship approaches the ground at 5 ft/sec with no payload and minimum fuel. Rotors are assumed to carry the heaviness throughout the landing. Only the dynamics resulting from the landing gear loads are considered since these dynamic loads are to be superimposed on the steady state loads.

Previous analytical and experimental work with the 5K and 3W airships have shown the necessity for a special landing gear characteristic. The metering pin type gear typical of airplanes has the tendency to stop the descent of the mass closest to the landing gear, then dissipate the available remaining stroke at low loads so that the oleo action is not available to absorb the momentum of the envelope which makes itself felt later. The solution to this problem is the "spring loaded orifice". In this gear the metering pin is replaced by a spring loaded orifice which does not allow the oleo action to begin until the orifice setting is overcome. The characteristic of this gear in simplified

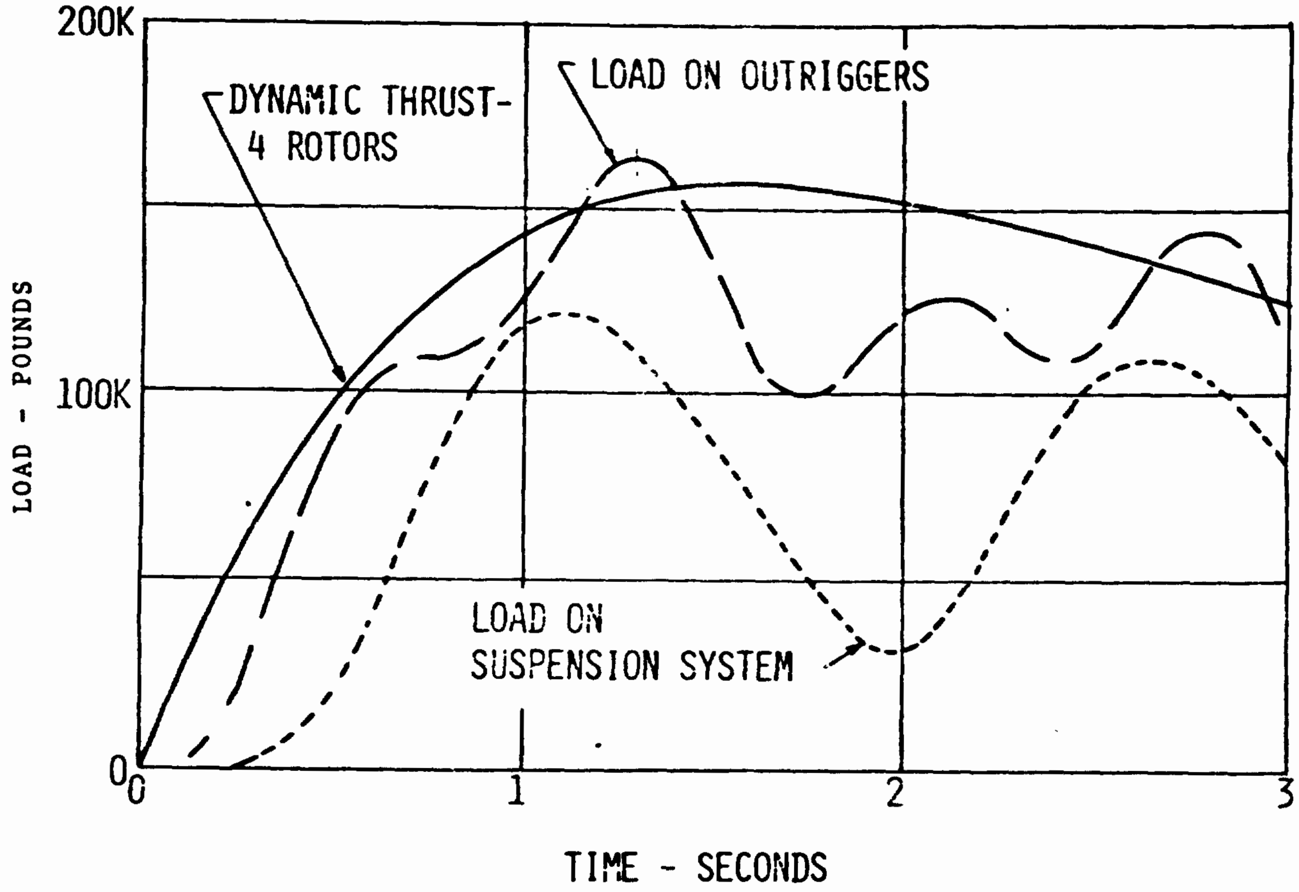

FIGURE B.1 - RESPONSE - DYNAMIC COLLECTIVE PITCH form is as follows. Let P_{max} = load required to open the orifice. When $P < P_{max}$ action is concentrated in tire deflection $P = K_T \Delta_T$.

When $P = P_{max}$ the oleo slips (closes) at a rate compatible with the closure rate between the ground and the helicopter mass (M_1).

When the closure rate becomes zero and then negative the oleo stroke remains constant and the action is again concentrated in the tire. The tire deflection decreases and the load decreases. When the tire deflection reaches zero the load also reaches zero and the tire may actually bounce clear off the ground momentarily.

For the landing conditions this behavior was programmed into the computer with the following constants.

P_{max} (4 helicopters) = 120,000 lbs

K_T = 360,000 lb/ft

M_1 = 3,068

K_{12} = 125,000 lb/ft

M_2 = 813

K_{23} = 75,000 lb/ft

M_3 = 9,000

Sinking Speed 5.0 ft/sec

The results are shown in Figure B.2.

In the two wheel landing condition it is assumed that diagonally opposite helicopters contact the ground with the other two helicopters dangling due to adverse terrain. The

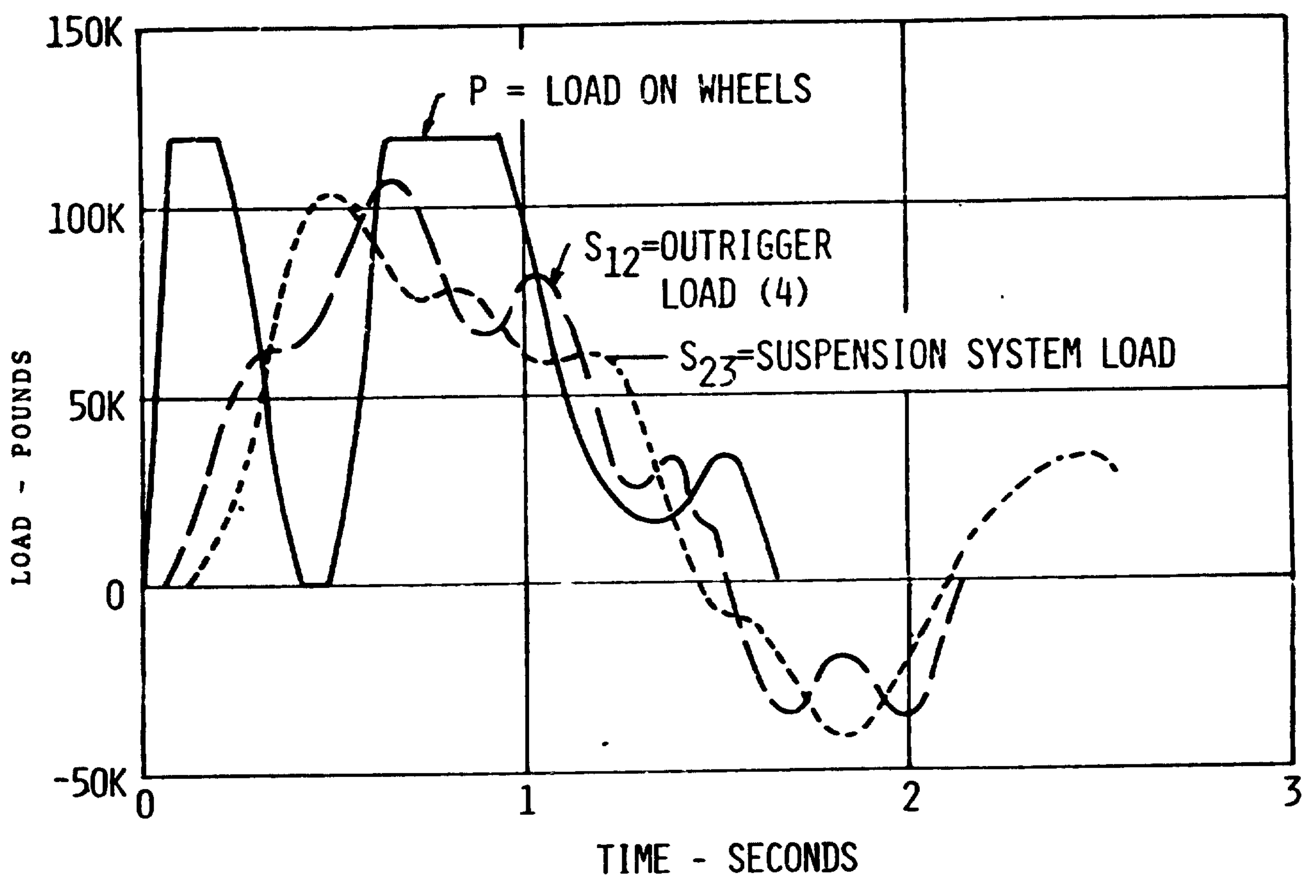

FIGURE B.2 - LANDING DYNAMICS - FOUR POINT sinking speed was reduced to 4 ft/sec. Even with the reduded sinking speed the stroke of the landing gears was exceeded, so a sinking speed of less than 4 ft/sec would actually be the limit for this condition. Nevertheless, the laods resulting from this calculation were actually used in the design since the purpose of imposing this condition was to produce negative design loads in members which tended to see only tension in the other six loading conditions.

In this condition, the dynamic response was simplified to a three mass system by placing the mass of the dangling ehlicopters in M_2. The dynamics were evaluated with the following constants (maximum fuel condition)

$$P_{max} = 60{,}000$$

$$K_T = 180{,}000$$

$$M_1 = 1{,}925$$

$$K_{12} = 62{,}500$$

$$M_2 = 2{,}738$$

$$K_{23} = 75{,}000$$

$$M_3 = 9{,}000$$

$$V_s = 4.0 \text{ ft/sec}$$

The results are shown in Figure B.3.

B.2 TABULATION OF DESIGN LOADS

The loads applied to the framework in the seven loading configurations are shown in Tables B.1 thru B.7 and were derived as follows:

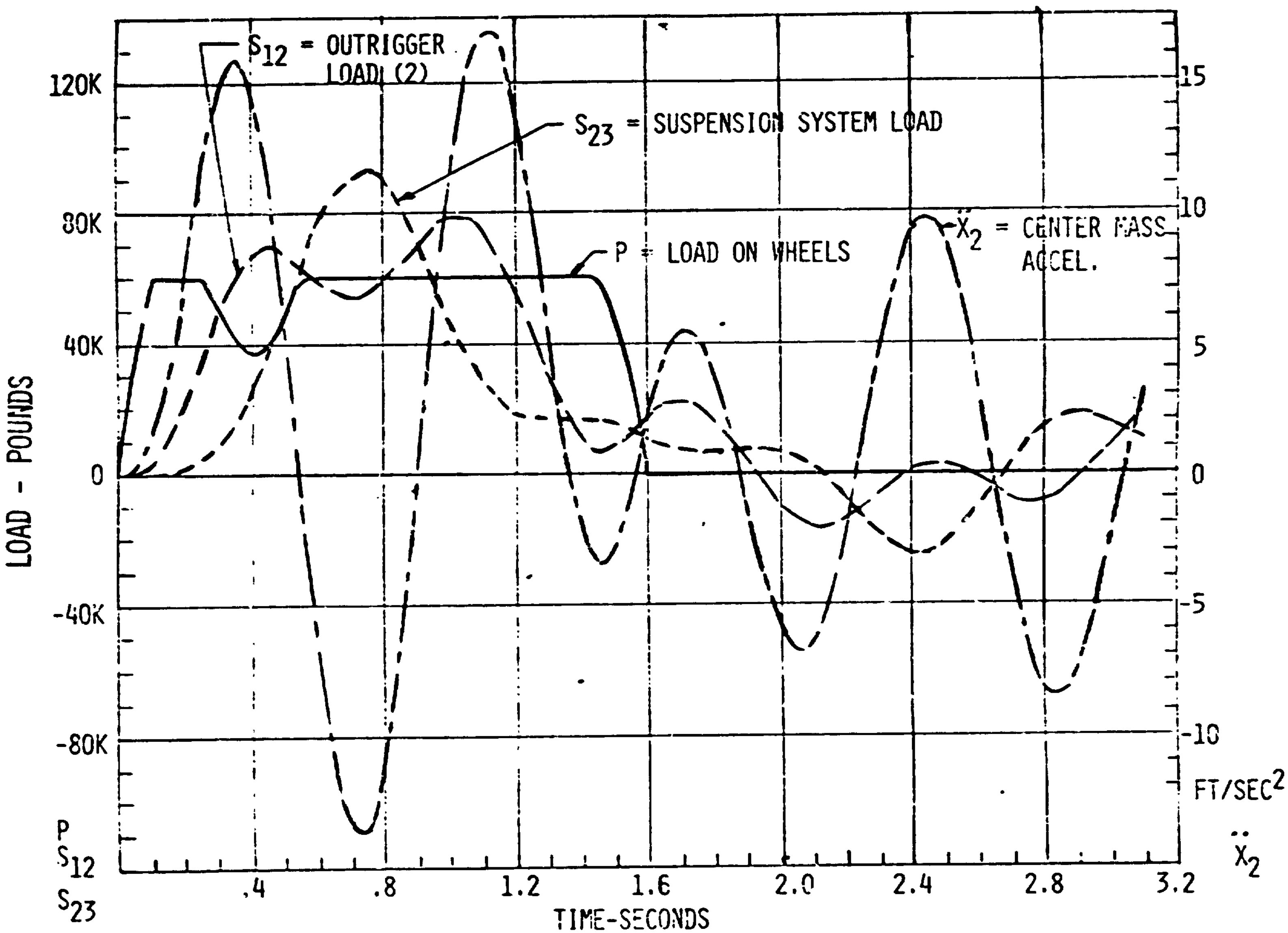

FIGURE B.3 - LANDING DYNAMICS - TWO POINT

Condition 1.1 - Dynamic Collective Pitch

In this condition the dynamic loads of Figure B.1 are superimposed on a static heavy hover condition.

Main rotor loads are applied vertically except that each rotor is tilted fore or aft such that the torque of the four rotors is balanced by the helicotper system and vertical load only is transmitted to the envelope. The rotor torque is based on 6000 HP and 204 rpm at each rotor.

Maximum Dynamic Outrigger Load	40,625 lb ea
Static Rotor Load	45,200
Static Mounted Weight	24,700
Net Outrigger Load	61,125 lbs

This condition occurs at t = 1.28 sec in the dynamic response when the acceleration of M_2 is 8.93 ft/sec^2 (0.277 g's). The masses of the framework and payload are subjected to a load factor of 1.277.

This condition is chosen at the point where the outrigger loads are a maximum. The dynamic load on the suspension system at this point is 112,022 lb compression.

This dynamic suspension load is superimposed to a static tension load of 100,000 lb and results in the 12,022 load applied to the envelope. The helicopter frame system is actually pushing up on the envelope by this amount.

These loads are displayed in Table B-1.

Condition 2.1 - One Engine Out

These loads are postulated from the results of Condition 1.1 but with the static condition represented by 38,000 lb on the helicopter with one engine out and its diagonally opposite

TABLE B.1. Heavy Lift Vehicle Limit Load Conditions

Loading Condition 1.1 Dynamic Collective - Minimum Fuel

OUTRIGGER LOADS	
LF	RF
$X_H = -1816.7$	$X_H = 1816.7$
$Y_H = 0$	$Y_H = 0$
$Z_H = 61125$	$Z_H = 61125$
$M_{XH} = 0$	$M_{XH} = 0$
$M_{YH} = 0$	$M_{YH} = 0$
$M_{ZH} = -1.853 \times 10^6$	$M_{ZH} = -1.853 \times 10^6$
$X_H = -1816.7$	$X_H = 1816.7$
$Y_H = 0$	$Y_H = 0$
$Z_H = 61125$	$Z_H = 61125$
$M_{XH} = 0$	$M_{XH} = 0$
$M_{YH} = 0$	$M_{YH} = 0$
$M_{ZH} = -1.853 \times 10^6$	$M_{ZH} = -1.853 \times 10^6$
LA	RA

OTHER JOINT LOADS						LOADS TO ENVELOPE
JOINT		W	X	Y	Z	
1	LF2	4576	0	0	-5845	$X = 0$
2	LA2	4576	0	0	-5845	$M_Y = 0$
3	RF2	4576	0	0	-5845	$Y = 0$
4	RA2	4576	0	0	-5845	$M_X = 0$
13	L2	0	0	0	0	$Z = +12022$
14	R2	0	0	0	0	$M_Z = 0$
16	F1	81848	0	0	-104549	
17	A1	81848	0	0	-104549	

mate throttled to an equal load. The other helicopters are pulling 52,400 lb each when dynamic collective pitch is applied. The dynamic rotor thrust is assumed to be:

$$1.8 \times 47{,}000 - 52{,}400 = 32{,}200 \text{ lb}$$

on the helicopters with good engines and

$$\frac{38{,}000}{52{,}400} \times 32{,}200 = 23{,}351 \text{ lb}$$

on the pair limited by a dead engine.

These loads are superimposed on the static condition with the rotor torque cut in half on the dead engine pair and a load factor of 1.20 on M_2. The results are as shown in Table B.2.

Condition 3.1 - Cross Wind Hover

This condition was originally structured to be a heavy hover condition in a 30 knot cross wind. The side load applied to the envelope is 30,000 lbs.

Subsequent to this analysis, wind tunnel data became available (see Book III of this Volume of the report) that would indicate that a 30 knot cross wind may produce a side load greatly in excess of 30,000 lbs. Thus this condition represents a cross wind loading of 30,000 lbs which corresponds more closely to a 20 knot cross wind condition than the original 30 knot condition.

Loads are derived to resist a 30,000 lb force at the center of the envelope superimposed on a 1 g heavy hover condition.

Results are displayed in Table B.3.

TABLE B.2. Heavy Lift Vehicle Limit Load Conditions

Loading Condition 2.1 One Engine Out Dynamic Collective

OUTRIGGER LOADS	
LF X_H = -1362.5 Y_H = 0 Z_H = 59900 M_{XH} = 0 M_{YH} = 0 M_{ZH} = -1.853×10^6	RF X_H = 1362.5 Y_H = 0 Z_H = 36651 M_{XH} = 0 M_{YH} = 0 M_{ZH} = -0.9265×10^6
X_H = -1362.5 Y_H = 0 Z_H = 36651 M_{XH} = 0 M_{YH} = 0 M_{ZH} = -0.9265×10^6 LA	X_H = 1362.5 Y_H = 0 Z_H = 59900 M_{XH} = 0 M_{YH} = 0 M_{ZH} = -1.853×10^6 RA

OTHER JOINT LOADS						LOADS TO ENVELOPE
JOINT		W	X	Y	Z	
1	LF2	4576	0	0	-5491	X = 0
2	LA2	4576	0	0	-5491	M_Y = 0
3	RF2	4576	0	0	-5491	Y = 0
4	RA2	4576	0	0	-5491	M_X = 0
13	L2	0	0	0	0	Z = -25298
14	R2	0	0	0	0	M_Z = 0
16	F1	81848	0	0	-98218	
17	A1	81848	0	0	-98218	

TABLE B.3 Heavy Lift Vehicle Limit Load Conditions
Loading Condition: 3.1 Heavy Hover - Cross Wind (30,000#)

OUTRIGGER LOADS	
LF X_H =- 1617.65 Y_H =-10,000 Z_H = 15227.94 M_{XH} = 0 M_{YH} = 0 M_{ZH} =-4.68 x 10^6	RF X_H = 1617.65 Y_H =-10,000 Z_H = 24772.06 M_{XH} = 0 M_{YH} = 0 M_{ZH} = -4.68 x 10^6
X_H =- 1617.65 Y_H = 5000 Z_H = 15227.94 M_{XH} = 0 M_{YH} = 0 M_{ZH} =-1.98 x 10^6 LA	X_H = 1617.65 Y_H = 5000 Z_H = 24772.06 M_{XH} = 0 M_{YH} = 0 M_{ZH} = -1.98 x 10^6 RA

OTHER JOINT LOADS						LOADS TO ENVELOPE
JOINT		W	X	Y	Z	
1	LF2		0	0	-4576	X = 0
2	LA2		0	0	-4576	M_Y = 0
3	RF2		0	0	-4576	Y = 30,000
4	RA2		0	0	-4576	M_X = -19.47 x 10^6
13	L2		0	0		Z =-100,000
14	R2		0	0		M_Z = 0
16	F1		0	0	-80848	
17	A1		0	0	-80848	

Condition 4.1 - Maximum Yawing Effort

The helicopters/rotors are subjected to differential fore and aft tilt of approximately 25° with pusher rotors also in the maximum differential configuration so that maximum yawing moment is created. The loads are applied in the direction which adds to the main rotor torque. A total yawing moment of 56.046×10^6 inch lbs results. This load is transmitted to the envelope in its entirety and superimposed on the heavy 1 g hover condition. Results are displayed in Table B.4.

Condition 5.1 - 4 Point Landing

This condition occurs with a sinking speed of 5 ft/sec, no payload, and minimum fuel. Static heaviness is 25,376 lb. The rotors are assumed to carry the heaviness throughout the landing.

Maximum dynamic outrigger load occurs at t = 0.66 sec and is 108,400 lbs for 4 outriggers.

The acceleration of M_2 at this point is approximately 1 g. The dynamic load from the above is superimposed on the static condition to provide a net up load of:

$$\frac{108{,}400}{4} + \frac{25{,}376}{4} - 24{,}700 = 8{,}644$$

on each outrigger. A load factor of 2 is applied to M_2 which produces a net up load on the suspension system of 17,776 lbs. See Table B.5 for results.

Condition 6.2 - 2 Point Landing

The dynamics of this condition produce a critical condition at t = 1.02 sec.

TABLE B.4 Heavy Lift Vehicle Limit Load Conditions

Loading Condition 4.1 Maximum Yawing Effort

OUTRIGGER LOADS	
LF	RF
X_H = 8600	X_H = -8600
Y_H = 0	Y_H = 0
Z_H = 20,000	Z_H = 20,000
M_{XH} = -400,000	M_{XH} = 400,000
M_{YH} = 0	M_{YH} = 0
M_{ZH} = -1.98×10^6	M_{ZH} = -1.98×10^6
X_H = 15,000	X_H = -15,000
Y_H = 0	Y_H = 0
Z_H = 20,000	Z_H = 20,000
M_{XH} = -400,000	M_{XH} = 400,000
M_{YH} = 0	M_{YH} = 0
M_{ZH} = -1.98×10^6	M_{ZH} = -1.98×10^6
LA	RA

OTHER JOINT LOADS					
JOINT		W	X	Y	Z
1	LF2				-4576
2	LA2				-4576
3	RF2				-4576
4	RA2				-4576
13	L2				0
14	R2				0
16	F1				-80848
17	A1				-80848

LOADS TO ENVELOPE	
X	= 0
M_Y	= 0
Y	= 0
M_X	= 0
Z	= -100,000
M_Z	= -56.064×10^6

TABLE B.5. Heavy Lift Vehicle Limit Load Conditions

Loading Condition 5.1 4 Point Landing - Minimum Fuel

OUTRIGGER LOADS	
LF	RF
X_H = 0	X_H = 0
Y_H = 0	Y_H = 0
Z_H = 8644	Z_H = 8644
M_{XH} = 0	M_{XH} = 0
M_{YH} = 0	M_{YH} = 0
M_{ZH} = Neg.	M_{ZH} = Neg.
X_H = 0	X_H = 0
Y_H = 0	Y_H = 0
Z_H = 8644	Z_H = 8644
M_{XH} = 0	M_{XH} = 0
M_{YH} = 0	M_{YH} = 0
M_{ZH} = Neg.	M_{ZH} = Neg.
LA	RA

OTHER JOINT LOADS						LOADS TO ENVELOPE
JOINT		W	X	Y	Z	
1	LF2	4576	0	0	-9152	X = 0
2	LA2	4576	0	0	-9152	M_Y = 0
3	RF2	4576	0	0	-9152	Y = 0
4	RA2	4576	0	0	-9152	M_X = 0
13	L2	0	0	0		Z =-17776
14	R2	0	0	0		M_Z = 0
16	F1	3936	0	0	-7872	
17	A1	3936	0	0	-7872	

TABLE B.6 Heavy Lift Vehicle Limit Load Conditions

Loading Condition 6.2 2-Wheel Landing (Diagonal)
Maximum Fuel

OUTRIGGER LOADS	
LF	RF
X_H = 0	X_H =
Y_H = 0	Y_H =
Z_H = 20,899	Z_H = -33,952
M_{XH} = 0	M_{XH} =
M_{YH} = 0	M_{YH} =
M_{ZH} = Neg.	M_{ZH} =
X_H =	X_H = 0
Y_H =	Y_H = 0
Z_H = -33,952	Z_H = 20,899
M_{XH} =	M_{XH} = 0
M_{YH} =	M_{YH} = 0
M_{ZH} =	M_{ZH} = Neg.
LA	RA

OTHER JOINT LOADS						LOADS TO ENVELOPE
JOINT		W	X	Y	Z	
1	LF2	4576	0	0	-5233	X = 0
2	LA2	4576	0	0	-5233	M_Y = 0
3	RF2	4576	0	0	-5233	Y = 0
4	RA2	4576	0	0	-5233	M_X = 0
13	L2	0	0	0	0	Z = -56,040
14	R2	0	0	0	0	M_Z = 0
16	F1	3936	0	0	-4501	
17	A1	3936	0	0	-4501	

$$P = 60{,}000, \; S_{12} = 78{,}710, \; S_{23} = 43{,}960 \text{ lb}$$

$$\ddot{X}_2 = 12.690$$

when the static 1 g loads are added the load factor on M_2 becomes

$$n_2 = -1 - \frac{12.690}{32.2} = 1.3941$$

The load factor on the dangling helicopters was arbitrarily increased to 1.50 with a compensating reduction of the load factor on the remaining weights in M_2 to n = 1.1434.

The resulting loads are:

$$Z_H = \frac{78{,}710}{2} + 12{,}537 - 30{,}993 = 20{,}899$$

on the wheel loaded helicopters and

$$Z_H = 12{,}537 - 1.5\,[30{,}993] = -33{,}952$$

on the dangling helicopter points. Other loads are as shown in Table B.6.

Condition 7.1 - Center Point Mooring - 65 mph

Envelope side load 110,000 lbs

$$q = (65 \times 1.467)^2 \times .0012 = 10.9 \text{ lbs/sq ft}$$

$$\mathcal{V}^{2/3} = (2.5 \times 10^6)^{2/3} = 18{,}420 \text{ sq ft}$$

$$C_Y = \frac{110{,}000}{10.9 \times 18{,}420} \cong .55$$

(See Figure B.4)

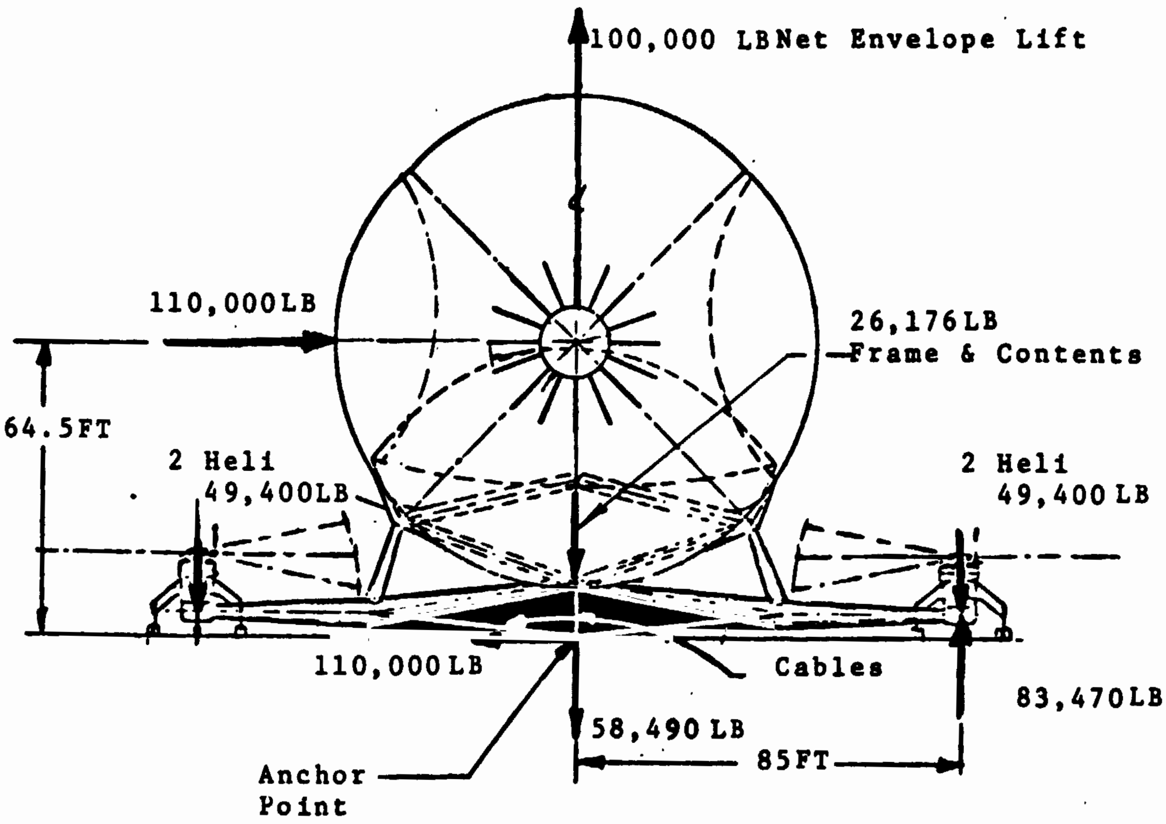

$$\frac{110,000 \times 64.5}{85} = \begin{array}{r} 83,470 \\ +100,000 \\ -\ 26,176 \\ -\ 49,400 \\ -\ \underline{49,400} \\ 58,490\ \text{LB} \end{array}$$

Figure B.4 Center Point Mooring System Loads

Anchor point at X = 0, Y = 0, Z = 0, load is Y = 110,000, Z = -58,490.

This load is carried to the frame by cables to end points of keel and to elbows of outriggers

Point	X	Y	Z	L	X/L	Y/L	Z/L
RF Elbow	535.384	-576	64	788.99	.67857	-.73005	.08112
RA Elbow	-535,384	-576	64	788.99	-.67857	-.73005	.08112
F1	240	0	150	283.02	.84800	0	.53000
A1	-240	0	150	283.02	-.84800	0	.53000

Cable loads to Elbows

$$P = \frac{110,000}{2 \times .73005} = 75337$$

$P_X = 51122$

$P_Y = 55000$

$P_Z = 6111$

Cable loads to Keel

$$P = \frac{58490 - 2\ (6111)}{2\ (.53000)} = \frac{46268}{1.06000} = 43,649$$

$P_X = 37014$

$P_Y = 0$

$P_Z = 23134$

The cable load at the elbow is carried up to the star frame through members

a) RF1-R2 drag strut

b) RF1-RF2 lift strut

c) RF1-F1 arm

	Geometry	Projections X	Y	Z	L	Cosines C_X	C_Y	C_Z
a)	RF1-R2	-535.384	108.0	236	594.98	-.89983	.18152	.39665
b)	RF1-RF2	- 55.384	108.0	236	265.38	-.20870	.40696	.88929
c)	RF1-F1	-295.384	576	86	653.01	-.45234	.88207	.13170

Cable load components on RF1

$$X = -51{,}122$$
$$Y = 55{,}000$$
$$Z = -6{,}111$$

$$-.89983\ P_a \quad -.20870\ P_b \quad -.45234\ P_c \quad - 51122 = 0$$
$$.18152\ P_a \quad +.40696\ P_b \quad +.88207\ P_c \quad - 55000 = 0$$
$$.39665\ P_a \quad +.88929\ P_b \quad +.13170\ P_c \quad - 6111 = 0$$
$$.39665\ P_a \quad +.88929\ P_b \quad +1.92749\ P_c \quad +120185 = 0$$
$$1.79579\ P_c \quad +126296 = 0$$
$$P_c = -70{,}329 \text{ lbs}$$

$$.89983\ P_a \quad +2.01738\ P_b \quad +4.37259\ P_c \quad +272646 = 0$$
$$1.80868\ P_b \quad +3.92025\ (-70{,}329) + 221524 = 0$$
$$P_b = +29{,}957$$
$$-.89938\ P_a \quad -.20870\ (29957) -.45234\ (-70{,}329) - 51122 = 0$$
$$P_a = -28{,}407$$

COMPONENTS ON ELBOW

		X	Y	Z
*P_a [Drag Strut]	= -28,407	+ 25561	- 5156	- 11268
P_b [Lift Strut]	= +29,957	- 6252	+ 12191	+ 26640
P_c [Arm]	= -70,329	31813	- 62035	- 9262
		51122	- 55000	+ 6110

*These member loads required to handle the cable load at the elbow are not otherwise accounted for in the analysis and must be added [on the right side only] to th. loads falling out of the mechanized analysis.

Total joint loads [cable loads plus weight] loads on affected joints.

Joint F1 [Keel Fwd End]	X	Y	Z
Direct Cable Load	- 37,014	0	- 23,134
Arm Load	- 31,813	62,035	+ 9,262
Wt. Load	0	0	- 3,936
	- 68,827	62,035	- 17,808
Joint RF2			
Lift Strut	6,252	- 12,191	- 26,640
Wt.	0	0	- 4,576
	6,252	- 12,191	- 31,216
Joint R2			
Two Drag Struts	0	+ 10,312	+ 22,536
Wt.	0	0	0
		10,312	22,536

These loads result from a re-creation of the original work and vary slightly from the loads tabulated in Table B.7.

TABLE B.7. Heavy Lift Vehicle Limit Load Conditions

Loading Condition 7.1 Center Point Mooring - Minimum Fuel
65 mph Wind Broadside

OUTRIGGER LOADS			
LF			RF
X_H	= 0	X_H	= 0
Y_H	= 0	Y_H	= 0
Z_H	= -24,700	Z_H	= 17,035
M_{XH}	= 0	M_{XH}	= 0
M_{YH}	= 0	M_{YH}	= 0
M_{ZH}	= 0	M_{ZH}	= 0
X_H	= 0	X_H	= 0
Y_H	= 0	Y_H	= 0
Z_H	= -24,700	Z_H	= 17,035
M_{XH}	= 0	M_{XH}	= 0
M_{YH}	= 0	M_{YH}	= 0
M_{ZH}	= 0	M_{ZH}	= 0
LA			RA

OTHER JOINT LOADS						LOADS TO ENVELOPE
	JOINT	W	X	Y	Z	
1	LF2	4576	0	0	-4576	X = 0
2	LA2	4576	0	0	-4576	M_Y = 0
3	RF2	4576	6251	-12190	-31213	Y = 110,000
4	RA2	4576	-6251	-12190	-31213	$M_X = -93.654 \times 10^6$
13	L2	0	0	0	0	Z = -100,000
14	R2	0	0	10303	22514	M_Z = 0
16	F1	3936	-68830	62035	-17810	
17	A1	3936	68830	62035	-17810	

APPENDIX C

DFTAILS OF STAR FRAME DESIGN

CONVERSION FACTORS FOR APPENDIX C

1.0 ft = 3.048×10^{-1} m

1.0 psi = $6.894 \times 10^{+3}$ N/m^2

C.1 GENERAL

This Appendix reports details of the analysis supporting the Starframe design (see Section 5.7 of Book I of this Volume of the Report).

C.2 SUSPENSION LOADS ON FRAME

The framework of the heavy lifter is attached to the envelope by a multitude of cables. Twenty cables attach to the internal suspension curtains and 40 cables to the external curtains.

As a matter of convenience, the reactions on the frame were computed from a simple elastic model of the arrangement. Both the framework and the envelope are taken as rigid bodies with six degrees of freedom in the relative motion between the bodies. Each cable in the system is replaced, (mathematically) by a linear spring. Each cable attaches to the framework (car) at X_c, Y_c, Z_c and to the envelope at X_e, Y_e, Z_e.

The projection of each cable on the 3 reference axes are taken as:

$$X = X_e - X_c$$

$$Y = Y_e - Y_c$$

$$Z = Z_e - Z_c$$

The length of the cable is:

$$\ell = \sqrt{X^2 + Y^2 + Z^2}$$

and the direction Cosines:

$$C_X = X \div \ell$$

$$C_Y = Y \div \ell$$

$$C_Z = Z \div \ell$$

For motions of the car relative to the envelope

$$\frac{d\ell}{dX_c} = -C_X$$

$$\frac{d\ell}{dY_c} = -C_Y$$

$$\frac{d\ell}{dZ_c} = -C_Z$$

In six degrees of freedom with the rotations taken about the reference axes using the right hand rule, X positive Fwd, Y positive to left, and Z positive up:

$$dX_c = \Delta_X + Z_c\,\theta_Y - Y_c\,\theta_Z$$
$$dY_c = \Delta_Y - Z_c\,\theta_X + X_c\,\theta_Z$$
$$dZ_c = \Delta_Z + Y_c\,\theta_X - X_c\,\theta_Y$$

The cable load resulting from the six components of relative motion:

$$P = -K\,(C_X\,dX_c + C_Y\,dY_c + C_Z\,dZ_c)$$

with three components:

$$P_X = -K\,(C_X{}^2\,dX_c + C_XC_Y\,dY_c + C_XC_Z\,dZ_c)$$
$$P_Y = -K\,(C_XC_Y\,dX_c + C_Y{}^2\,dY_c + C_ZC_Y\,dZ_c)$$
$$P_Z = -K\,(C_XC_Z\,dX_c + C_YC_Z\,dY_c + C_Z{}^2\,dZ_c)$$

Combining these equations, taking moments about the reference axes and taking the summation over all the cables results in the following set of equations in Table C.1 relating the six components of force at the origin to the six components of relative deflection.

These equations are general in that no symmetry has been assumed in the derivation. For the case of the heavy lifter design being considered, double symmetry exists and most of the cross product terms are zero. Exceptions are X, θ_Y and Y, θ_X terms.

The frame analysis integrated computer program solves the above set of equations for the input geometry and springs constants to produce deflections as a function of forces X, Y, Z, M_X, M_Y and M_Z, computes cable loads and components and accumulates components at each suspension joint on the frame for subsequent use in the frame member analyses.

Table C.2 is the set of cable geometries and spring constants used in the analysis and the resulting matrix representing the above set of general equations and its inverse.

Table C.1 MATRIX - X, M_Y, Y, M_X, Z M_Z, AS FUNCTION OF Δ_X, θ_Y, Δ_Y, θ_X, Δ_Z, θ_Z

ΔX	θY	ΔY	θX	ΔZ	θZ	
ΣKC_X^2	$\Sigma KC_X\ (Z_cC_X - X_cC_Z)$	ΣKC_XC_Y	$\Sigma KC_X\ (Y_cC_Z - Z_cC_Y)$	ΣKC_XC_Z	$\Sigma KC_X\ (X_cC_Y - Y_cC_X)$	X
$\Sigma KC_X\ (Z_cC_X - X_cC_Z)$	$\Sigma K\ (Z_cC_X - X_cC_Z)^2$	$\Sigma KC_Y\ (Z_cC_X - X_cC_Z)$	$\Sigma K(X_cC_Z-Z_cC_X)(Z_cC_Y - Y_cC_Z)$	$\Sigma KC_Z(Z_cC_X-X_cC_Z)$	$\Sigma K(Y_cC_X-X_cC_Y)(X_cC_Z - Z_cC_X)$	M_Y
ΣKC_XC_Y	$\Sigma KC_Y\ (Z_cC_X - X_cC_Z)$	ΣKC_Y^2	$\Sigma KC_Y\ (Y_cC_Z - Z_cC_Y)$	ΣKC_YC_Z	$\Sigma KC_Y\ (X_cC_Y - Y_cC_X)$	Y
$\Sigma KC_X\ (Y_cC_Z - Z_cC_Y)$	$\Sigma K(X_cC_Z-Z_cC_X)(Z_cC_Y - Y_cC_Z)$	$\Sigma KC_Y\ (Y_cC_Z - Z_cC_Y)$	$\Sigma K\ (Y_cC_Z - Z_cC_Y)^2$	$\Sigma KC_Z(Y_cC_Z - Z_cC_Y)$	$\Sigma K(Y_cC_X-X_cC_Y)(Y_cC_Z - Z_cC_Y)$	M_X
ΣKC_XC_Z	$\Sigma KC_Z\ (Z_cC_X - X_cC_Z)$	ΣKC_YC_Z	$\Sigma KC_Z\ (Y_cC_Z - Z_cC_Y)$	ΣKC_Z^2	$\Sigma KC_Z\ (X_cC_Y - Y_cC_X)$	Z
$\Sigma KC_X\ (X_cC_Y - Y_cC_X)$	$\Sigma K(Y_cC_X-X_cC_Y)(X_cC_Z - Z_cC_X)$	$\Sigma KC_Y\ (X_cC_Y - Y_cC_X)$	$\Sigma K(Y_cC_X-X_cC_Y)(Y_cC_Z - Z_cC_Y)$	$\Sigma KC_Z(X_cC_Y - Y_cC_X)$	$\Sigma K\ (Y_cC_X - X_cC_Y)^2$	M_Z

ORIGINAL PAGE IS OF POOR QUALITY

Table C.2 SUSPENSION CABLE GEOMETRY & STIFFNESS

I	XC	YC	ZC	XE	YE	ZE	K
1	.480000E 03	.468000E 03	.300006E 03	.600000E 03	.525988E 03	.401038E 03	.300000E 03
2	.480000E 03	.468000E 03	.300006E 03	.600000E 03	.366232E 03	.243304E 03	.300000E 03
3	.480000E 03	.468000E 03	.300006E 03	.972000E 03	-.411535E 03	.118553E 04	.200000E 03
4	.480000E 03	.468000E 03	.300006E 03	.756000E 03	-.411535E 03	.118553E 04	.200000E 03
5	.480000E 03	.468000E 03	.300006E 03	.540000E 03	-.411535E 03	.118553E 04	.200000E 03
6	.480000E 03	.468000E 03	.300006E 03	.324000E 03	-.411535E 03	.118553E 04	.200000E 03
7	.480000E 03	.468000E 03	.300006E 03	.360000E 03	.525988E 03	.401038E 03	.300000E 03
8	.480000E 03	.468000E 03	.300006E 03	.360000E 03	.366232E 03	.243304E 03	.300000E 03
9	.240000E 03	.468000E 03	.300006E 03	.360000E 03	.525988E 03	.401038E 03	.300000E 03
10	.240000E 03	.468000E 03	.300006E 03	.360000E 03	.366232E 03	.243304E 03	.300000E 03
11	.240000E 03	.468000E 03	.300006E 03	.120000E 03	.525988E 03	.401038E 03	.300000E 03
12	.240000E 03	.468000E 03	.300006E 03	.120000E 03	.366232E 03	.243304E 03	.300000E 03
13	.000000E 00	.468000E 03	.300006E 03	.120000E 03	.525988E 03	.401038E 03	.300000E 03
14	.000000E 00	.468000E 03	.300006E 03	.120000E 03	.366232E 03	.243304E 03	.300000E 03
15	.000000E 00	.468000E 03	.300006E 03	.108000E 03	-.411535E 03	.118553E 04	.200000E 03
16	.000000E 00	.468000E 03	.300006E 03	-.108000E 03	-.411535E 03	.118553E 04	.200000E 03
17	.000000E 00	.468000E 03	.300006E 03	-.120000E 03	.525988E 03	.401038E 03	.300000E 03
18	.000000E 00	.468000E 03	.300006E 03	-.120000E 03	.366232E 03	.243304E 03	.300000E 03
19	-.240000E 03	.468000E 03	.300006E 03	-.120000E 03	.525988E 03	.401038E 03	.300000E 03
20	-.240000E 03	.468000E 03	.300006E 03	-.120000E 03	.366232E 03	.243304E 03	.300000E 03
21	-.240000E 03	.468000E 03	.300006E 03	-.360000E 03	.525988E 03	.401038E 03	.300000E 03
22	-.240000E 03	.468000E 03	.300006E 03	-.360000E 03	.366232E 03	.243304E 03	.300000E 03
23	-.480000E 03	.468000E 03	.300006E 03	-.360000E 03	.525988E 03	.401038E 03	.300000E 03
24	-.480000E 03	.468000E 03	.300006E 03	-.360000E 03	.366232E 03	.243304E 03	.300000E 03
25	-.480000E 03	.468000E 03	.300006E 03	-.324000E 03	-.411535E 03	.118553E 04	.200000E 03
26	-.480000E 03	.468000E 03	.300006E 03	-.540000E 03	-.411535E 03	.118553E 04	.200000E 03
27	-.480000E 03	.468000E 03	.300006E 03	-.756000E 03	-.411535E 03	.118553E 04	.200000E 03
28	-.480000E 03	.468000E 03	.300006E 03	-.972000E 03	-.411535E 03	.118553E 04	.200000E 03
29	-.480000E 03	.468000E 03	.300006E 03	-.600000E 03	.525988E 03	.401038E 03	.300000E 03
30	-.480000E 03	.468000E 03	.300006E 03	-.600000E 03	.366232E 03	.243304E 03	.300000E 03
31	.480000E 03	-.468000E 03	.300006E 03	.600000E 03	-.525988E 03	.401038E 03	.300000E 03
32	.480000E 03	-.468000E 03	.300006E 03	.600000E 03	-.366232E 03	.243304E 03	.300000E 03
33	.480000E 03	-.468000E 03	.300006E 03	.972000E 03	.411535E 03	.118553E 04	.200000E 03
34	.480000E 03	-.468000E 03	.300006E 03	.756000E 03	.411535E 03	.118553E 04	.200000E 03
35	.480000E 03	-.468000E 03	.300006E 03	.540000E 03	.411535E 03	.118553E 04	.200000E 03
36	.480000E 03	-.468000E 03	.300006E 03	.324000E 03	.411535E 03	.118553E 04	.200000E 03
37	.480000E 03	-.468000E 03	.300006E 03	.360000E 03	-.525988E 03	.401038E 03	.300000E 03
38	.480000E 03	-.468000E 03	.300006E 03	.360000E 03	-.366232E 03	.243304E 03	.300000E 03
39	.240000E 03	-.468000E 03	.300006E 03	.360000E 03	-.525988E 03	.401038E 03	.300000E 03
40	.240000E 03	-.468000E 03	.300006E 03	.360000E 03	-.366232E 03	.243304E 03	.300000E 03
41	.240000E 03	-.468000E 03	.300006E 03	.120000E 03	-.525988E 03	.401038E 03	.300000E 03
42	.240000E 03	-.468000E 03	.300006E 03	.120000E 03	-.366232E 03	.243304E 03	.300000E 03
43	.000000E 00	-.468000E 03	.300006E 03	.120000E 03	-.525988E 03	.401038E 03	.300000E 03
44	.000000E 00	-.468000E 03	.300006E 03	.120000E 03	-.366232E 03	.243304E 03	.300000E 03
45	.000000E 00	-.468000E 03	.300006E 03	.108000E 03	.411535E 03	.118553E 04	.200000E 03
46	.000000E 00	-.468000E 03	.300006E 03	-.108000E 03	.411535E 03	.118553E 04	.200000E 03
47	.000000E 00	-.468000E 03	.300006E 03	-.120000E 03	-.525988E 03	.401038E 03	.300000E 03
48	.000000E 00	-.468000E 03	.300006E 03	-.120000E 03	-.366232E 03	.243304E 03	.300000E 03
49	-.240000E 03	-.468000E 03	.300006E 03	-.120000E 03	-.525988E 03	.401038E 03	.300000E 03
50	-.240000E 03	-.468000E 03	.300006E 03	-.120000E 03	-.366232E 03	.243304E 03	.300000E 03
51	-.240000E 03	-.468000E 03	.300006E 03	-.360000E 03	-.525988E 03	.401038E 03	.300000E 03
52	-.240000E 03	-.468000E 03	.300006E 03	-.360000E 03	-.366232E 03	.243304E 03	.300000E 03
53	-.480000E 03	-.468000E 03	.300006E 03	-.360000E 03	-.525988E 03	.401038E 03	.300000E 03
54	-.480000E 03	-.468000E 03	.300006E 03	-.360000E 03	-.366232E 03	.243304E 03	.300000E 03
55	-.480000E 03	-.468000E 03	.300006E 03	-.324000E 03	.411535E 03	.118553E 04	.200000E 03
56	-.480000E 03	-.468000E 03	.300006E 03	-.540000E 03	.411535E 03	.118553E 04	.200000E 03
57	-.480000E 03	-.468000E 03	.300006E 03	-.756000E 03	.411535E 03	.118553E 04	.200000E 03
58	-.480000E 03	-.468000E 03	.300006E 03	-.972000E 03	.411535E 03	.118553E 04	.200000E 03
59	-.480000E 03	-.468000E 03	.300006E 03	-.600000E 03	-.525988E 03	.401038E 03	.300000E 03
60	-.480000E 03	-.468000E 03	.300006E 03	-.600000E 03	-.366232E 03	.243304E 03	.300000E 03

Table C.2 (CONTINUED)

MATRIX A(I,J)

	ΔX	θY	ΔY	θX	ΔZ	θZ	
1	.634282E 04	.177295E 07					X
2	.177295E 07	.117731E 10					My Y
3			.484735E 04	-.118416E 07			Mx Z
4			-.118416E 07	.132770E 10		.219698E 10	Mz
5							
6							

MATRIX B(I,J),A(I,J) INVERSE

1	.272267E-03	-.410017E-06	-.143185E-21	-.586124E-24	-.213550E-38	.584427E-23
2	-.410017E-06	.146686E-08	.295283E-25	.120874E-27	.440395E-42	-.246441E-25
3	-.143185E-21	.295283E-25	.263768E-03	.235252E-06	.329520E-20	.397634E-42
4	-.586124E-24	.120874E-27	.235252E-06	.963001E-09	.350863E-23	.162771E-44
5	-.213550E-38	.440395E-42	.329520E-20	.350863E-23	.207907E-03	.593045E-59
6	.584427E-23	-.246441E-25	.397634E-42	.162771E-44	.593045E-59	.455170E-09

MATRIX I(I,J),A(I,J)*B(I,J)

1	.100000E 01	.325261E-18	.578634E-53	.752316E-36	.267276E-50	-.376158E-35
2	.238942E-30	.100000E 01	.162943E-49	.667006E-52	.243019E-66	.000000E 00
3	.120371E-34	-.293874E-38	.100000E 01	-.199443E-36	-.173334E-32	-.407832E-55
4	.776892E-50	-.169215E-53	-.119878E-31	.100000E 01	.295823E-30	.334096E-51
5	.167048E-51	-.815663E-55	.000000E 00	-.752316E-36	.100000E 01	-.169794E-71
6	-.157772E-29	.924446E-32	-.427642E-49	-.167048E-51	-.593473E-66	.100000E 01

Matrix A expresses loads at the origin corresponding to the six components of deflection of the frame relative to the envelope.

Matrix B is the inverse of A, for calculating the six components of deflection from known loads.

C.3 JOINT LOADS ON FRAME FROM OUTRIGGERS

The outrigger geometry is shown in Figure C.1 and further defined in the following. Equations are written for the Left Front Outrigger and extended to the other three outriggers by considerations of symmetry.

The outrigger attaches to the starframe at joints LF2, F1 and L2 which have been re-designated as D, E and F, respectively for this analysis. Loads are applied at the helicopter gimbal (point H). Joints D, E and F are assumed to provide resistance for 3 components of force but no moments. The drag strut is pin ended at both ends but the lift strut is pinned at the elbow joint with the pin axis parallel to the "X" axis of the reference system. These features make the outrigger reactions statically determinate.

Geometry

Joint	X	Y	Z
H (Gimbal)	672	1020	125
LF1 (Elbow)	535.384	576	64
D (LF2)	480	468	300
E (F1)	240	0	150
F (L2)	0	468	300

Six equilibrium equations and three geometric constraints are available to determine the three components of reaction at points D, E, and F. Note: The sign convention on these forces is taken so that no reversal of sign is necessary when applying these loads to the starframe joints.

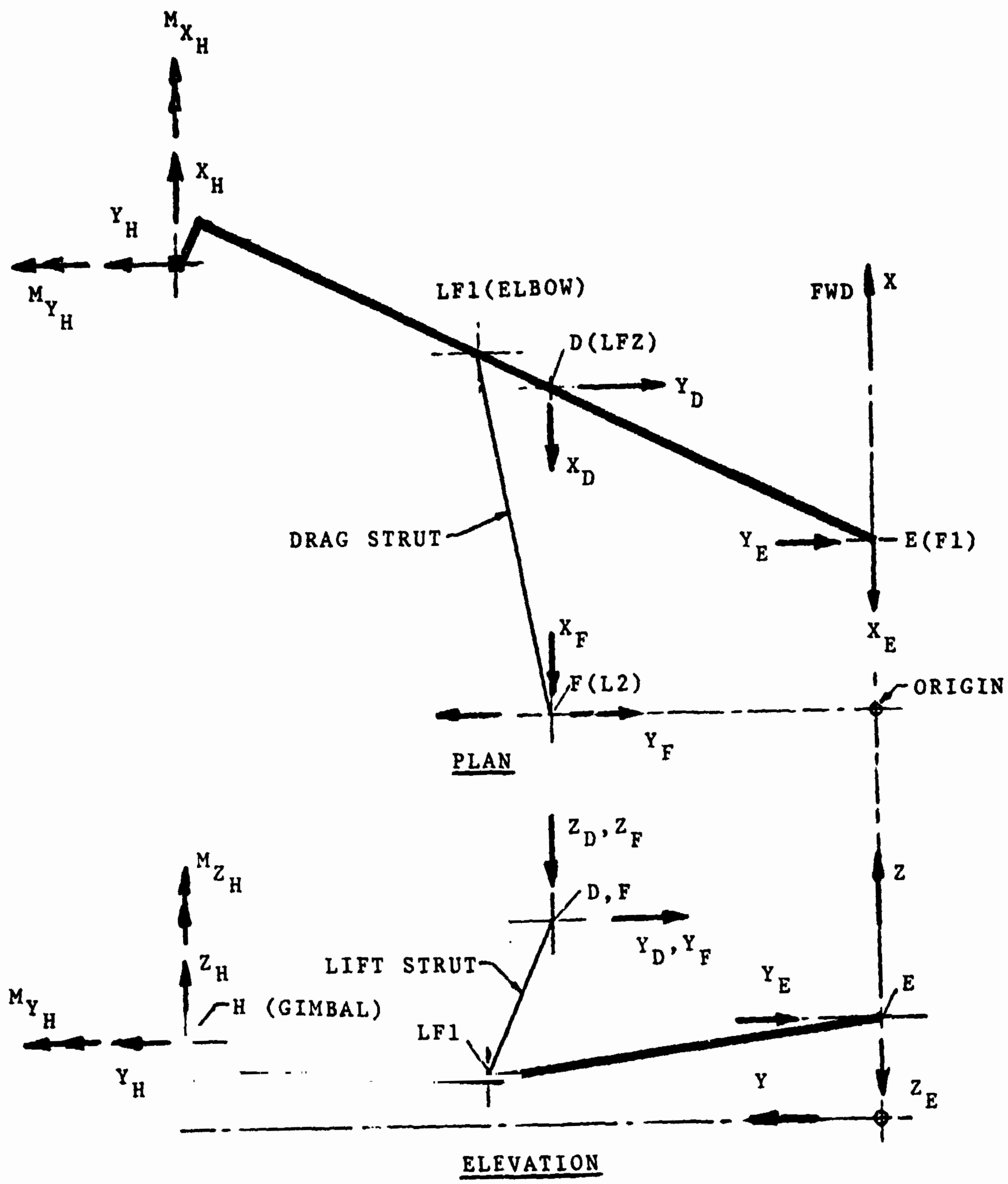

Figure C.1 OUTRIGGER GEOMETRY (SEE TABULATED COORDINATES)

Taking moments about DF

$$1)\quad 552Z_H + Mx_H + 175\ Y_H + 468\ Z_E - 150\ Y_E = 0$$

From requirement that reactions at F have a resultant which passes through the elbow point

$$2)\quad Y_F = \frac{108}{535.384}\ X_F$$

$$3)\quad Z_F = \frac{-\ 236}{535.384}\ X_F$$

Taking moments about the X axis through the elbor [lift strut]

$$4)\quad 108\ Z_D + 236\ Y_D = 0$$

$\Sigma F_X = 0,\ \Sigma F_Y = 0,\ \Sigma F_Z = 0$ Outrigger Free Body

$$5)\quad X_H - X_D - X_E - X_F = 0$$

$$6)\quad Y_H - Y_D - Y_E - Y_F = 0$$

$$7)\quad Z_H - Z_D - Z_E - Z_F = 0$$

Taking moments about the Y axis through the gimbal:

$$8)\quad 125\ X_D + 125\ X_F + 25\ X_E + 192\ Z_D + 432\ Z_E + 672\ Z_F - Mx_H = 0$$

Taking moments about the Z axis through the gimbal

9) $552\ (X_D + X_F) + 1020\ X_E - 192\ Y_D - 432\ Y_E$

$$- 672\ Y_E - M_{Z_H} = 0$$

These nine equations are solved as a subroutine of the integrated computer program by matrix manipulation for the nine components of reaction at the starframe joints for each of the four outriggers. For the left front outrigger the signs of the reactions are a direct result of the equations. For the other 3 outriggers the joints D, E, F are interpreted to be the appropriate joints in the frame from considerations of symmetry. The signs of the reactions as related to the Left Front solution is taken from the following table where the layout in each block of 4 is as follows:

Left Front	Right Front
Left Rear	Right Rear

Positive signs in this display mean that the sign is the same as the left front solution. Negative signs mean the sign of the reaction is opposite that for the left front solution.

GIMBAL LOADS		REACTIONS X	REACTIONS Y	REACTIONS Z
	X	+ +	+ -	+ +
		+ +	- +	- -
	Y	+ -	+ +	+ -
		- +	+ +	+ -
	Z	+ +	+ -	+ +
		- -	+ -	+ +
	M_X	+ -	+ +	+ -
		- +	+ +	+ -
	M_Y	+ +	+ -	+ +
		+ +	- +	- -
	M_Z	+ -	+ +	+ -
		+ -	- -	- +

C.4 FRAME MEMBER LOAD ANALYSIS

The loads in the members of the starframe are evaluated by the method of joints utilizing joint loads compiled from three sources:

1) The tabulation of "other joint loads" from Tables B.1 through B.7.

2) Joint loads on the starframe resulting from loads applied at the helicopter gimbals (Section C.3).

3) Joint loads representing the suspension system reaction (Section C.2).

Joint loads X, Y, Z are positive forward, to the left and up. Frame members are identified in Figure C.2. The geometry of he frame is described by the X, Y, Z coordinates of the joints (Table C.3) where the origin of the coordinate system is in the ground plan at the geometric center of the plan form. Coordinates are also positive forward, to the left and up from the origin. Direction cosines of the frame members are developed in Table C.4.

Member loads are determined by setting the unbalanced force equal to zero at each joint in succession with the results as shown in Table C.5. X, Y, and Z forces shown in these equations refer to the joint loads compiled from three sources as described above for the subject joint. Joints and members are as identified in Figure C.2. Subscripts on the "P" values are frame member identifications. Equations are written for the Left-Front quadrant. The equations for the other quadrants are written from considerations of symmetry.

C.5 FRAME MEMBER CRITICAL LOADS AND DESIGN

The integrated frame analysis program accepts the loading condition data from Tables B.1 through B.7 and processes the data to produce loads in each member of the framework. The equations developed in Sections C.2, C.3 and C.4 and supporting geometric data are an integral part of the computer program. Since the framework has two planes of symmetry all members not in the planes of symmetry occur 4 times in the structure, members in the planes of symmetry occur twice with the exception of the keel which lies in one plane and passes through the other.

Table C.3 FRAME JOINT LOCATIONS

JOINT	X	Y	Z
F1	240	0	150
LF2	480	468	300
LF6	300	292.50	356.25
LF4	240	468	300
C2	0	0	450
L2	0	468	300
LA4	-240	468	300
LA6	-300	292.50	356.25
LA2	-480	468	300
A1	-240	0	150
RA2	-480	-468	300
RA6	-300	-292.50	356.25
RA4	-240	-468	300
R2	0	-468	300
C2	0	0	450
RF4	240	-468	300
RF6	300	-292.50	356.25
RF2	480	-468	300
F1	240	0	150

Table C.4

FRAME MEMBER LENGTHS - PROJECTIONS - COSINES

	MEM.	X	Y	Z	L	X/L	Y/L	Z/L
1	LF2-LF4	- 240	0	0	240	-1	0	0
2	LF2-F1	- 240	-468	-150	546.92	-.43882	-.85570	-.27426
3	LF2-LF6	- 180	-175.5	56.25	257.61	-.69872	-.68126	.21835
4	LF4-LF6	60	-175.5	56.25	192.97	.31094	-.90949	.29150
5	L2-LF6	300	-175.5	56.25	352.09	.85207	-.49846	.15976
6	LF4-F1	0	-468	-150	491,45	0	-.95228	-.30522
7	LF4-L2	- 240	0	0	240	-1	0	0
8	LF6-C2	- 300	-292.50	93.75	429.35	-.69872	-.68126	.21835
9	L2-C2	0	-468	150	491.45	0	-.95228	.30522
10	LA6-C2	300	-292.50	93.75	429.35	.69872	-.68126	.21835
11	LA4-L2	240	0	0	240	+1	0	0
12	LA4-A1	0	-468	-150	491.45	0	-.95228	-.30522
13	L2-LA6	- 300	-175.5	56.25	352.09	-.85207	-.49846	.15976
14	LA4-LA6	- 60	-175.5	56.25	192.97	-.31094	-.90949	.29150
15	LA2-LA6	180	-175.5	56.25	257.61	.69872	-.68126	.21835
16	LA2-A1	240	-468	-150	546.92	.43882	-.85570	-.27426
17	LA2-LA4	240	0	0	240	+1	0	0
18	C2-A1	- 240	0	-300	384.19	-.62469	0	-.78087
19	F1-A1	- 480	0	0	480	-1	0	0
20	C2-F1	240	0	-300	384.19	.62469	0	-.78087
21	RF2-RF4	- 240	0	0	240	-1	0	0
22	RF2-F1	- 240	468	-150	546.92	-.43882	.85570	-.27426
23	RF2-RF6	- 180	175.5	56.25	257.61	-.69872	.68126	.21835
24	RF4-RF6	60	175.5	56.25	192.97	+.31094	+.90949	+.29150
25	R2-RF6	300	175.5	56.25	352.09	.85207	.49846	.15976
26	RF4-F1	0	468	-150	491.45	0	+.95228	-.30522
27	RF4-R2	- 240	0	0	240	-1	0	0
28	RF6-C2	- 300	292.50	93.75	429.35	-.69872	.68126	.21835
29	R2-C2	0	468	150	491.45	0	.95228	.30522
30	RA6-C2	300	292.50	93.75	429.35	.69872	.68126	.21835
31	RA4-R2	240	0	0	240	1	0	0
32	RA4-A1	0	468	-150	491.45	0	.95228	-.30522
33	R2-RA6	- 300	175.5	56.25	352.09	-.85207	.49846	.15976
34	RA4-RA6	- 60	175.5	56.25	192.97	-.31094	.90949	.29150
35	RA2-RA6	180	175.5	56.25	257.61	.69872	.68126	.21835
36	RA2-A1	240	468	-150	546.92	.43882	.85570	-.27426
37	RA2-RA4	240	0	0	240	+1	0	0
38	F1-L2	- 240	468	150	546.92	-.43882	.85570	.27426
39	A1-L2	240	468	150	546.92	.43882	.85570	.27426
40	F1-R2	- 240	-468	150	546.92	-.43882	-.85570	.27426
41	A1-R2	240	-468	150	546.92	-.43882	-.85570	.27426

Table C.5 - MEMBER LOAD EQUATIONS

Joint	Equation	Results
LF2	$\Sigma F_X = 0$	$P_1 = X - .76923Y + .79999Z$
	$\Sigma F_Y = 0$	$P_2 = .58432Y + 1.82309Z$
	$\Sigma F_Z = 0$	$P_3 = .73394Y - 2.28990Z$
LA2	Sym	$P_{17} = -X -.76923Y + .79999Z$
		$P_{16} = .58432Y +1.82309Z$
		$P_{15} = .73394Y -2.28990Z$
RF2	Sym	$P_{21} = X +.76923Y + .79999Z$
		$P_{22} = -.58432Y +1.82309Z$
		$P_{23} = -.73394Y -2.28990Z$
RA2	Sym	$P_{37} = -X +.76923Y + .79999Z$
		$P_{36} = -.58432Y +1.82309Z$
		$P_{35} = -.73394Y -2.28990Z$
LF4	$\Sigma F_X = 0$	$P_4 = .54976Y -1.71525Z$
	$\Sigma F_Y = 0$	$P_6 = .52505Y +1.63817Z$
	$\Sigma F_Z = 0$	$P_7 = X +.17094Y - .53334Z + P_1$
LA4	Sym	$P_{14} = .54976Y -1.71525Z$
		$P_{12} = .52505Y +1.63817Z$
		$P_{11} = -X +.17094Y - .53334Z + P_{17}$
RF4	Sym	$P_{24} = -.54976Y -1.71525Z$
		$P_{26} = -.52505Y +1.63817Z$
		$P_{27} = X -.17094Y - .53334Z + P_{21}$

Table C.5 - MEMBER LOAD EQUATIONS [CONT]

Joint	Equation	Results
RA4	Sym	$P_{34} = -.54976Y - 1.71525Z$
		$P_{32} = -.52505Y + 1.63817Z$
		$P_{31} = -X - .17094Y - .53334Z + P_{37}$
LF6	$\Sigma F_X = 0$	$P_5 = -.91216\ P_4$
	$\Sigma F_Y = 0$	$P_8 = P_3 + .66736\ P_4$
LA6	Sym	$P_{13} = -.91216\ P_{14}$
		$P_{10} = P_{15} + .66736\ P_{14}$
RF6	Sym	$P_{24} = -.91216\ P_{25}$
		$P_{28} = P_{23} + .66736\ P_{24}$
RA6	Sym	$P_{33} = -.91216\ P_{34}$
		$P_{30} = P_{35} + .66735\ P_{34}$
L2	$\Sigma F_X = 0$	$P_9 = .52505Y - 1.63818Z - .52344\ (P_5 + P_{13})$
	$\Sigma F_Y = 0$	$P_{38} = .32179Y - 1.13942\ (X + P_7 - P_{11}) + .91154Z - .97086\ (P_5 - P_{13})$
	$\Sigma F_Z = 0$	$P_{39} = .32179Y + 1.13942\ (X + P_7 - P_{11}) + .91154Z + .97086\ (P_5 - P_{13})$
R2	Sym	$P_{29} = -.52505Y - 1.63818Z - .52344\ (P_{25} - P_{33})$
		$P_{40} = -.32179Y - 1.13942\ (X + P_{27} - P_{31}) + .91154Z - .97086\ (P_{25} - P_{33})$
		$P_{41} = -.32179Y + 1.13942\ (X + P_{27} - P_{31}) + .91154Z + .97086\ (P_{25} - P_{33})$

Table C.5 - MEMBER LOAD EQUATIONS [CONT]

Joint	Equation	Results
C2	$\Sigma F_X = 0$ $\Sigma F_Y = 0$	$P_{18} = .80041X + .64031Z + .41944 (P_8 + P_{28}) - .69907 (P_{10} + P_{30}) - .19544 (P_9 + P_{29})$ $P_{20} = -.80041X + .64031Z + .41944 (P_{10} + P_{30}) - .69907 (P_8 + P_{28}) - .19544 (P_9 + P_{29})$
F1	$\Sigma F_X = 0$	$P_{19} = X + .43882 (P_2 + P_{22} - P_{38} - P_{40}) - .62469 P_{20}$

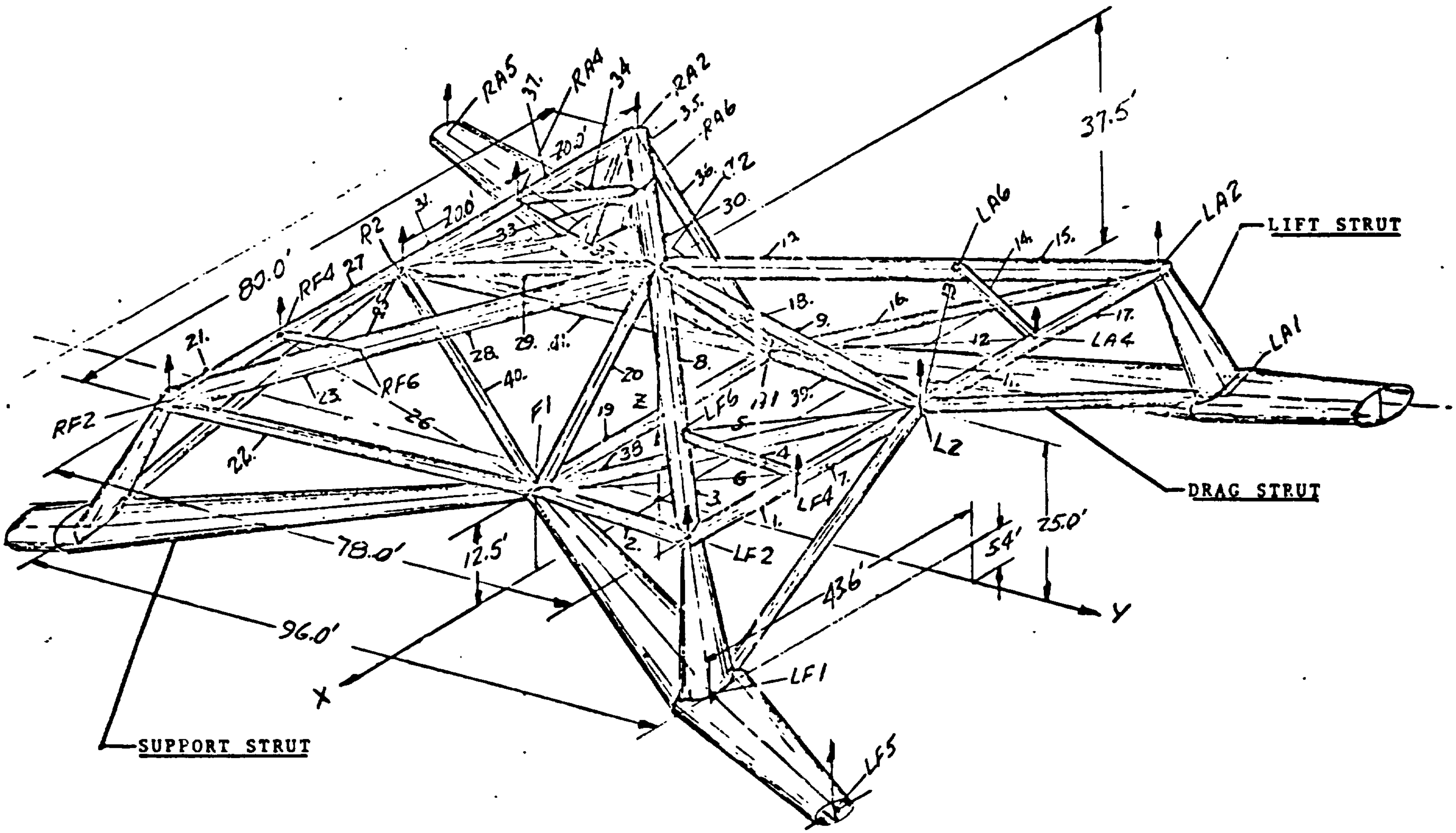

Figure C.2 INTERCONNECTING STRUCTURE (CONSISTING OF FOUR LIFT STRUTS, FOUR DRAG STRUTS, FOUR SUPPORT STRUTS AND ONE INTERNAL STAR FRAME)

Table C.6 presents the maximum and minimum loads occurring in each member or its symmetrical opposites for each of the seven design loading conditions.

Note that critical loads occur in Condition 1.1 (Dynamic Collective) for most of the main members. In several cases the Condition 2.1 (One Engine Out Dynamic Collective) is slightly more critical. The 2 wheel landing condition produces critical loads in many of the main members representing approximately a 50% reversal of the Condition 1.1 loads. The maximum yawing effort condition is critical on certain lightly loaded members and the center point mooring condition appears to be critical for the keel only. Refer to Figure C.2 for identification of the members.

All frame members are 3 boom girders of welded steel construction. Characteristics are as described in Section A.2.4 with $E = 30 \times 10^6$, $D/t = 40$, $F_{cy} = 180{,}000$ psi, $F_{TU} = 180{,}000$ in the as-welded condition. Material is HP9420 steel.

The theoretical optimum design of the frame members is shown in Table C.7. P_c and P_T are the maximum compression and maximum tension loads of Table C.5 multiplied by a Factor of Safety of 1.5, expressed in Kips.

The unsupported length L is taken from the geometry, Table C.4.

The structural index P/L^2 is in lbs/in^2.

The optimum effective stress σ_{0_e} is taken from Section A.2.4 with $E = 30 \times 10^6$ and $D/t = 40$.

TABLE C.6 - FRAME MEMBER LOADS [LIMIT]

LOADING COND.			1.1	2.1	3.1	4.1	5.1	6.2	7.1
MEMBER			D.C.	O.E.O	X.W.H	M.Y.E	4PT.L	2PT.L	C.P.M
1	LF2-LF4		-	-	-	-	-	-62.2	-19.5
			112.9	116.9	59.6	55.8	12.1	44.8	2.1
2	LF2-F1		-	-	-	-	-	-89.7	-22.1
			154.9	161.2	79.7	82.9	11.4	61.4	-
3	LF2-LF6		-266.9	-274.8	-126.4	-115.8	-25.2	-104.2	-
			-	-	-	-	-	150.8	37.2
4	LF4-LF6		0	- 1.9	-7.5	- 9.0	- 1.3	- 4.2	-11.2
			.9	-	-	-	-	-	-
-	L2-LF6		-.8	-	-	-	-	-	-
			-	1.7	6.9	8.3	1.2	3.8	10.2
6	LF4-F1		- 1.5	-	-	-	-	-	-
			-	3.2	13.1	16.0	2.2	7.0	15.9
7	LF4-L2		-	-	-	-	-	-63.5	-20.7
			113.2	116.4	57.2	56.4	13.2	43.5	-
8	LF6-C2		-266.3	-276.0	-131.2	-129.6	-261.3	-106.9	-
			-	-	-	-	-	148.0	34.8
19	F1-A1		-	-	-	-	-	-18.5	-106.6
	KEEL		74.1	52.8	15.0	13.0	1.7	-	-
20	F1-C2		-	-	-	-	-	- 7.7	-
			159.4	135.5	80.7	79.6	17.9	-	2.9
38	F1-L2		-	-32.0	-14.3	- 3.7	-	-99.3	-
			12.0	55.5	41.5	25.2	5.0	107.5	21.9
	LF1-L2		-20.4	-19.4	-16.1	- 25.1	-2.8	-6.9	-34.0*
	DRAG STRUT		-	-	7.7	13.8	-	11.1	8.1
	LF1-LF2	Z	108.2	106.2	29.6	42.7	15.3	-60.1	-43.7
	LIFT STRUT	X	- 5.6	- 4.7	- 9.4	18.4	.8	3.0	2.2
	LF1-F1	X	21.7	20.7	25.5	-26.0	3.3	13.1	9.5
	ARM	Y	53.2	52.1	-31.8	-17.0	7.5	29.5	-21.5
		Z	-55.0	-53.9	-22.8	-17.3	-7.8	30.6	22.2
9	L2-C2		-27.2	-28.8	-33.7	-37.1	-8.4	- 9.8	-42.4

*Includes tether cable loads.

TABLE C.6 FRAME MEMBER LOADS [LIMITS] (Continued)

Condition 7.1

Drag Strut Loads $C_X = \pm.89983$

	X_F	Load	Added Load-Cable	Total Load
LF	7313	8127	0	8127
RF	-5044	-5605	-28407	-34012
LA	-7313	8127	0	8127
RA	5044	-5605	-28407	-34012

TABLE C.7 FRAME MEMBER DESIGN (THEOR. OPTIMUM)

MEMBER Name	MEMBER I.D.	Loads P_c	Loads P_T	Length L	P_c/L^2	σ_{o_e}	A_c *	ΔA	A	Theo. Wt.	b_{opt}	D_{opt}	t_{cap}
Shoulder	LF2-LF4 LF4-L2	95	175	480	.41	89	.711	.26	.974	183	25	1.74	.059
Keel	F1-A1	160	111	480	.69	106	1.01	-	1.01	207	27.26	2.06	.052
W Strut (End)	LF2-F1	135	242	547	.45	92	.977	.37	1.343	287	28.89	2.035	.070
W Strut (Center)	F1-L2	149	161	547	.50	95	1.05	-	1.05	246	29.39	2.11	.053
Bi Pod	F1-C2	12	240	384	.08	51.3	.15	1.18	1.33	154	15.17	.80	.176
Pyramid	LF2-LF6 LF6-C2	412	226	687	.87	114.5	2.40	-	2.40	707	40.54	3.19	.080
Drag Strut		51	21	595	.144	62.8	.541	-	.541	139	26.17	1.51	.038
Cross Strut	L2-C2	63.6	-	491	.26	76.8	.552	-	.552	116	23.75	1.53	.038

$$* \quad A_c = \frac{P_c}{1.5 \times \sigma_{o_e}}$$ (Ref. Page A-7)(Compression Cap Area Required)

ORIGINAL PAGE IS
OF POOR QUALITY

The required boom area in compression A_c is $P_c \div \sigma_{0_e}$ (1.5) (Ref. Page A.8)

ΔA is the additional boom area required when P_T exceeds the tension strength of the strut designed on the basis of compression alone

$$\Delta A = \frac{P_T}{180} - A_c$$

where A is the total area $A_c + \Delta_c$

The theoretical weight is 0.286 $(1.5\ A_c + \Delta_A)$.

b_{opt} is taken from Section A.2.4 with $E = 30 \times 10^6$ and represents optimum dimension for the compression strut from center to center of corner tubes.

D_{opt} is taken from Section A.2.4 - with $E = 30 \times 10^6$ represents the optimum boom tube diameter for the compression load with $D/t = 40$ and lattice arrangement as in Section A.2.3 - D_{opt} is measured to the center of the wall thickness.

APPENDIX D

DETAILS OF OUTRIGGER ANLAYSIS

CONVERSION FACTORS FOR APPENDIX D

1.0 Kip	=	$4.536 \times 10^{+2}$ kg
1.0 Ksi	=	$6.89 \times 10^{+6}$ N/sq m
1.0 lb/in	=	1.786 kg/m
1.0 psi	=	$6.89 \times 10^{+3}$ N/sq m
1.0 sq in	=	6.45×10^{-2} sq m

D.1 GENERAL

This Appendix provides details of the outrigger analysis as described in Section 5.8 of Book I of this Volume of the report.

D.2 MAIN STRUT SHEARS AND MOMENTS

The outer arm of the main strut has a chord plane in WL 64 and its axis extends outward and forward making an angle of 26.4093° with the lateral direction as shown in Drawing 76-082. The spar lies in a vertical plane through the axis. The helicopter loads are applied at the gimbal which is located 61 inches above the chord plane and 75.124 inches aft of the strut axis measured normal to the plane of the spar.

Working with this geometry and the gimbal loads tabulated in Tables B.1 through B.7 the equations for the shears and moments on three sections of the outrigger are derived. Section 2 is a theoretical rib station normal to the spar containing the gimbal point. Section 3 is located at the intermediate rib shown on the drawing and Section 4 is at the "elbow" containing the theoretical intersection point of the lift strut and drag strut with the main strut axis (see drawing). The equations are as follows:

SECTION (2)

H	=	$.09564X_H - .44478Y_H$	Chordwise Shear
V	=	Z_H	Beam Shear
P	=	$.44478X_H + .89564Y_H$	Axial Tension
M_C	=	$33.414X_H + 67.284Y_H - M_{ZH}$	
M_B	=	$.89564M_{XH} - .44478MY_H$	
T	=	$75.124Z_H + .89564M_{YH} + .44478M_{XH}$	

SECTION (3)

$H = .09564X_H - .44478Y_H$

$V = Z_H$

$P = .44478X_H + .89564Y_H$

$M_C = M_{CZ}' + 217.259H_Z'$

$M_B - M_{BZ} + 217.259Y_Z'$

$T = 75.124Z_H + .89564M_{YH} + .44478M_{XH}$

SECTION (4)

$H = .09564X_H - .44478Y_H$

$V = Z_H$

$P = .44478X_H + .89564Y_H$

$M_C = M_{CZ}' + 458.427H_Z'$

$M_B = M_{BZ}' + 458.427Y_Z'$

$T = 75.124Z_H + .89564M_{YH} + .44478M_{XH}$

The shears and moments resulting from these equations and the helicopter loads corresponding to the seven loading conditions are tabulated in Table D.1. Shears in Kips, moments in in. lbs times 10^{-6}. Values shown are limit loads and are to be multiplied by a factor of safety of 1.5 to produce design ultimate loads. In most cases critical stresses are produced by the loads of Condition 1.1.

D.3 SECTION PROPERTIES

The section properties of the main strut of the outrigger are evaluated as follows:

1) A trial cross section (at the elbow) is developed and evaluated (Figure D.1).

TABLE D.1 - OUTRIGGER SHEARS AND MOMENTS

LOADING CONDITION

			1.1	2.1	3.1	4.1	5.1	6.2	7.1
G	X_H	(K)	-1.82	-1.36	-1.62	8.60	0	0	0
I	Y_H	(K)	0	0	-10.00	0	0	0	0
M	Z_H	(K)	61.12	59.90	15.23	20.00	8.64	-33.95	-24.70
B	M_{XH}		0	0	0	-.40	0	0	0
A	M_{YH}		0	0	0	0	0	0	0
L	M_{ZH}		-1.85	-1.85	-4.68	-1.98	0	0	0
	H		-1.63	-1.22	3.00	7.70	0	0	0
	V		61.12	59.90	15.23	20.00	8.64	-33.95	-24.70
2	P		-.81	-.60	-9.68	3.82	0	0	0
	M_C		1.789	1.804	4.626	2.267	0	0	0
	M_B		0	0	0	-.358	0	0	0
	T		4.481	4.401	1.045	1.850	.649	-2.550	-1.855
	H		-1.63	-1.22	3.00	7.70	0	0	0
	V		61.12	59.90	15.23	20.00	8.64	-33.95	-24.70
3	P		-.81	-.60	-9.68	3.82	0	0	0
	M_C		1.435	1.539	5.278	3.940	0	0	0
	M_B		13.279	13.014	3.309	3.987	1.877	-7.376	-5.366
	T		4.481	4.401	1.045	1.850	.649	-2.550	-1.855
	H		-1.63	-1.22	3.00	7.70	0	0	0
	V		61.12	59.90	15.23	20.00	8.64	-33.95	-24.70
4	P		-.81	-.60	-9.68	3.82	0	0	0
	M_C		1.042	1.245	6.001	5.796	0	0	0
	M_B		28 019	27.460	6.982	8.810	3.961	-15.564	-11.323
	T		4.481	4.401	1.045	1.850	.649	-2.550	-1.855

$$Y = 36\,[1 - (X/72)^2]^{\frac{1}{2}}$$

$$dy/dx = -\tfrac{1}{4}\,X/Y$$

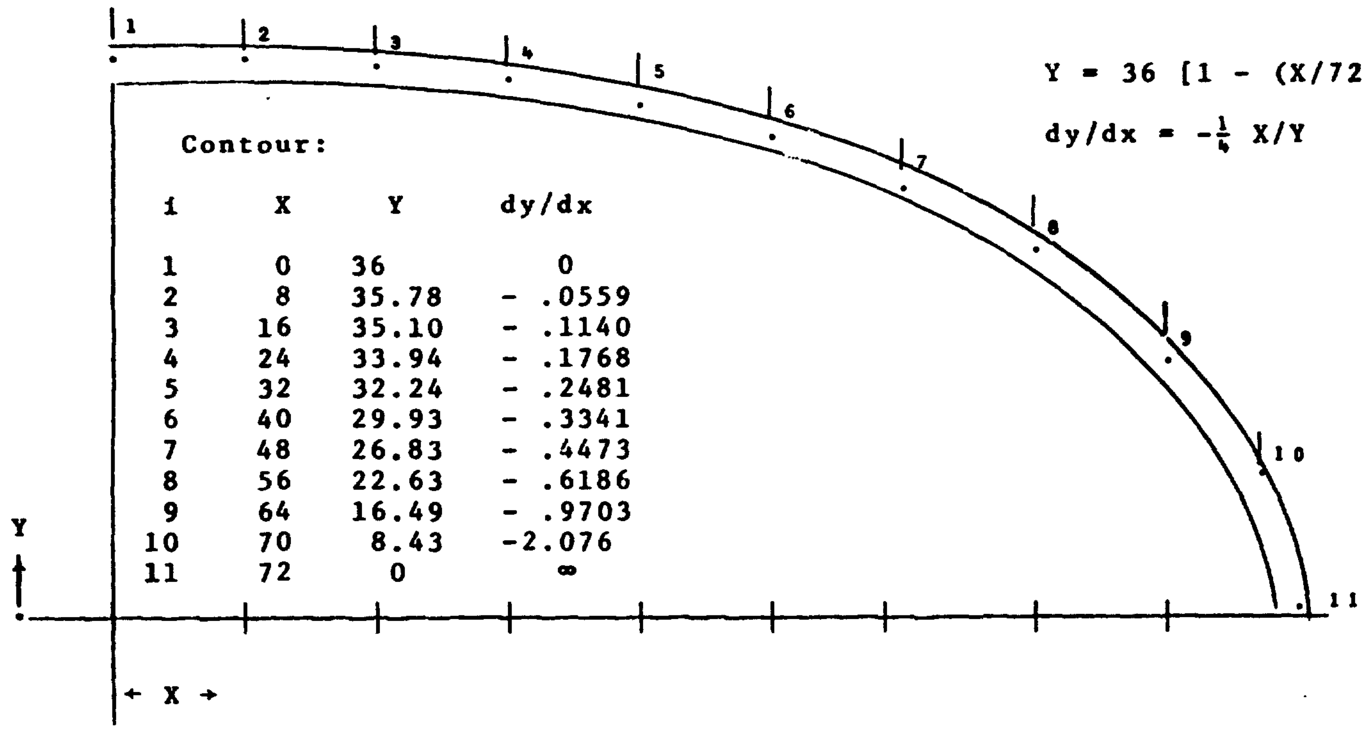

Contour:

i	X	Y	dy/dx
1	0	36	0
2	8	35.78	- .0559
3	16	35.10	- .1140
4	24	33.94	- .1768
5	32	32.24	- .2481
6	40	29.93	- .3341
7	48	26.83	- .4473
8	56	22.63	- .6186
9	64	16.49	- .9703
10	70	8.43	-2.076
11	72	0	∞

Figure D.1 Trial Section Properties of Outrigger - Max. Section 72 x 144

2) A preliminary calculation of the critical bending stresses indicates that reductions in face sheet gages and spar cap areas are possible.

3) A revised section property using reduced material areas was projected from the trial section data.

4) Section properties at the midway Section (3) and the outboard Section (2) are projected from the properties at Section (4) by appropriate ratios.

Item	X	Y	A		$A_X{}^2$		$A_Y{}^2$	
1	0	35.10	2.76		0		3400	
2	8	34.88	.64	2.59	40	3939	779	3965
3	16	34.20	.64		164		749	
4	24	34.04	.65		374		753	
5	32	31.35	.66		676		648	
6	40	29.03	.67		1072		565	
7	48	25.93	.70		1613		471	
8	56	21.73	.75	2.55	2352	10455	354	586
9	63.2	15.69	.75		2996		185	
10	69.2	7.93	.75		3591		47	
11	71.1	0	.30		1516		0	
			7.90		14394		7961	

Item 1: $I_y = 57576$, $I_x = 31804$

Spar Cap	4.0^2
$\frac{1}{6} \times 72 \times .04$	.48
Sand.	.64
Reinfor.	.40
	5.52/2

OUTRIGGER REVISED SECTION PROPERTIES

[Based on Trial Section]

At Max Section reduce spar cap area by 1.0 sq in.

Use .032 gage skins Items 2 thru 7
.020 gage skins Items 8 thru 11

$$\frac{2.26}{2.76} \times 3400 = 2784$$

$$\frac{.032}{.040} \times 3965 = 3172$$

$$\frac{.020}{.040} \times 586 = \frac{293}{6249}$$

$$I_x = 24,996$$

$$\left(\frac{M_x e}{I_x} = \frac{42.03 \times 10^6 \times 35.1}{24,996} = 59,020 \text{ psi} \right)$$

$$\frac{.032}{.040} \times 3939 = 3151$$

$$\frac{.020}{.040} \times 10455 = \frac{5227}{8378}$$

$$I_y = 33,512$$

$$\left(\frac{M_y c}{I_y} = \frac{9.002 \quad 10 \quad 71.1}{33,512} = 19,100 \text{ psi} \right)$$

Extension to mid and outboard sections - maintain .032 cover skins throughout - assume true conic section.

$$I_x = K_x b^3 + 2a^2 A_s$$

$$K_x = \frac{(3172 + 293)4}{71.1^3} = .03856$$

$$I_y = K_y b^3 = K_y (\overline{71.1^3}) = 4(3151 + 5227), \; K_y = .09324$$

Section	a	b	A_s	I_x	I_y	Bare Cap
4	35.1	71.1	4.52	24996	33512	3.0
3	24.9	50.5	3.09	8798	12008	1.95
2'	16.1	32.6	1.53	2129	3230	.77

D.4 STRESS ANALYSIS

Bending Stresses

Maximum bending stresses occur in Condition 1.1 in region of the center spar cap. Maximum Stresses at the T.E. and L.E. occur in Condition 3.1.

Section	$M_{x_{max}}^{*} \times 10^{-6}$	f_b	$M_{y_{max}}^{*} \times 10^{-5}$	$f_{b_{L.E.,T.E.}}$
4	42.03	59020	9.002	19099
3	19.92	56380	7.917	33295
2'	0	0	6.939	70304**

*Ultimate, includes factor of safety of 1.50

**Local reinforcements will be required for a short distance inward from the outboard station at the L.E. and T.E.

Torsion Analysis

Torque Box Area = πab

Section	a	b	πab	T_{max}	q_T	τ_T
4	35.1	71.1	7860	6.72×10^6	428	6.7 KSI
3	24.9	50.5	3960	6.72×10^6	850	13.3
2'	16.1	32.6	1650	6.72×10^6	2040	32 KSI

Stability of the Sandwich Shell

Core thicknesses are designed to provide elastic stability to 60,000 psi for bending stresses and 40,000 psi for shear stresses.

The chordwise and beamwise shear forces will add and subtract from the torsional shear and must be taken into account for local stresses but the overall buckling is evaluated only on the basis of the bending and torsion as a reasonable approximation.

$$M.S. = \frac{1}{\sqrt{\left(\frac{M}{M_A}\right)^2 + \left(\frac{T}{T_n}\right)^2}} - 1$$

Section	M/M_a	T/T_a	M.S.
4	.984	.17	.001
3	.940	.33	.004
2'	0	.80	+.25

Direct Shear Stresses

Since the torsional shear stresses are low except near the outer end, the addition of direct shear stresses will not be a problem except near the outer end. Therefore, a simple approximation will suffice.

For beam shear assume $\frac{2}{3}$ of vertical shear goes into the spar web with $\frac{1}{6}$ around the ends with an additional factor of 1.05 included. For chordwise shear, use 1.5 times the average over the chord is used.

Direct Shear - Outboard Section

Added to torsion shear Condition 1.1

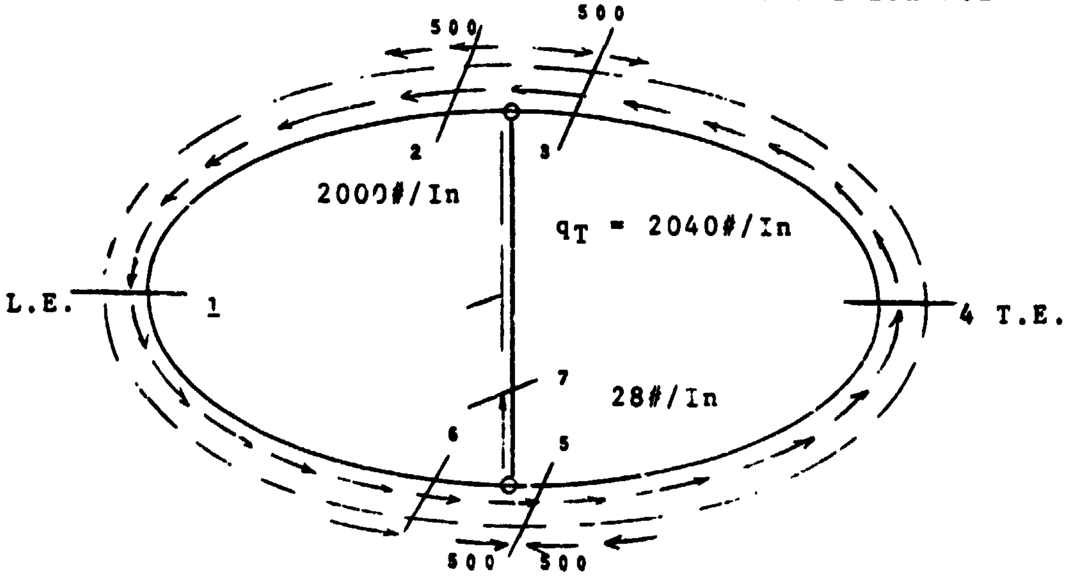

$$H = -2445 \text{ lbs} \quad \frac{H}{4b} \quad 1.5 = \frac{2445 \times 1.5}{4 \times 32.6} = 28.2 \text{ Lb/In}$$

$$V = 92{,}000 \text{ lbs} \quad \frac{V}{2a} = \frac{92{,}000}{2 \times 16.1} = 2{,}860 \text{ Lb/In}$$

Spar Web $q = \frac{2}{3} \times 2860 \times 1.05 = 2{,}000$ Lb/In

L.E. & T.E. $q = \frac{1}{6} \times 2860 \times 1.05 = 500$ Lb/In

Cut	q_T	q_H	q_Y	q_{Tot}	t_f	Shear Stress KSI
1	2040	0	-500	1540	.020	38.5
2	2040	-18	+500	2522	.032	39.4
3	2040	-18	-500	1522	.032	23.8
4	2040	0	+500	2540	.032	39.7
5	2040	+18	-500	1558	.032	24.3
6	2040	+18	+500	2558	.032	40.0
7	0	0	2000	2000	.025	40.0

Spar Web

Since the outrigger area is a conical geometry the shear flows will fall off inversely with the square of the depth.

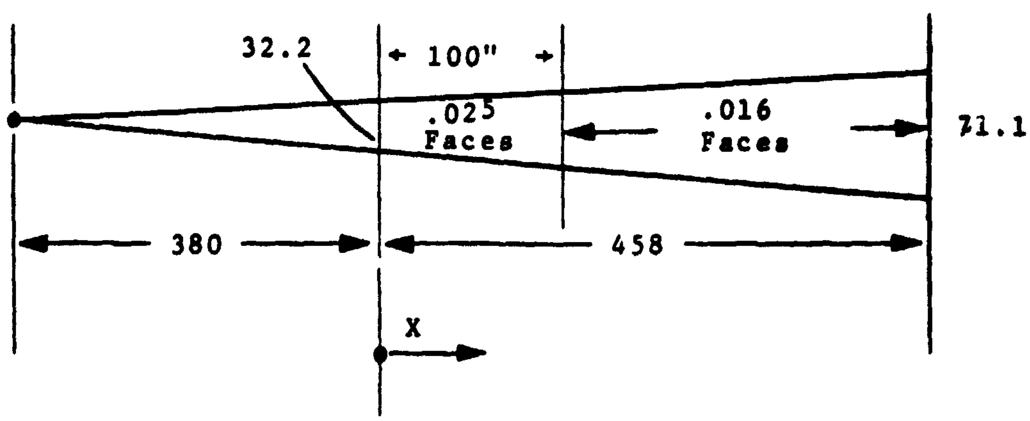

$$\frac{32.2}{38.9} \times 458 = 380$$

SPAR SHEAR FLOWS

X	q		
0	2000		
50	1560	.025	Faces
100	1250		
150	1030		
200			
250			
300		.016	Faces
350			
400			
458			

APPENDIX E

ENVELOPE ANALYSIS

CONVERSION FACTORS FOR APPENDIX E

1.0 ft	=	3.048×10^{-1} m
1.0 ft/sec	=	3.048×10^{-1} m/s
1.0 in	=	2.54×10^{-2} m
1.0 kt	=	5.144×10^{-1}
1.0 lb	=	4.535×10^{-1} kg
1.0 lb/ft	=	1.49 kg/m
1.0 lb/st ft	=	$4.788 \times 10^{+1}$ N/sq m
1.0 mph	=	4.47×10^{-1} m/s

E.1 GENERAL

This Appendix reports details of the HLA envelope analysis (see Section 5.9 of Book I of this volume of the report).

E.2 ENVELOPE PRESSURE REQUIREMENTS*

Section 5.9.2 of Book I of this volume of the report delineates the critical design conditions considered in determining the required envelope pressure. This section provides additional data relative to the development of the pressure requirements.

E.2.1 Masted Out

When masted out the airship is secured through attachments to the interconnecting structure which permits the airship to weathervane freely. The stable position which it assumes is broadside to the direction of the wind.

The shape of the cross section of the envelope when masted out at 65 MPH was determined for various levels of pressure. It was found that a pressure of 5" H_2O measured at the interconnecting structure was required to provide acceptable envelope deformations. The cross sectional shape of the envelope when subjected to 65 MPH and with 5" H_2O pressure is shown in Section

E.2.2 Landing

The dynamic interaction between the car and the envelope was studied. It was found that the critical condition for the envelope occurs after impact when the motion of the envelope and the car were out of phase. In the four-point landing at a 5 ft/sec sinking speed the condition produced a dynamic load of 50,000 lbs on the envelope in addition to the 100,000 lb static load. The static load was reacted by the net lift of the envelope. The dynamic load was

---

reacted by the mass of envelope which included the weight of the envelope and helium and the apparent mass of the air surrounding the envelope.

The apparent air mass was taken as 85% of the displaced volume of the envelope (Reference 2).

The maximum bending moment occurred at the center of the envelope.

E.2.3 Flight - Maneuver

The critical condition for maneuver occurs in the dynamic collective condition in which the envelope is subjected to a 50,000 lb dynamic load from the interconnecting structure in addition to this 100,000 lb static load of the structure supported by the envelope. Since these loads are the same as those used for the landing condition the dynamic and static moments will also be the same.

E.2.4 Flight - Gust

The envelope is designed to resist a 50 FPS gust when flying at 65 knots. The aerodynamic moment is determined from the formula

$$M_A = C_M \frac{U}{V} \cdot q \forall = \frac{1}{2} C_M U V \rho \forall$$

Where U = gust velocity ft/sec

V = airship velocity ft/sec

ρ = air density

$\forall$ = envelope volume cu ft

$C_M = 0.11 + \frac{3F}{80}$

F = fineness ratio = $\frac{342}{107}$ = 3.2

$$M_A = \frac{1}{2} \left(.11 + \frac{3 \times 3.2}{80}\right) \quad 50 \times 109.71 \cdot .002378 \cdot 2{,}500{,}000$$

$$M_A = 3{,}831{,}827 \text{ ft lbs}$$

This moment is probably conservative since it was derived for an envelope with an empennage.

E.2.5 Flight - Maximum Yaw

The maximum yaw condition occurs in a tight turn. The dynamic moment was determined for this condition and found to be low when compared to the other flight conditions.

The yawing moment is resisted by the interconnecting structure therefore there are apt to be high shear stresses in the vicinity of the external catenary which could cause wrinkling of the envelope. This condition was investigated and found to be not critical.

E.2.6 Summary

The static, dynamic and aerodynamic moments determined for the above flight and landing design conditions are summarized in Table 5.2 of Book I of this volume of the report. The pressure required for the critical condition is also determined in Section 5.9.3 of Book I of this volume of the report.

E.3 ENVELOPE SHAPE ANALYSIS

E.3.1 Center Point Mooring Condition

This section provides details of the analysis of the envelope shape when moored as discussed in Section 5.9.7.1 of Book I of this volume of the report.

The external pressure distribution of Figure 5.12 of Book I of this volume of the report is combined with an internal gas pressure based on 25 lbs per square foot at the shoulder beams level (approximately 5" H_2O).

Loads are applied to a one-foot strip of the envelope cross section representing the center 120 ft of the envelope. Loads originating on the ends of the envelope are introduced to the cross section by shear forces. Table E.1 shows the pressure and shear loads used in the calculations. Pressure loads are taken as constant over an arc length representing 15° on the undistorted cylindrical envelope. Shear loads are introduced as increments to the hoop tension at the junction of the 15° arc segments. Juncture points are identified in Table 5.19 by their location (on the undistorted envelope) as an angle measured from bottom center in the clockwise direction.

E.3.1.1 Analysis - 18 Arc Solution

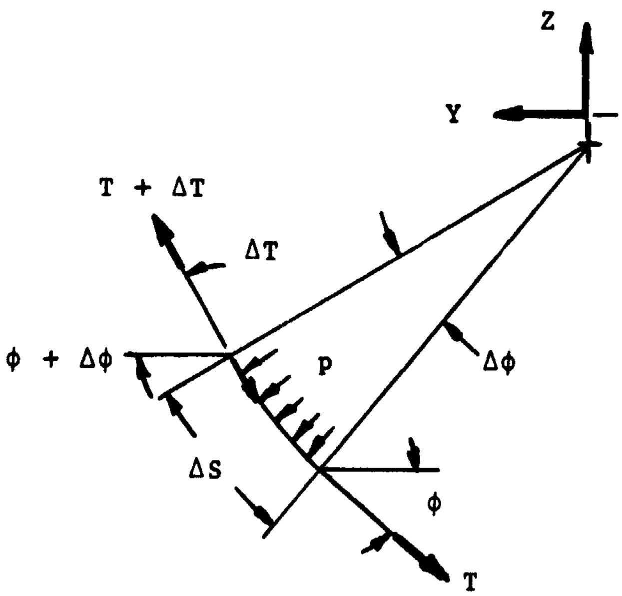

TABLE E.1 - PRESSURE AND SHEAR LOADS - CENTER POINT MOORING

65 MPH, q = 10.8 PSF

Point	External Pressure p/q	External Pressure p	Internal Pressure	Net Outward Pressure	Shear Force ΔT
45°	-1.30	-14.00	25.31	30.17	0
60	- .45	- 4.86	26.02	21.16	.5
75	.45	4.86	26.80	17.07	- 6.9
90	- .90	9.73	27.63	17.90	-13.9
105	.45	4.86	28.42	23.56	-19.9
120	- .45	- 4.86	29.13	33.99	-24.5
135	-1.30	-14.00	29.71	43.71	-27.5
150	-2.00	-21.62	30.12	51.74	-28.5
165	-2.30	-24.86	30.33	55.19	-27.7
180	-1.95	-21.08	30.33	51.41	-25.5
195	-1.10	-11.89	30.12	42.01	-20.5
210	- .50	- 5.40	29.71	35.11	-14.7
225	- .50	- 5.40	29.13	34.53	- 7.9
240	- .50	- 5.40	28.42	33.82	+ .5
265	- .50	- 5.40	27.63	33.03	6.9
270	- .50	- 5.40	26.80	32.20	13.9
285	- .50	- 5.40	26.02	31.42	20.9
300	- .50	- 5.40	25.31	30.71	25.5
315					

From equilibrium of incremental Arc:

1) $\frac{\Delta\phi}{2} = \frac{P}{2T} \Delta S, \quad \Delta S = \frac{\pi}{12} R_0$

2) $\Delta Y = \Delta S \frac{\text{Sin } \Delta\phi/2}{\Delta\phi/2} \text{ Cos} \left[\phi + \frac{\Delta\phi}{2}\right]$

3) $\Delta Z = \Delta S \frac{\text{Sin } \Delta\phi/2}{\Delta\phi} \text{ Sin} \left|\phi + \frac{\Delta\phi}{2}\right|$

4) $Y = Y_0 + \Sigma\Delta Y$

5) $Z = Z_0 + \Sigma\Delta Z$

6) $T = T_0 + \Sigma\Delta T$

Constraints:

7) At points 6 and 12 $Y^2 + Z^2 = a^2$

At points 18 $Y_{18} = -Y_0$, $Z_{18} = Z_0$

8) At the catenary curtain attachments [Pts 6 and 12] the resultant of the hoop tension forces including the ΔT forces at the juncture must pass through the origin.

The cross sectional shape is determined by integrating the above equations step by step to find values of T_0, ϕ_0, ϕ_{6+}, ϕ_{12+} which satisfy the constraints.

The problem is programmed for the digital computer to proceed as follows:

1) For an estimated value of T_0 and ϕ_0 integrate to point (6) determining Y_6 and Z_6; compute the error:

$$e_1 = \sqrt{Y_6^2 + Z_6^2} - a$$

where "a" is a pre-selected length of the internal curtain and cables from the origin. Make a correction to ϕ_0

$$\Delta\phi_0 = \left(\frac{e_1}{Z_6 + Z_0} \right) C_1$$

where C_1 is a convergence factor determined by experiment to insure convergence.

2) Repeat step one with the new values of ϕ_0 as many times as necessary to reduce e_1 to zero within a specified tolerance. [The tolerance was taken as .01 ft.]

3) Using the values of Y_6, Z_6 and ϕ_6 from (2) above:

a) Guess ϕ_{6+}

b) Compute T_{6+} required to meet constraint (8) and carry the calculation to point 12. Iterate on ϕ_{6+} until the dimensional constraint at point (12) is satisfied.

4) In a similar fashion iterate on ϕ_{12+} until point 18 falls on the proper radius from the origin.

The final step is to repeat the entire process with different values of T_0 until point 18 falls precisely on the attachment point to the starframe.

Since the undeflected cylindrical cross section is designed as a circle with a radius of 53.5 ft the approximate radial length "a" of the internal suspension system was guessed to lie between 52.0 and 53.0 ft.

Computer runs were made for a = 52.0 and a = 53.0. Later studies of the symmetrical rigging condition showed that a = 52.5 ft provided a satisfactory cross sectional shape with the lift of the envelope distributed approximately 50-50 between the internal and external systems which was judged to be a good balance. The cross sectional shape for the center point mooring condition is shown in Figure E.1 and represents an interpolation between the computer runs for a = 52.0 and a = 53.0 The hoop tensions T are also shown.

E.3.2 Symmetrical Loads

This section provides details of the analysis of the envelope shape due to symmetrical loads as discussed in Section 5.9.7.2 of Book I of this volume of the report.

In the initial series of computer runs the shape was computed for an equatorial super pressure of 3, 4 and 5 inches of water respectively and with ZX = -208, -104, -312 where ZX = -208 represents the nominal condition with the vertical load split between the internal system and the external system on a 50-50 basis.

Input data for these 9 runs is shown in Table E.2. The shear forces Q are introduced for simplicity as 5 equal forces tangent to the envelope at 5 points as shown in Figure 5.13 of Book I of this volume of the report.

The hoop tension and coordinates at point (1) are computed from the geometry of Figure 5.13 of Book I of this volume of the report and the Loads P_{01}, P_{02}, P_{03} and ZX.

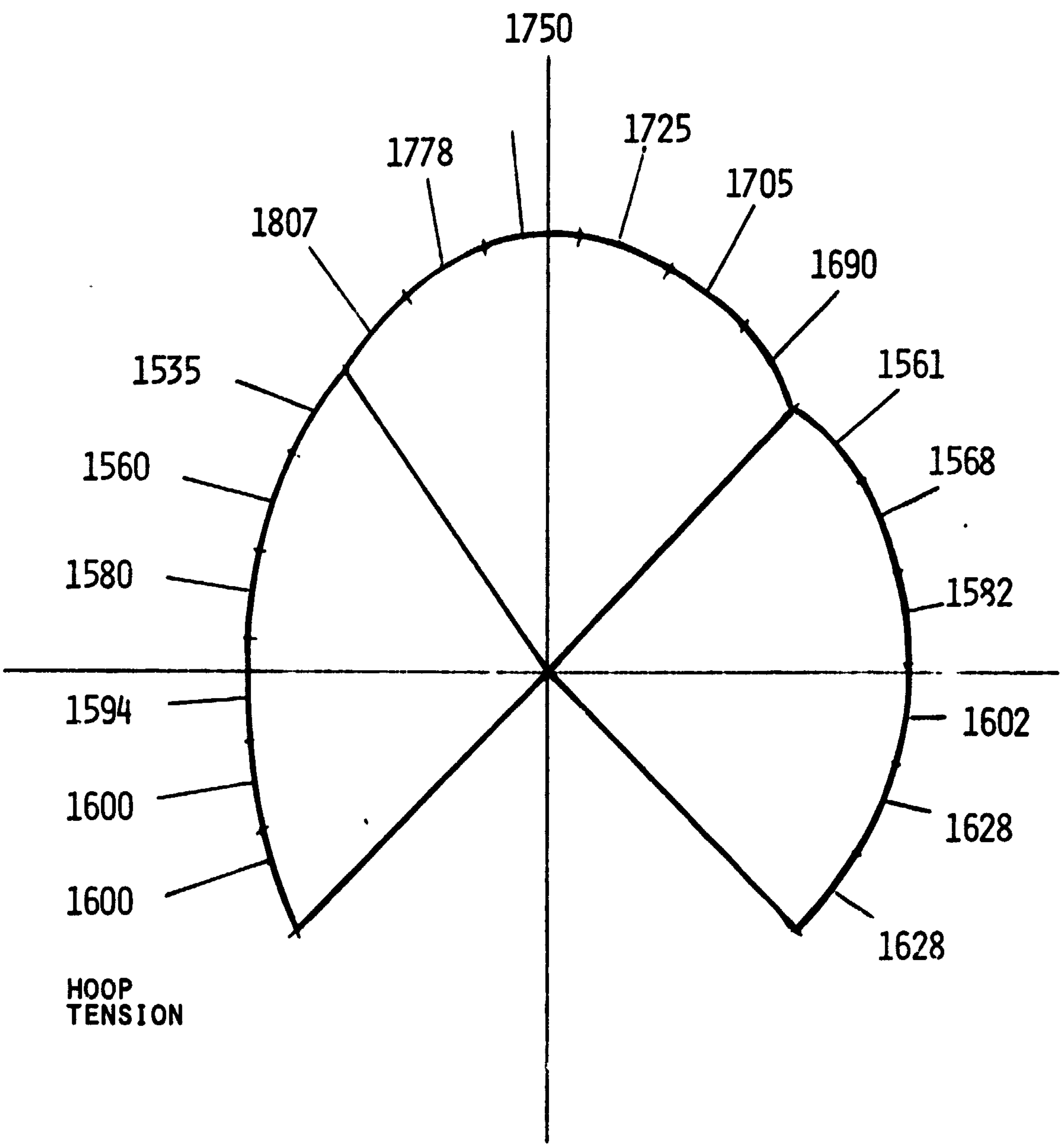

FIGURE E.1 ENVELOPE SHAPE - CENTER POINT MOORING

TABLE E.2 - INPUT DATA SYMMETRICAL LOADINGS

INITIAL CONDITION

Condition	1	2	3	4	5	6	7	8	9
Ref Pressure	3"	3"	3"	4"	4"	4"	5"	5"	5"
				P_1+5.2			P_1+10.2		
P_{01}	12.84			18.04			23.24		
P_{02}	13.36			18.56			23.76		
P_{03}	13.95			19.15			24.35		
P_1	14.51			19.71			24.91		
P_2	15.23			20.43			25.63		
P_3	15.97			21.17			26.37		
P_4	16.69	same as 1	same as 1	21.79	same as 4	same as 4	27.09	same as 7	same as 7
P_5	17.34			22.54			27.74		
P_6	17.56			23.06			28.26		
P_7	18.23			23.43			28.63		
P_8	18.43			23.63			28.83		
ΔT_1	-23.3	-30.7	-15.5	same as 1	same as 2	same as 3	same as 1	same as 2	same as 3
ΔT_2	-23.3	-30.7	-15.5						
ΔT_3	-23.3	-30.7	-15.5						
ΔT_4	-23.3	-30.7	-15.5						
Ao	474.26	474.26	474.26	664.27	664.27	664.27	854.28	854.28	854.28
ZX	-208	-312	-104	-208	-312	-104	-208	-312	-104
ZEEI	139	69	207	139	69	207	139	69	207

The integration of the section shape is carried out using a nominal value of ϕ_1 and ZEEI as a starting point and adjusting these values by an iterative procedure to meet the constraints of symmetry at top center.

For each condition (defined by ZX and super pressure) this procedure produces the cross section shape, hoop tensions and the radius "a" of the internal suspension system. A plot of these results (Figure E.2) provides a device for determining what value of "a" is needed to produce a chosen split of the vertical loads between the internal and external system rigging condition and to access the changes in this distribution with changing pressure condition.

Observe from the figure that "a" = 52.5 feet provides the nominal rigging condition of ZX = 0208 at 4" H_2O which corresponds to a 50-50 distribution of vertical load between the internal and external systems. Note also that ZX drops to about -175 when the pressure goes up to 5" H_2O and increases to about -235 at 3" H_2O. The corresponding values for the vertical component of the internal curtain load are 135, 156, and 108 for pressures of 4, 5 and 3" of H_2O respectively. Thus, the vertical load distribution external/internal shifts from 50/50 at 4" to 42/58 at 5" and 56/44 at 3".

An additional run with no unbalanced vertical load was made for comparison with the rigging condition. A detail calculation of the CG of the cross sections showed that the CG of the unloaded (air inflated zero fabric weight) section lies at .15 ft below the nominal center and moves to .75 ft above the nominal center for the 1G rigging condition. This condition corresponds to approximately 100,000 lb net lift load on the suspension system. The vertical spring constant considering cross section deflections alone is therefore on the order of 111,000 lbs per ft. When the additional deflections of cable stretch, envelope shear, and envelope bendings are included (not evaluated at this time) it is anticipated that the net

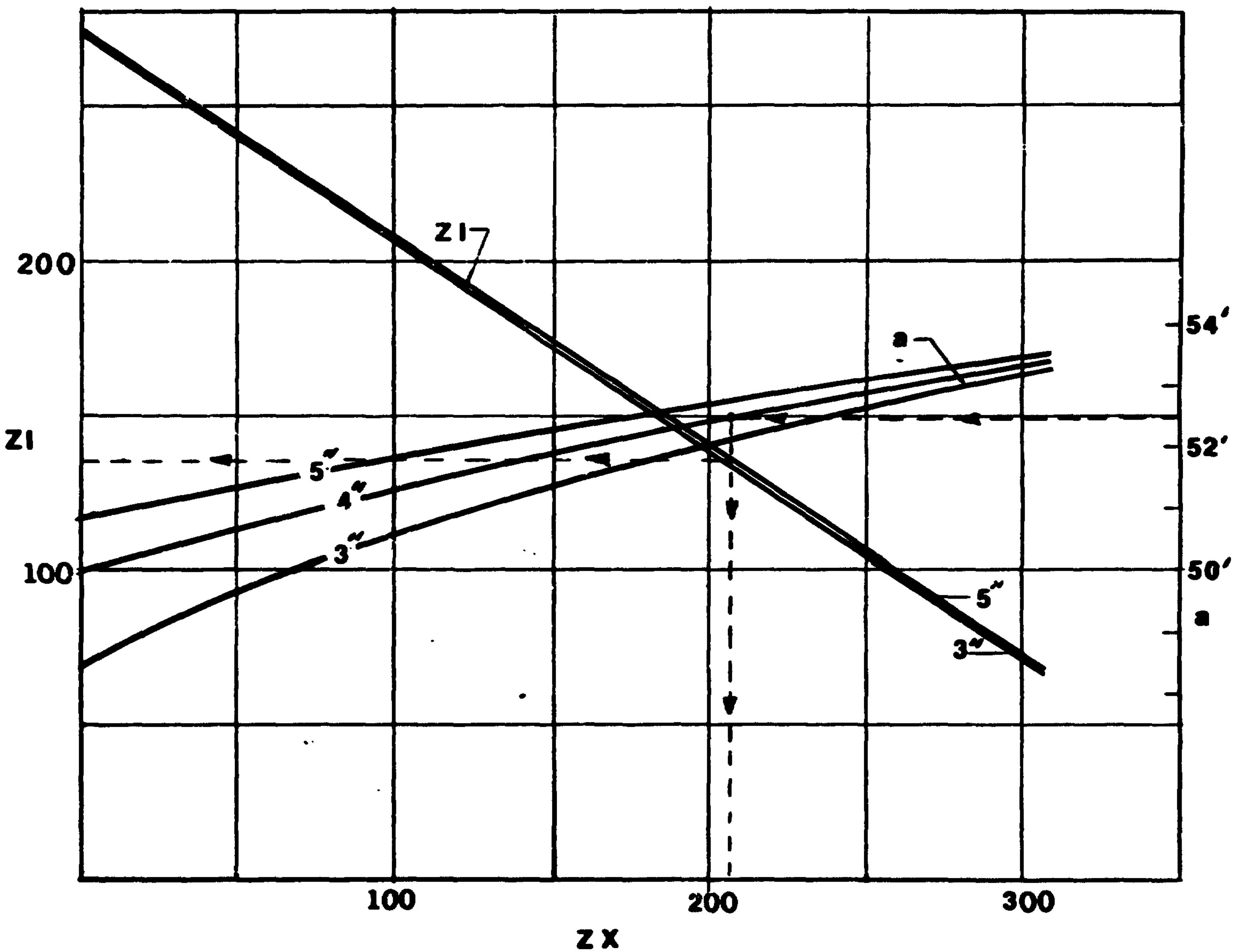

FIGURE E.2 SUSPENSION LOAD DISTRUBUTION VERSUS CABLE GEOMETRY vertical stiffness will be consistent with the K_{12} = 75,000 lbs per ft used in the dynamics analysis of a previous section of this report.

Further analysis of the data showed that although the nominal rigging condition places 50% of the vertical load into the internal system, the envelope stiffness is such that incremental loads will distribute 25% of the internal, 51% to the upper external curtain, 11% to the lower external and the remainder to variation of fabric tension components on the shoulder beam (gas pressure).

As discussed previously, the above analysis was based on an external suspension configuration which places the system on the outside of the envelope with the envelope deflected inward by the shoulder beam of the starframe.

This arrangement requires that all internal suspension cables as well as all starframe members must penetrate the envelope. To alleviate this problem an alternative arrangement was investigated. In the alternate arrangement (the one chosen for the baseline design) the "external" catenary system is actually inside the envelope with the envelope allowed to bulge between the catenary attachment lines. This arrangement eliminates structural penetrations of the envelope except for main outrigger support members. Analysis shows that the alternate system is not quite as stiff as the other system but is much more secure from the possibility of going slack under high inward or outward radial loads. The alternate system is therefore the chosen design.

APPENDIX F

ROTOR PERFORMANCE DATA

CONVERSION FACTORS FOR APPENDIX F

1.0 KIP	=	$4.535 \times 10^{+2}$ kg
1.0 kt	=	5.144×10^{-1} m/s
1.0 HP	=	$7.46 \times 10^{+2}$ W
1.0 lb	=	4.535×10^{-1} kg
t_K	=	$(5/9)(t_F + 459.67)$

Piasecki Aircraft Corporation
ISLAND ROAD, INTERNATIONAL AIRPORT
PHILADELPHIA, PENNSYLVANIA 19153

Figure F-1
HOVER POWER VS. GROSS WEIGHT
47,000 to 50,000-LB. SINGLE-ROTOR
(WITH TAIL-ROTOR) HELICOPTER

S.L., 59° F., O.G.E.

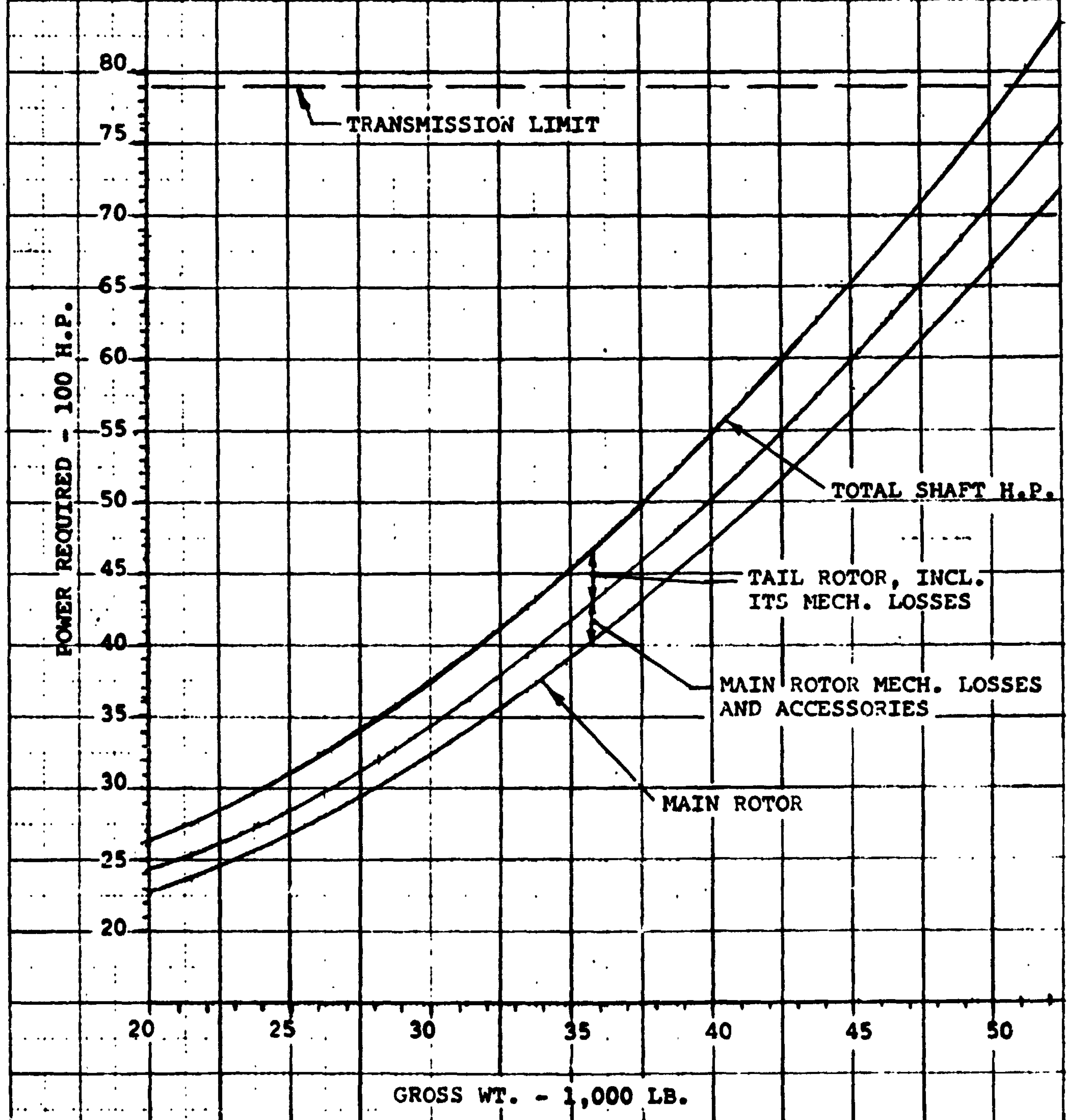

Figure F-2

HOVER POWER VS. GROSS WT.
47,000 TO 50,000-LB. SINGLE-ROTOR
(WITH TAIL-ROTOR) HELICOPTER

5,000 FT., 41.2 DEG.F., — O.G.E.

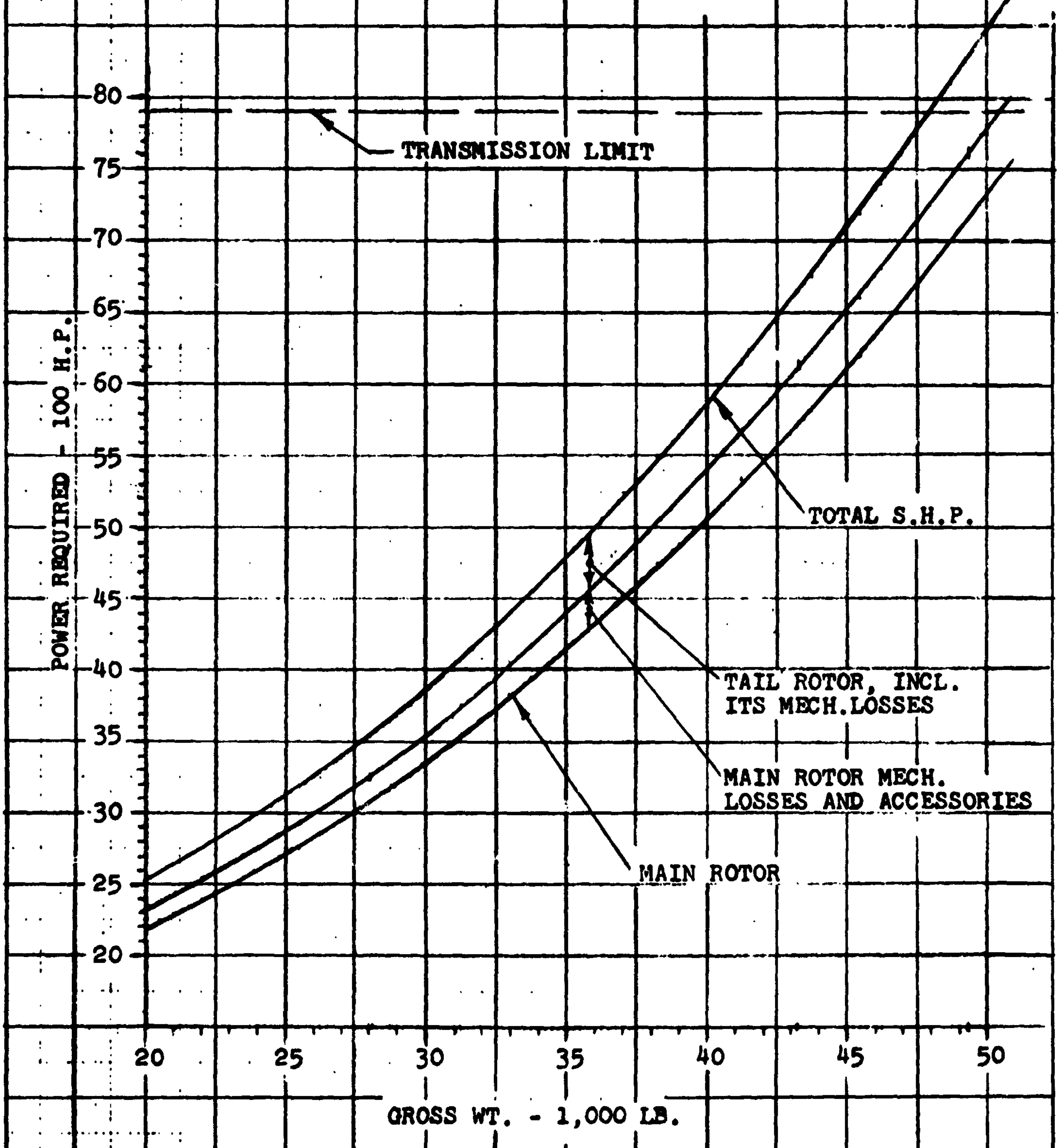

Figure F-3

Piasecki Aircraft Corporation
ISLAND ROAD, INTERNATIONAL AIRPORT
PHILADELPHIA, PENNSYLVANIA

HOVER POWER VS. GROSS WT.
47,000 TO 50,000-LB. SINGLE-ROTOR
(WITH TAIL-ROTOR) HELICOPTER

8,000 FT., 30.5 DEG. F., O.G.E.

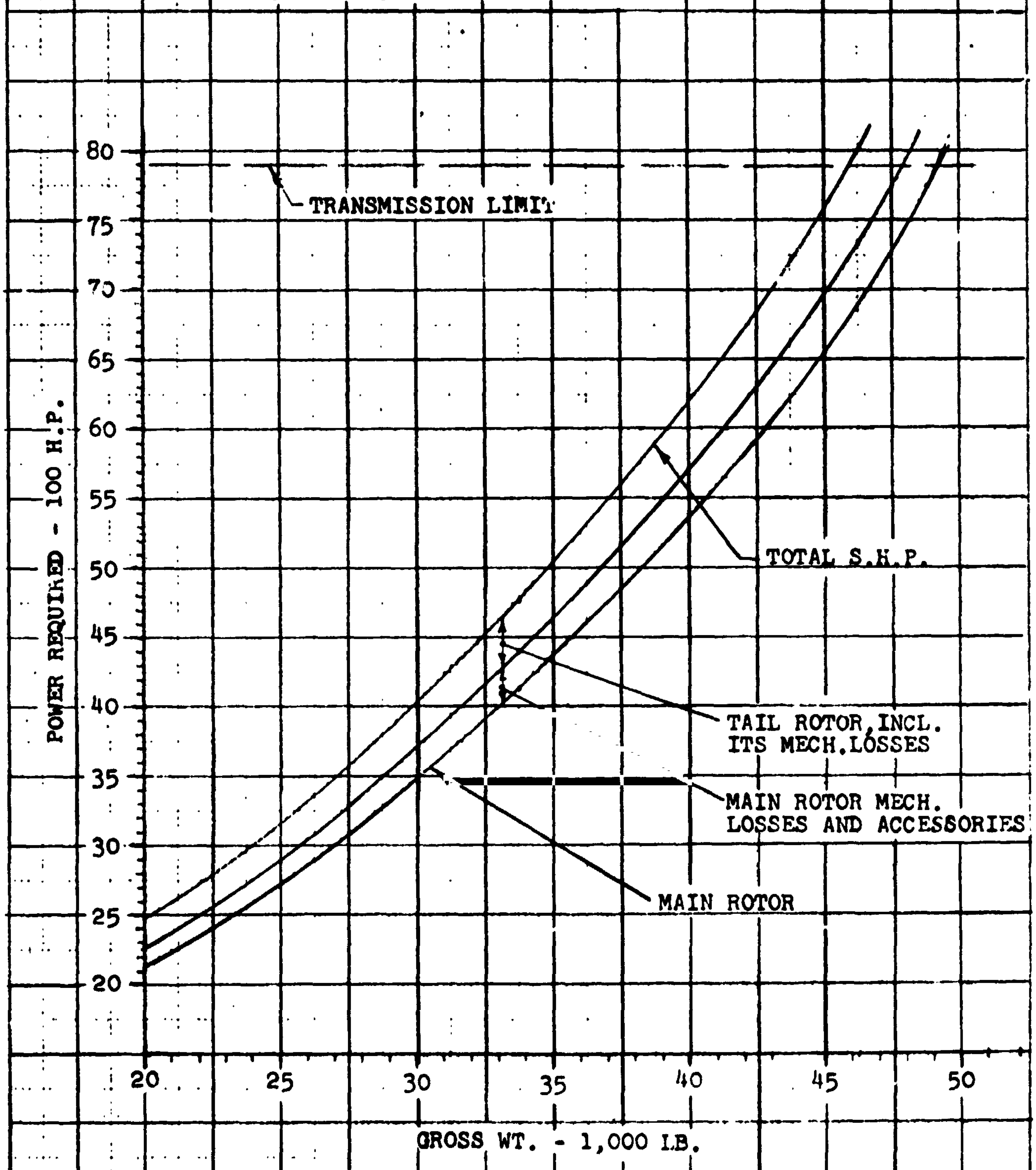

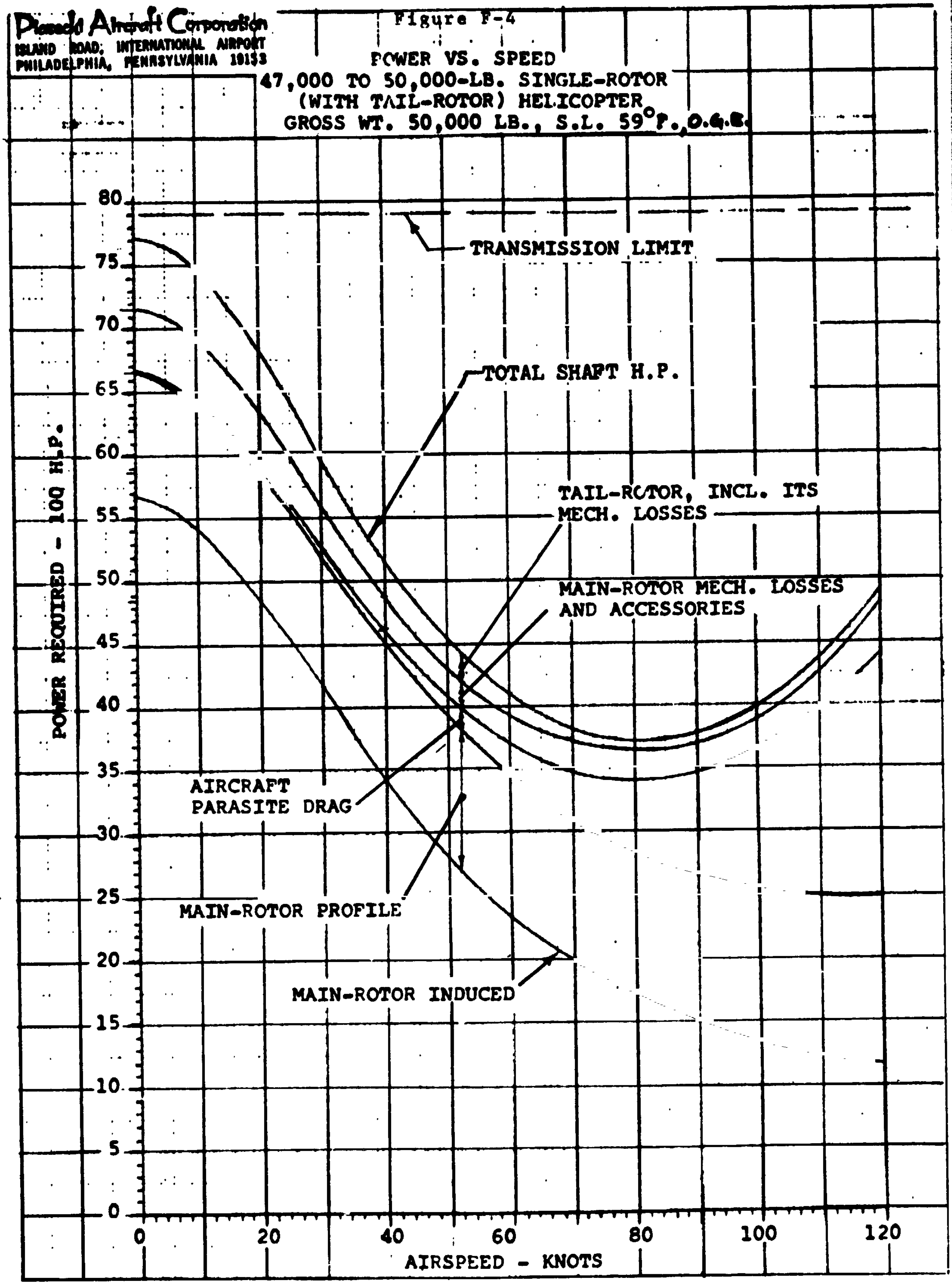

Piasecki Aircraft Corporation
ISLAND ROAD, INTERNATIONAL AIRPORT
PHILADELPHIA, PENNSYLVANIA 19153
Figure F-4
POWER VS. SPEED
47,000 TO 50,000-LB. SINGLE-ROTOR
(WITH TAIL-ROTOR) HELICOPTER
GROSS WT. 50,000 LB., S.L. 59°F. O.A.T.
TRANSMISSION LIMIT
TOTAL SHAFT H.P.
TAIL-ROTOR, INCL. ITS MECH. LOSSES
MAIN-ROTOR MECH. LOSSES AND ACCESSORIES
AIRCRAFT PARASITE DRAG
MAIN-ROTOR PROFILE
MAIN-ROTOR INDUCED
POWER REQUIRED - 100 H.P.
0
5
10
15
20
25
30
35
40
45
50
55
60
65
70
75
80
0
20
40
60
80
100
120
AIRSPEED - KNOTS

Figure F-5

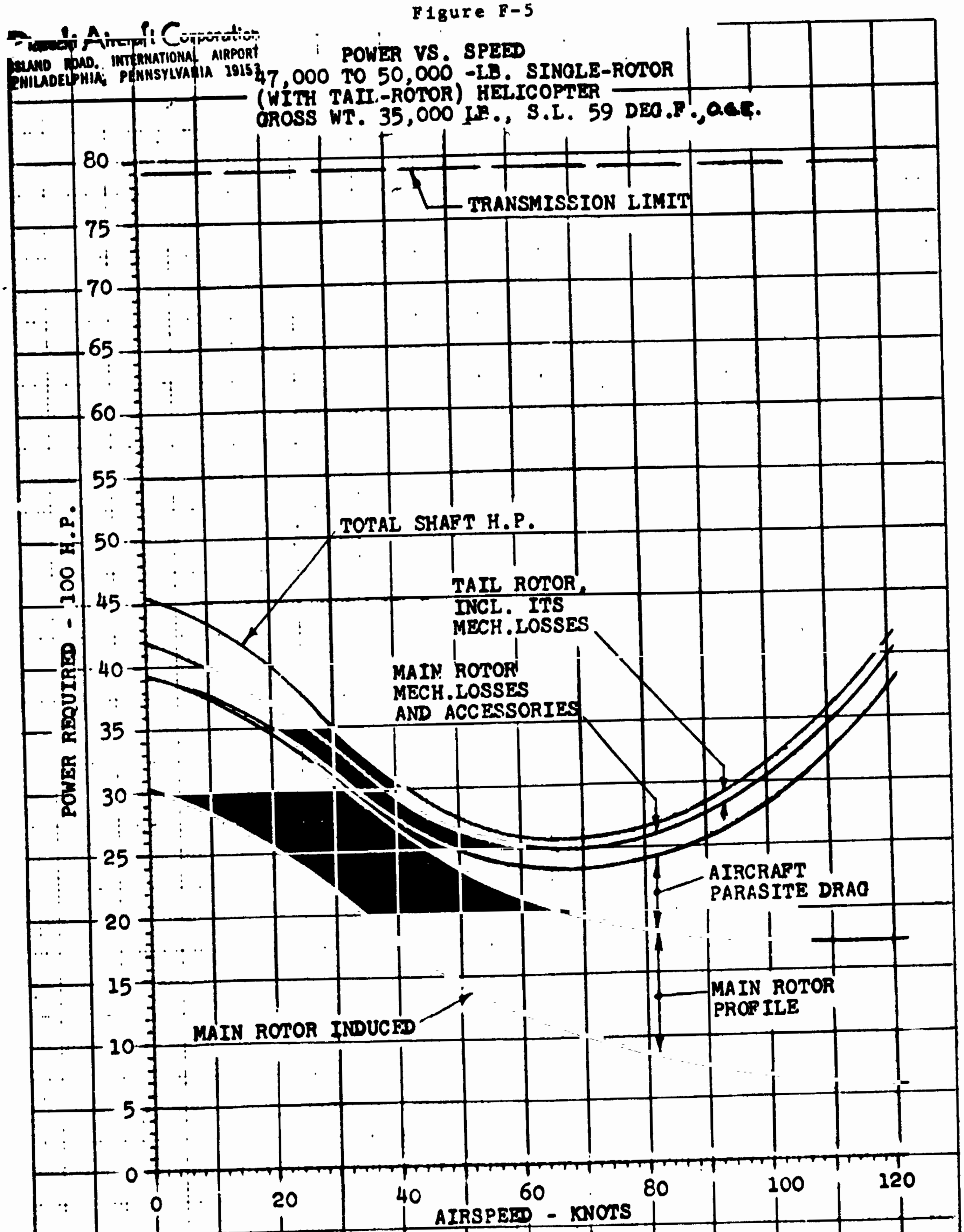

Piasecki Aircraft Corporation
ISLAND ROAD, INTERNATIONAL AIRPORT
PHILADELPHIA, PENNSYLVANIA 19153
POWER VS. SPEED
47,000 TO 50,000 -LB. SINGLE-ROTOR
(WITH TAIL-ROTOR) HELICOPTER
GROSS WT. 35,000 LB., S.L. 59 DEG.F., O.G.E.
TRANSMISSION LIMIT
TOTAL SHAFT H.P.
TAIL ROTOR, INCL. ITS MECH.LOSSES
MAIN ROTOR MECH.LOSSES AND ACCESSORIES
AIRCRAFT PARASITE DRAG
MAIN ROTOR PROFILE
MAIN ROTOR INDUCED
POWER REQUIRED - 100 H.P.
AIRSPEED - KNOTS
0
5
10
15
20
25
30
35
40
45
50
55
60
65
70
75
80
0
20
40
60
80
100
120

[illegible] Aircraft Corporation
ISLAND ROAD, INTERNATIONAL AIRPORT
PHILADELPHIA, PENNSYLVANIA 19153

Figure F-6

POWER VS. SPEED
47,000 to 50,000-LB. SINGLE-ROTOR
(WITH TAIL-ROTOR) HELICOPTER
GROSS WT.20,000 LB.,S.L.59 DEG.F., [illegible]

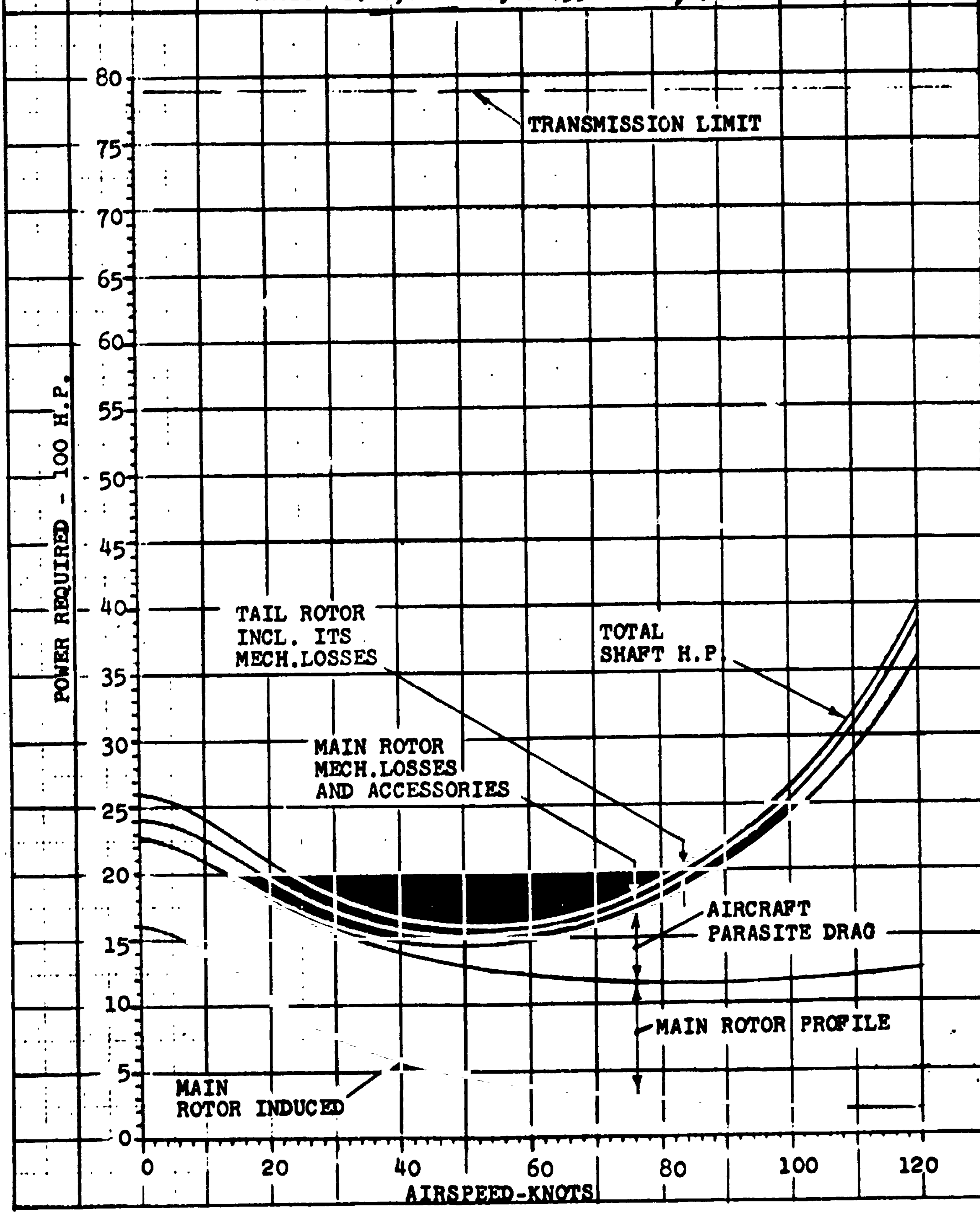

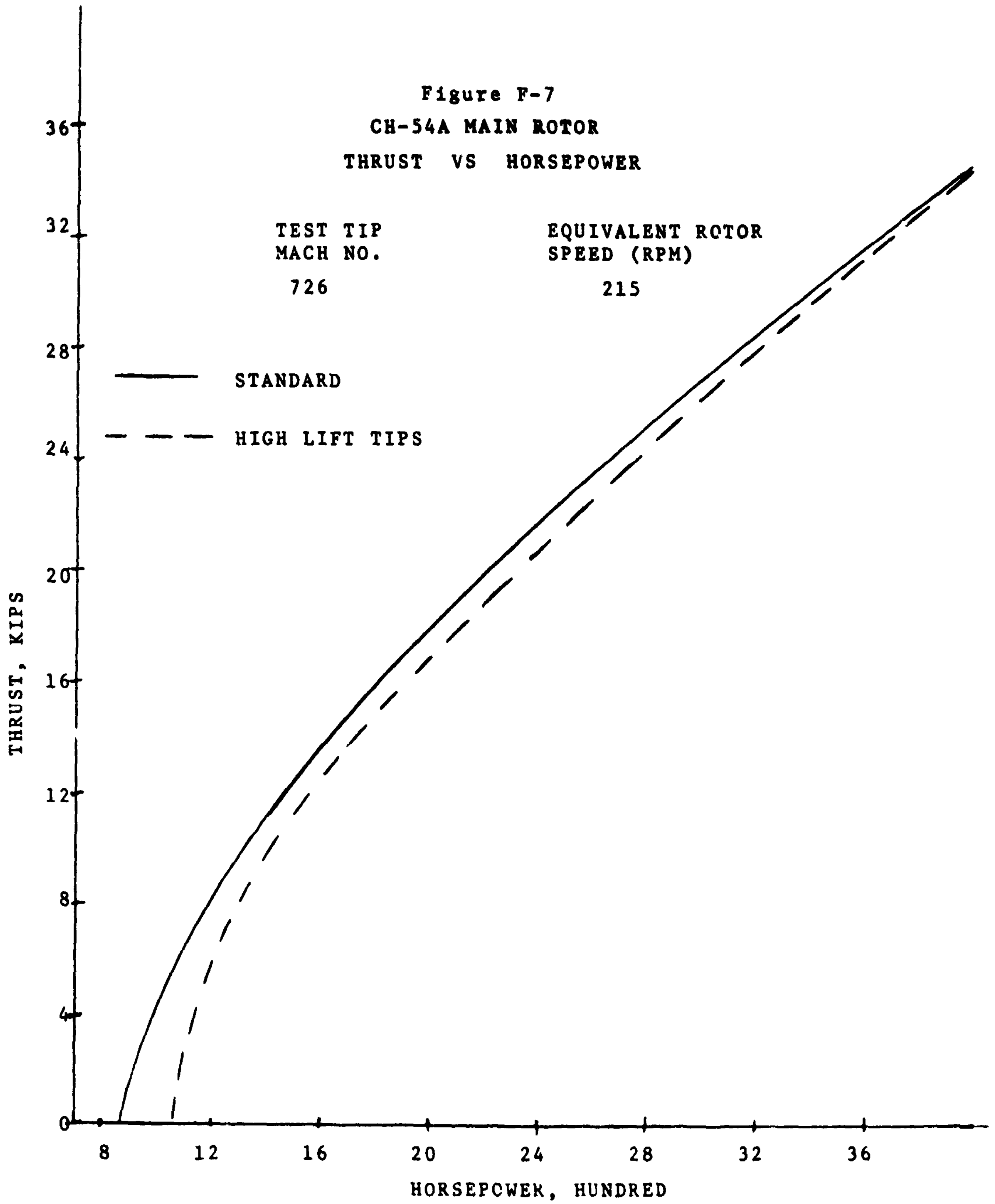
Figure F-7
CH-54A MAIN ROTOR
THRUST VS HORSEPOWER
TEST TIP
MACH NO.
726
EQUIVALENT ROTOR
SPEED (RPM)
215
STANDARD
HIGH LIFT TIPS
THRUST, KIPS
0
4
8
12
16
20
24
28
32
36
8
12
16
20
24
28
32
36
HORSEPOWER, HUNDRED

HELICOPTER WEIGHT STATEMENT

NAME ____________

DATE ____________

PAGE 5

MODEL CH-54B

REPORT SER-64361

SUMMARY WEIGHT STATEMENT
ROTORCRAFT ONLY
~~ESTIMATED - CALCULATED~~ - ACTUAL

(Cross out those not applicable)

CONTRACT DAAJ01-70-C-0306

ROTORCRAFT, GOVERNMENT NUMBER 70-18489

ROTORCRAFT, CONTRACTOR NUMBER S.S. 64097

MANUFACTURED BY Sikorsky Aircraft

			MAIN	AUXILIARY
ENGINE	MANUFACTURED BY		Pratt & Whitney	
ENGINE	MODEL	(2)	JFTD12A-5A	
ENGINE	NUMBER	R.H. L.H.	#677766 #677767	
PROPELLER	MANUFACTURED BY			
PROPELLER	MODEL			
PROPELLER	NUMBER			

MIL-STD-451 PART I

NAME

DATE

ROTORCRAFT
SUMMARY WEIGHT STATEMENT
WEIGHT EMPTY

PAGE 6
MODEL CH-54B
REPORT SER-64361

1							
2	ROTOR GROUP						3976.6
3	BLADE ASSEMBLY					2178.0	
4	HUB					453.9	
5	HINGE AND BLADE RETENTION					1344.7	
6		FLAPPING			583.5		
7		LEAD LAG			332.6		
8		PITCH			416.9		
9	BLADE ATTACH. HDWE.	~~XXXXXX~~			11.7		
10	WING GROUP						
11	WING PANELS-BASIC STRUCTURE						
12	CENTER SECTION-BASIC STRUCTURE						
13	INTERMEDIATE PANEL-BASIC STRUCTURE						
14	OUTER PANEL-BASIC STRUCTURE-INCL TIPS			LBS			
15	SECONDARY STRUCT-INCL FOLD MECH			LBS			
16	AILERONS-INCL BALANCE WTS			LBS			
17	FLAPS						
18	-TRAILING EDGE						
19	-LEADING EDGE						
20	SLATS						
21	SPOILERS						
22							
23	TAIL GROUP						532.8
24	TAIL ROTOR					440.3	
25	-BLADES				149.6		
26	-HUB				290.7		
27	STABILIZER-BASIC STRUCTURE						
28	FINS-BASIC STRUCTURE-INCL DORSAL			LBS		92.5	
29	SECONDARY STRUCTURE -STABILIZER AND FINS						
30	ELEVATOR - INCL BALANCE WEIGHT			LBS			
31	RUDDER - INCL BALANCE WEIGHT			LBS			
32							
33	BODY GROUP						2924.9
34	FUSELAGE OR HULL - BASIC STRUCTURE					2498.7	
35	BOOMS - BASIC STRUCTURE						
36	SECONDARY STRUCTURE - FUSELAGE OR HULL					242.4	
37	- BOOMS						
38	- DOORS, PANELS & MISC					183.8	
39							
40							
41	ALIGHTING GEAR - LAND TYPE						1728.0
42	LOCATION	*ROLLING	STRUCT	CONTROLS	SUPPORTS		
43		ASSEMBLY					
44	MAIN GEAR	206.0	613.0	67.3	608.1		
45	NOSE GEAR	39.5	164.4	1.6			
46	TAIL SKID		22.1	6.0			
47							
48							
49							
50	ALIGHTING GEAR GROUP - WATER TYPE						
51	LOCATION	FLOATS	STRUTS	CONTROLS			
52							
53							
54							
55							
56							
57							

ORIGINAL PAGE IS
OF POOR QUALITY

*WHEELS, BRAKES, TIRES, TUBES AND AIR

MIL-STD-451 PART I
NAME
DATE

ROTORCRAFT
SUMMARY WEIGHT STATEMENT
WEIGHT EMPTY

PAGE 1
MODEL CH-46
REPORT SER-64301

1							
2	FLIGHT CONTROLS GROUP						1165.0
3	COCKPIT CONTROLS					142.6	
4	AUTOMATIC STABILIZATION					109.6	
5	SYSTEM CONTROLS - ROTOR	NON ROTATING				245.1	
6		ROTATING				268.6	
7	- FIXED WING						
8	- HYD. BOOST					399.1	
9							
10	ENGINE SECTION OR NACELLE GROUP						125.4
11	INBOARD						
12	CENTER					125.4	
13	OUTBOARD						
14	DOORS, PANELS AND MISC						
15							
16	PROPULSION GROUP						6941.4
17			X AUXILIARY	X	X MAIN	X	
18	ENGINE INSTALLATION						
19	ENGINE					1871.1	
20	TIP BURNERS						
21	LOAD COMPRESSOR						
22	REDUCTION GEAR BOX, ETC						
23	ACCESSORY GEAR BOXES AND DRIVES						
24	SUPERCHARGER-FOR TURBOS						
25	AIR INDUCTION SYSTEM					56.9	
26	EXHAUST SYSTEM					21.8	
27	COOLING SYSTEM						
28	LUBRICATING SYSTEM					62.6	
29	TANKS				28.0		
30	BACKING BD, TANK SUP & PADDING						
31	COOLING INSTALLATION				30.0		
32	PLUMBING, ETC				4.6		
33	FUEL SYSTEM					858.6	
34	TANKS - UNPROTECTED						
35	- PROTECTED -7.62MM		75.0		199.1		
36	BACKING BD, TANK SUP & PADDING		101.3		154.7		
37	PLUMBING, ETC		74.6		253.9		
38	WATER INJECTION SYSTEM						
39	ENGINE CONTROLS					35.1	
40	STARTING SYSTEM					77.[illegible]	
41	PROPELLER INSTALLATION						
42	DRIVE SYSTEM					3958.1	
43	GEAR BOXES				3096.0		
44	LUBE SYSTEM				75.4		
45	~~XXXXXXXXXXXXX~~ ROTOR BRAKE				47.0		
46	TRANSMISSION DRIVE				234.7		
47	ROTOR SHAFT				505.0		
48	JET DRIVE						
49							
50							
51							
52	AUXILIARY POWER PLANT GROUP						182.5
53							
54							
55							
56							
57							

ROTORCRAFT
SUMMARY WEIGHT STATEMENT
WEIGHT EMPTY

1							
2							
3							
4	INSTRUMENT AND NAVIGATIONAL EQUIPMENT GROUP						263.5
5	INSTRUMENTS					263.5	
6	NAVIGATIONAL EQUIPMENT						
7							
8							
9	HYDRAULIC AND PNEUMATIC GROUP						318.5
10	HYDRAULIC					318.5	
11	PNEUMATIC						
12							
13							
14	ELECTRICAL GROUP						465.4
15	A C SYSTEM					260.8	
16	D C SYSTEM					204.6	
17							
18							
19	ELECTRONICS GROUP						448.9
20	EQUIPMENT					318.7	
21	INSTALLATION					130.2	
22							
23							
24	ARMAMENT GROUP - INCL GUNFIRE PROTECTION				LBS		
25	PASSIVE DEFENSE PROVISIONS						78.0
26	FURNISHINGS AND EQUIPMENT GROUP						218.9
27	ACCOMMODATIONS FOR PERSONNEL					131.3	
28	MISCELLANEOUS EQUIPMENT	X INCL			LBS BALLASTX	53.5	
29	FURNISHINGS						
30	EMERGENCY EQUIPMENT					34.1	
31							
32							
33							
34	AIR CONDITIONING AND ANTI-ICING EQUIPMENT						119.8
35	AIR CONDITIONING					94.4	
36	ANTI-ICING					25.4	
37							
38							
39	PHOTOGRAPHIC GROUP						
40	EQUIPMENT						
41	INSTALLATION						
42							
43	AUXILIARY GEAR GROUP						199.4
44	AIRCRAFT HANDLING GEAR					14.3	
45	LOAD HANDLING GEAR					185.1	
46	ATO GEAR						
47							
48							
49							
50							
51							
52							
53							
54	MANUFACTURING VARIATION						42.3
55							
56							
57	TOTAL-WEIGHT EMPTY - PAGES 2, 3 AND 4						19,731.3

F-13

ORIGINAL PAGE IS
OF POOR QUALITY

NAME
DATE

SUMMARY WEIGHT STATEMENT

PAGE 9
MODEL CH-54B
REPORT SER-64361

	LOAD CONDITION	SEA LEVEL MISSION			MILITARY OPERATIONAL MISSION		
2							
3	CREW - NO. (2)			400			400
4	PASSENGERS - NO.						
5	FUEL LOCATION	TYPE	GALS		TYPE	GALS	
6	UNUSABLE	JP-4	2.5	16	JP-4	2.5	16
7	INTERNAL	JP-4	387.8	2,521	JP-4	368.8	2,397
8							
9							
10							
11	EXTERNAL						
12							
13							
14							
15	BOMB BAY						
16							
17							
18							
19	OIL						
20	UNUSABLE		0.8	6		0.8	6
21	ENGINE		2.0	15		2.0	15
22							
23							
24							
25	BAGGAGE						
26	CARGO (WITH CARGO HANDLING SYSTEM)			24,306			24,430
27							
28	ARMAMENT						
29	GUNS - LOCATION TYPE**	QUANTITY	CALIBER				
30							
31							
32							
33							
34	AMM						
35							
36							
37							
38	BOMB INSTL*						
39	BOMBS						
40							
41	TORPEDO INSTL*						
42	TORPEDOES						
43							
44	ROCKET INSTL*						
45	ROCKETS						
46							
47	EQUIPMENT - PYROTECHNICS						
48	-PHOTOGRAPHIC						
49							
50	-*OXYGEN						
51	CARGO SUSPENSION SYSTEM (4 POINT) (INCL. IN CARGO)			(813)			(813)
52	-MISCELLANEOUS						
53	SEAT CUSHIONS - PILOT & CO-PILOT			5			5
54	CARGO HOIST (SINGLE POINT) (INCL. IN CARGO)			(1,149)			(1,149)
55	USEFUL LOAD			27,269			27,269
56							
57	GROSS WEIGHTS - PAGES 2-5			47,000			47,000

*IF NOT SPECIFIED AS WEIGHT EMPTY **FIXED, FLEXIBLE, ETC.

The guaranteed empty weight of the CH-54B is 19,864 lbs (Reference 3). The estimated weight for the adapter assembly required to interface the helicopter to the interconnecting structure is 886 lbs each. Thus, the total weight considered in Table 5.5 of Book I of this volume of the report is 4 (19,864 + 886) = 83,000 lbs.

It should be noted that equipment on board the helicopters not needed in the HLA application can be removed which would reduce the vehicle empty weight somewhat. This has not been done in that the philosophy has been to minimize helicopter modifications in the interest of minimizing the cost to achieve a flight research capability.

APPENDIX G

ESTIMATED EMPTY WEIGHT OF OPERATIONAL HLA CONFIGURATION

CONVERSION FACTORS FOR APPENDIX G

1.0 cu ft	=	2.83×10^{-2} sq m
1.0 lb	=	4.535×10^{-1} kg
1.0 n m	=	$1.853 \times 10^{+3}$ m

ESTIMATED EMPTY WEIGHT OF OPERATIONAL HLA CONFIGURATION[1]

Weight Empty (Pounds)			124,435
Propulsion Module[2,3]		64,500	
Envelope Group		30,500	
Envelope	17,750		
Ballonets	2,100		
Pressure System	3,100		
Misc. Envelope and Fairings	2,075		
Internal Suspension Curtains	1,140		
Internal Suspension Cables	1,900		
External Suspension	2,435		
Interconnecting Structure		26,000	
Internal Starframe (includes Drag Strut)	7,100		
Support and Lift Struts	18,900		
Control Car		1,500	
Furnishings		200	
Navigational Instruments		75	
Airconditioning		200	
Precision Hover Sensor		540	
Automatic Flight Control System Electronics		20	
Fly-By-Wire Control System		850	
Electronics	350		
Interconnecting Cabling and Supports	500		
Vehicle Sensors and Cabling		50	

[1] 75 Ton Payload, 100 nautical mile range, hull volume approximately 2×10^6 Ft^3

[2] Includes adaptor to support strut

[3] Weight based upon removing cockpit and tail sections from existing CH-54B helicopter at existing manufacturing breakpoints. A dedicated propulsion module employing current materials and propulsion technology would reduce the propulsion module weight somewhat.